Exceptional service in the national interest

Sandia National Laboratories

UR LLE

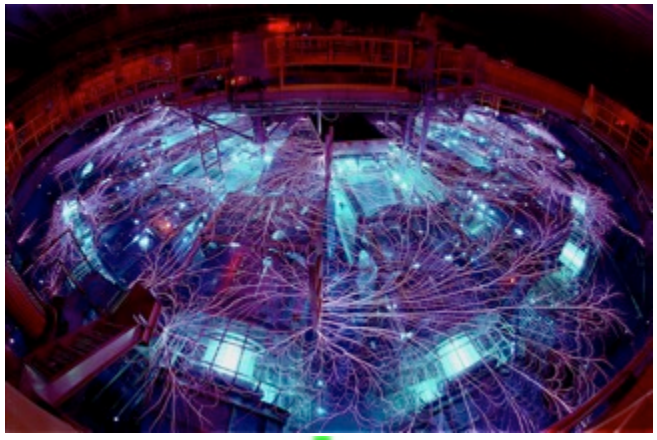

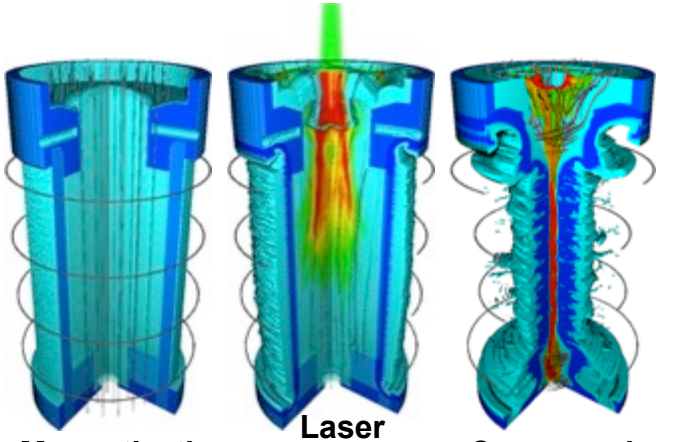

Introduction to Magnetically Driven Implosions and MagLIF

Kyle Peterson

on behalf of the entire MagLIF team

Sandia National Laboratories,

Albuquerque, NM, USA

National Implosion Stagnation Physics Group,

Livermore, CA, October 27, 2015

Sandia National Laboratories is a multi-program laboratory managed and operated by Sandia Corporation, a wholly owned subsidiary of Lockheed Martin Corporation, for the U.S. Department of Energy's National Nuclear Security Administration under contract DE-AC04-94AL85000.

Outline

- Overview of MDI and MagLIF on Z (speaker: Kyle Peterson, ~45 mins)
  - What are the advantages and disadvantages to using pulsed power as opposed to lasers as a driver?
  - Similarities and differences of MDI and IDI,DDI implosions
  - Why magnetized implosions? What is unique about MagLIF?
  - What is our current understanding of magnetically driven implosions and stagnation?
  - What are the biggest challenges for MagLIF and what are we doing to address them?
  - What is the current state of our simulation tools and plans for the future?

Outline

- Diagnosing MagLIF stagnation conditions (speaker: Mathew Gomez, ~30 mins)
  - Challenges for diagnosing MagLIF implosions and stagnation
  - Estimation of burn duration
  - Temperature measurements
  - Plasma density measurements
  - Estimation of liner opacity and mix fraction
  - Estimation of hot fuel volume

Outline

- Diagnosing MDI stagnation conditions with nuclear diagnostics & alternative platforms (speaker: Patrick Knapp, ~30 mins)
  - Complications of nuclear diagnostics on Z
  - Effects of magnetization
  - Measurements of yield, ion temperature, magnetization, areal density, and mix
  - Nuclear diagnostic needs & wishlist
  - Alternative platforms to study stagnation conditions on Z
    - **D_2 Gas puff**: Platform to look at energy conversion
    - **Cold Compression**: Stability and confinement
  - Diagnostic signatures of non-thermal neutron generation (gas-puffs)

The Z pulsed power generator provides a compact MJ-class target physics platform

Sandia National Laboratories

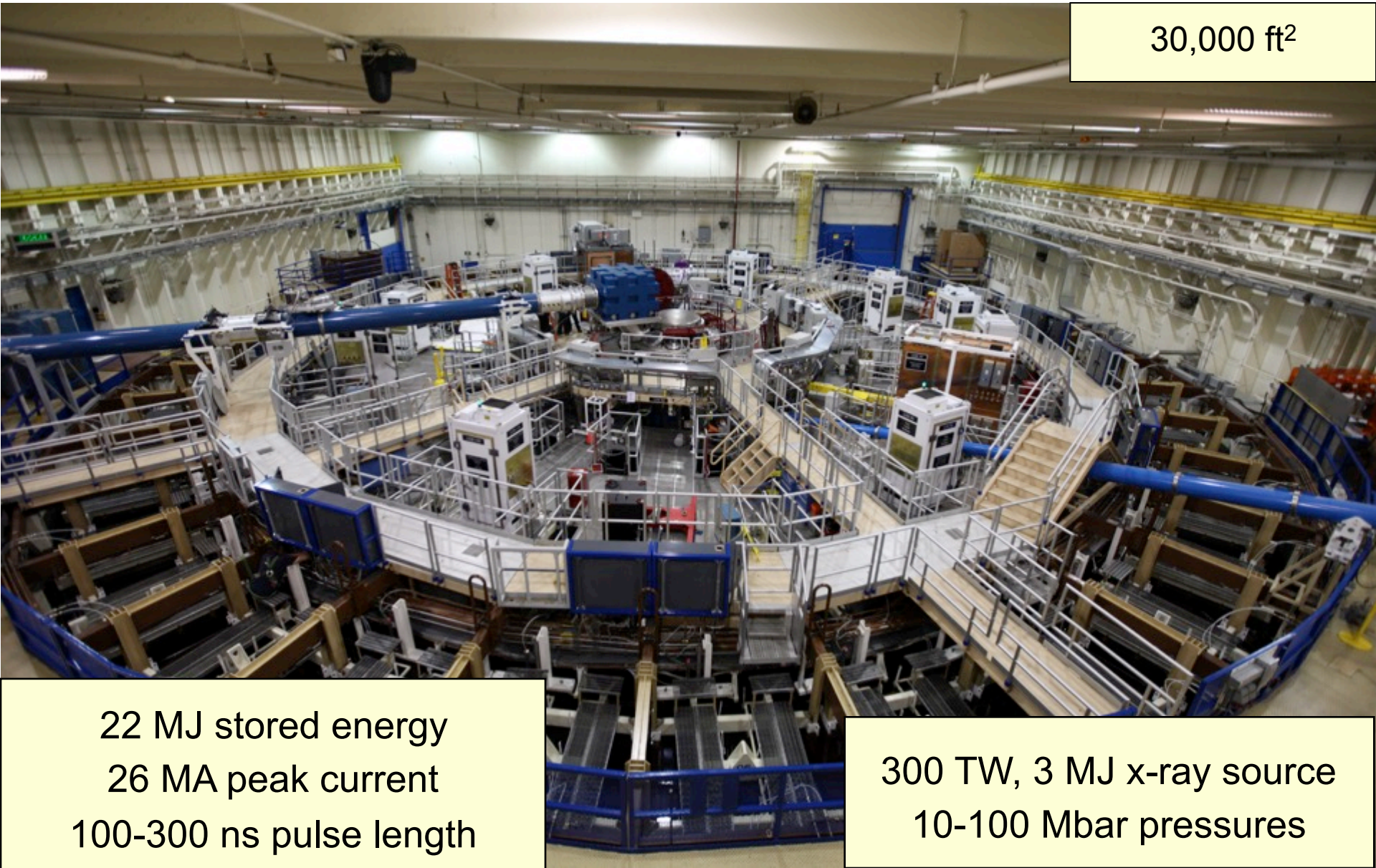

30,000 ft^2

22 MJ stored energy
26 MA peak current
100-300 ns pulse length

300 TW, 3 MJ x-ray source
10-100 Mbar pressures

Magnetic direct drive is based on efficient use of large currents to create high pressures

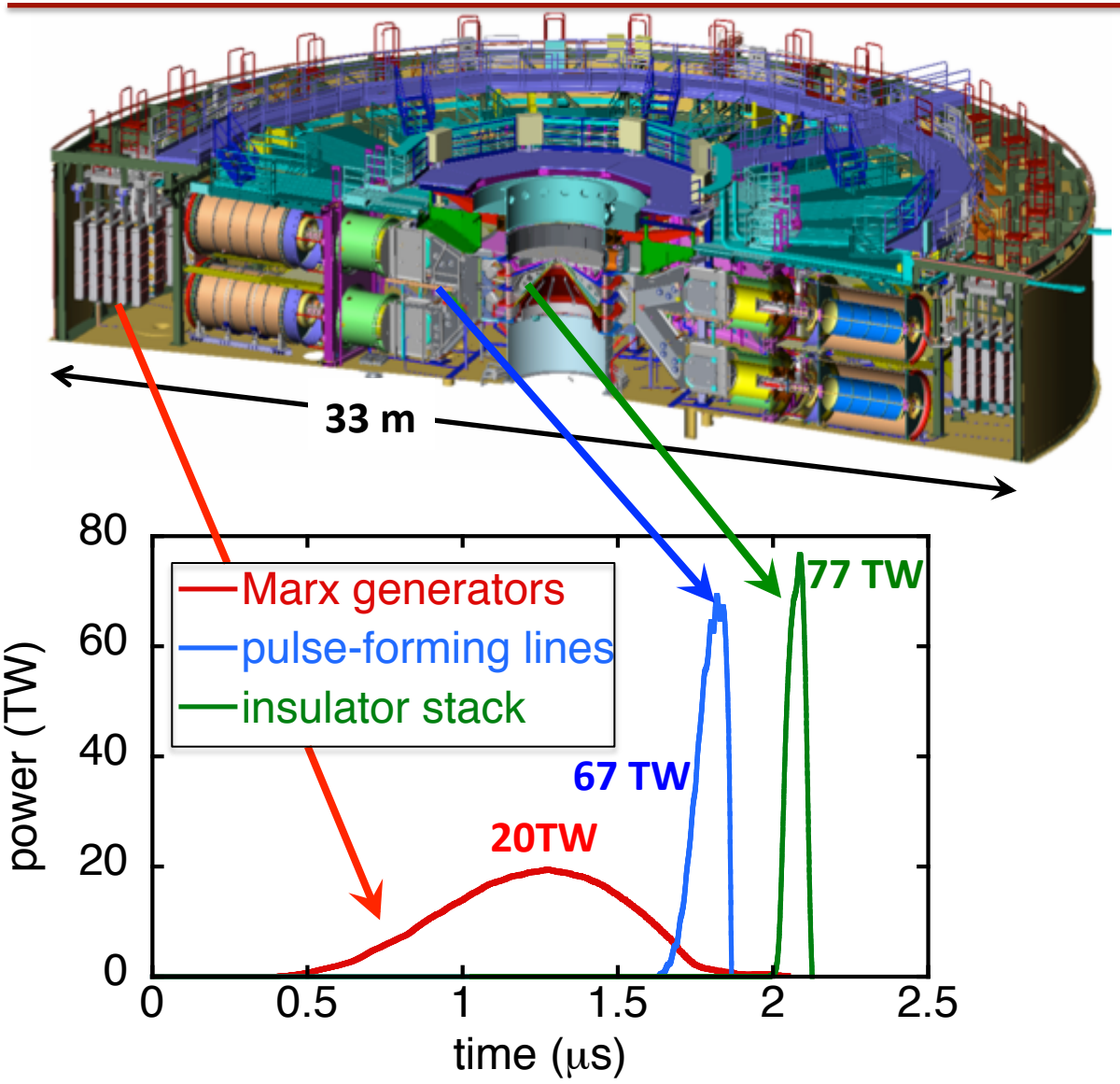

Z today couples ~0.5 MJ out of 20 MJ stored to magnetized liner inertial fusion (MagLIF) target (0.1 MJ in DD fuel).

Pulsed-power drive is energy efficient

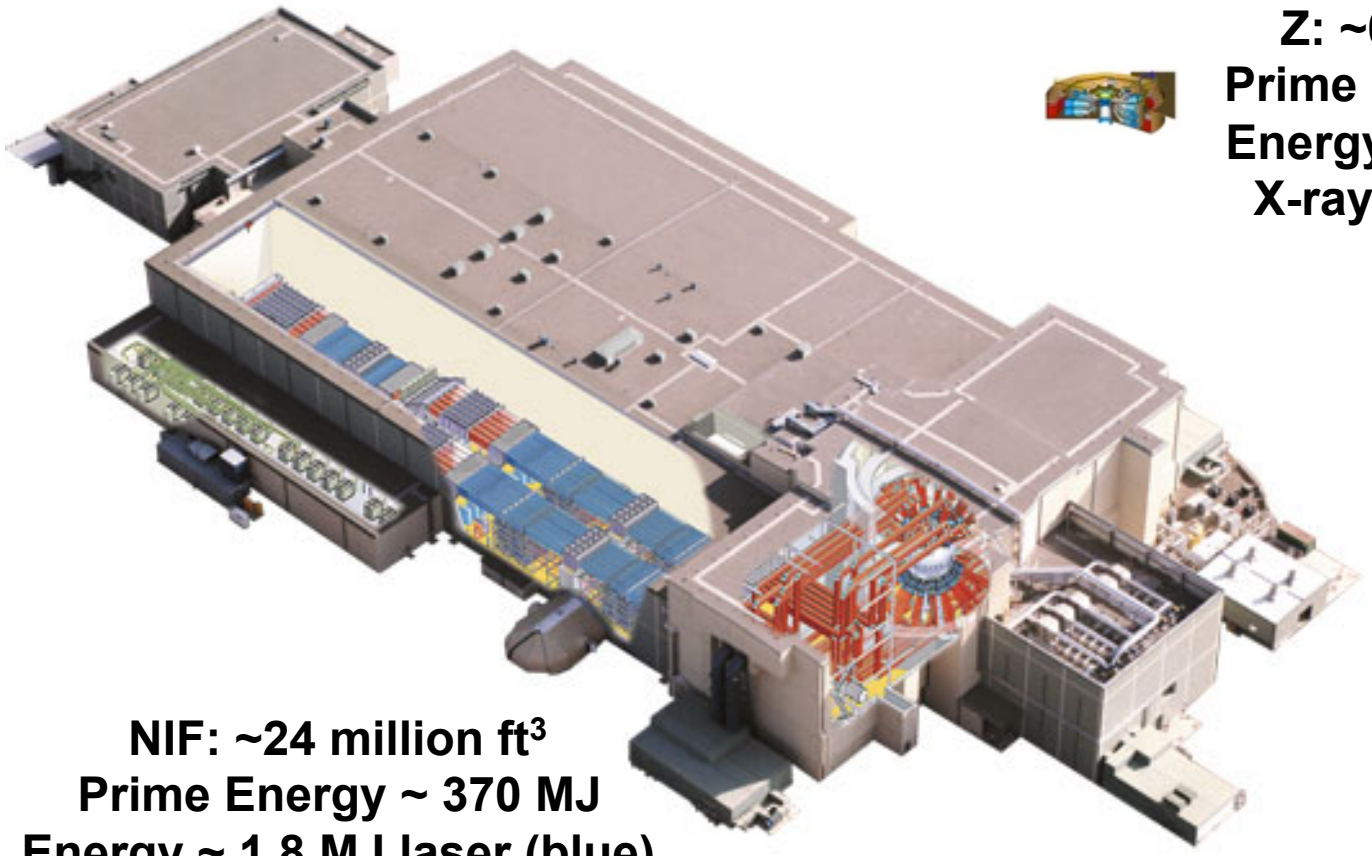

Z: ~0.2 million ft^3
Prime Energy ~ 22 MJ
Energy to load ~3 MJ
X-ray energy ~3 MJ

NIF: ~24 million ft^3
Prime Energy ~ 370 MJ
Energy ~ 1.8 MJ laser (blue)
X-ray Energy ~1 MJ

We use magnetic fields on Z in several ways to create High Energy Density matter for stockpile stewardship applications

Dynamic Material Properties

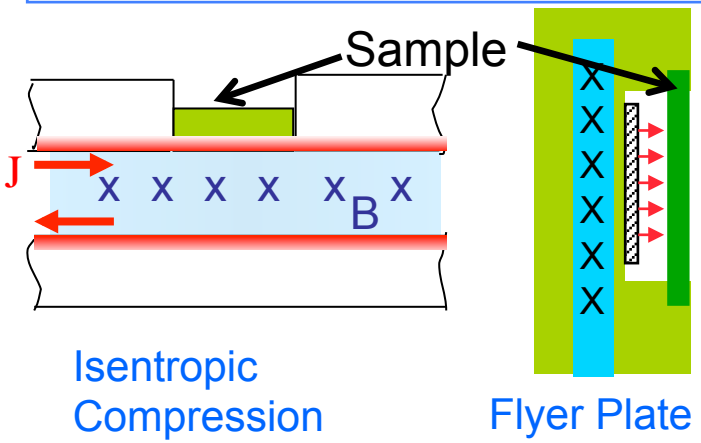

CY13 Z shot distribution

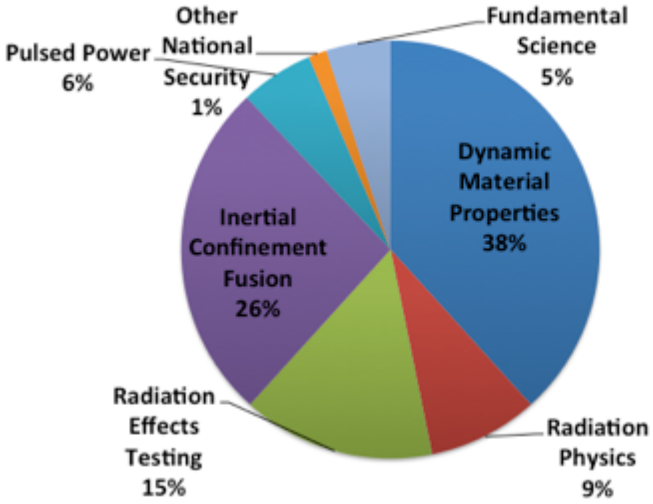

Z-Pinch X-ray Sources (RES, Rad. Physics)

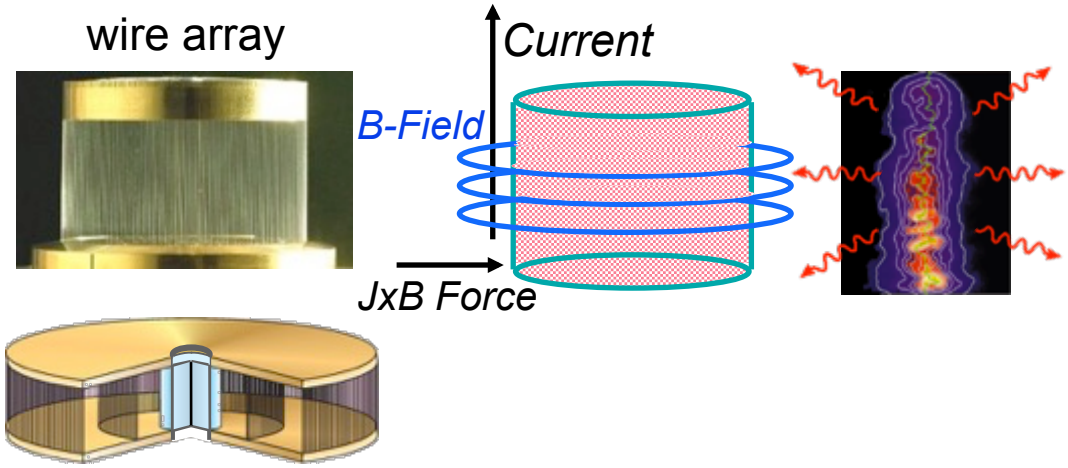

Inertial Confinement Fusion

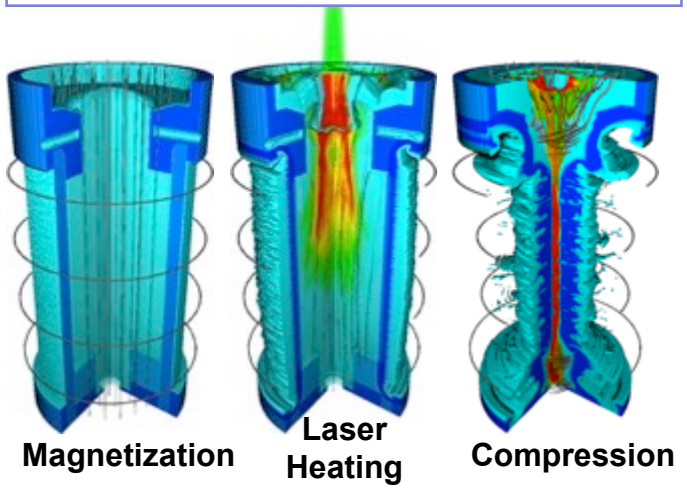

In MDI, the driver and target are strongly coupled

Adding 2.5mm of liner height (0.8nH) decreases peak current ~1MA

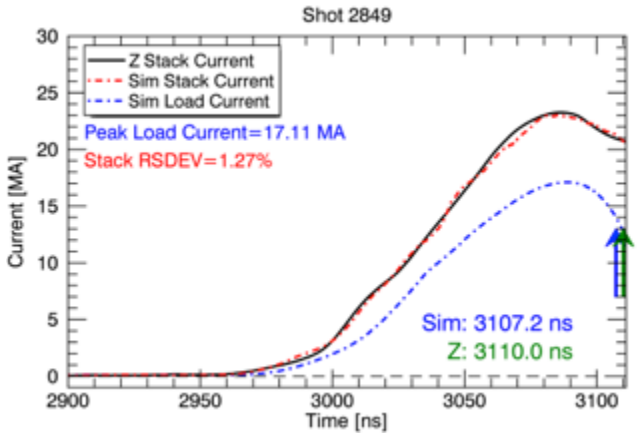

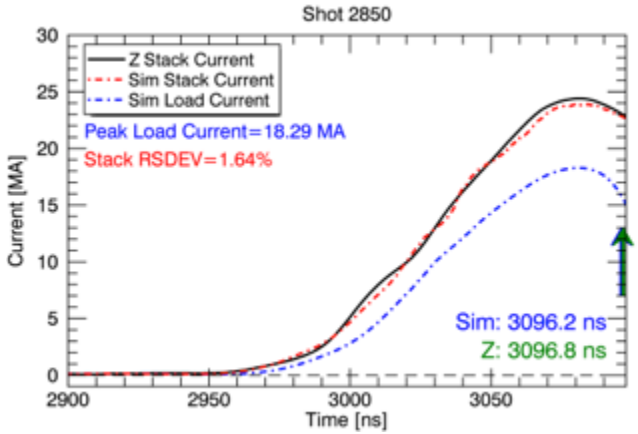

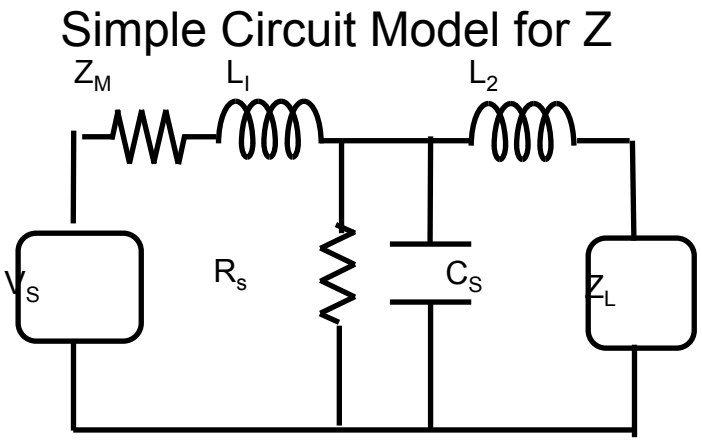

- Target inductance must be minimized
  - maximizes current delivery
  - minimizes power flow losses
- Current delivery sensitive to both initial inductance and dL/dt

Magnetic drive pressures on Z can be comparable to the drive pressure in radiation driven capsules

Sandia National Laboratories

Magnetically-Driven Cylinder

$$P = \frac{B^2}{2\mu_o} = 141\left(\frac{I_{MA}/30}{R_{mm}}\right)^2 \text{ MBar}$$

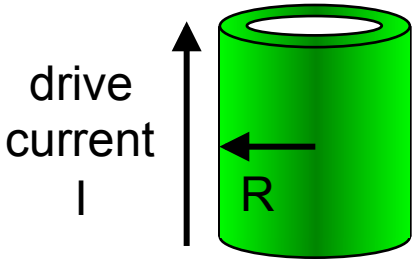

140 MBar at 30 MA and 1 mm

Radiation-Driven Sphere

$$P = \frac{(2/5)(1-\alpha)\sigma T^4}{C_s} = 3T^{3.5} \text{ MBar}$$

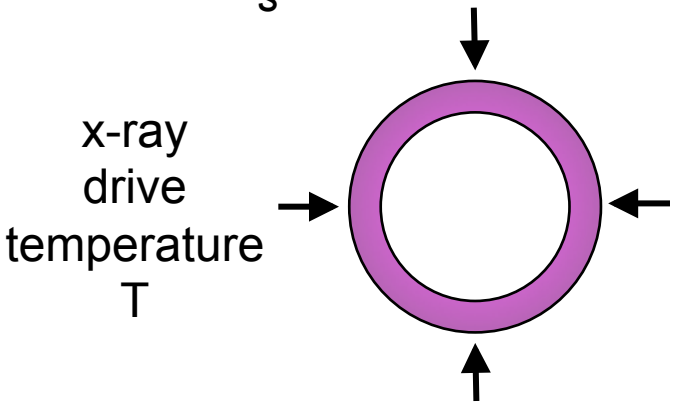

140 MBar at 300 eV

Magnetic implosions can efficiently perform work on the fuel while reaching very high pressures, if the current can reach small radius

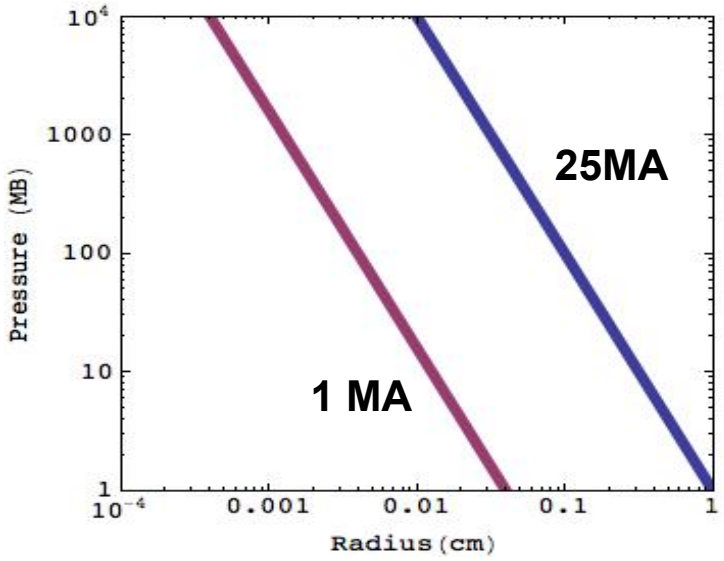

What limits current delivery to small radius?

- Ideal driver limits (dL/dt >0 eventually causes dI/dt<0)
- Power flow losses
- Asymmetric current delivery (displacement of magnetic center from geometric center)
- 3D current redistribution
- Current shunting in target

$$B_\theta(G) \sim \frac{I(\mathrm{A})}{5R(\mathrm{cm})} \qquad P \sim \frac{B^2}{8\pi} \sim \frac{I^2}{R^2}$$

A current carrying cylinder is driven more strongly the farther it converges

A magnetic implosion continues to extract energy as it implodes:

$$E_{kin} \sim I^2 \log\left(\frac{R_0}{R_f}\right)$$

Though there are differences in the details of each of the three main approaches that offer different risks and benefits, all ICF implosions go through similar stages

Cylindrical magnetically driven implosions

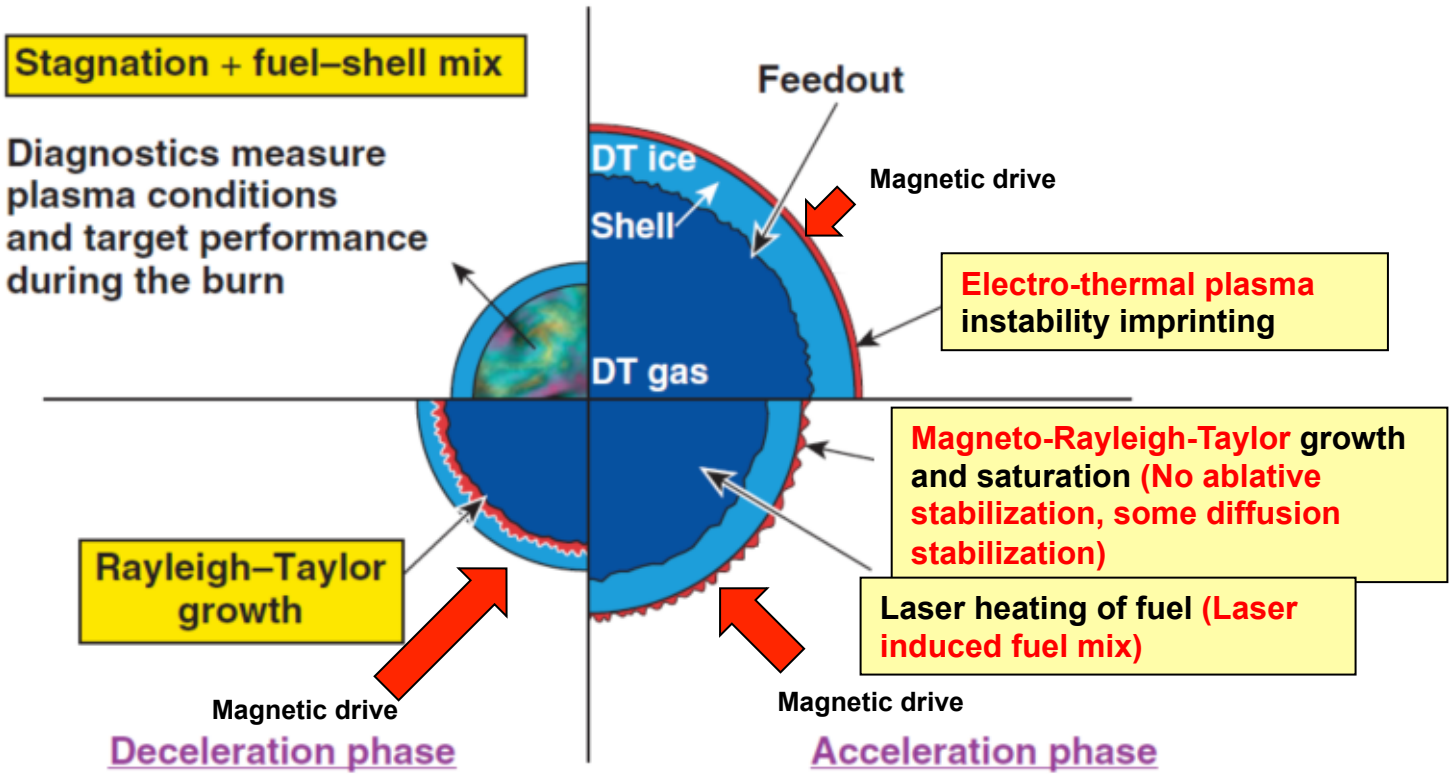

In both the acceleration and deceleration phases, light fluid is supporting a heavy fluid against "gravity"— the classical Rayleigh–Taylor instability.

We have spent many years testing our liner implosion modeling, and have made some interesting advances

Sandia National Laboratories

Single-mode magneto-Rayleigh-Taylor growth

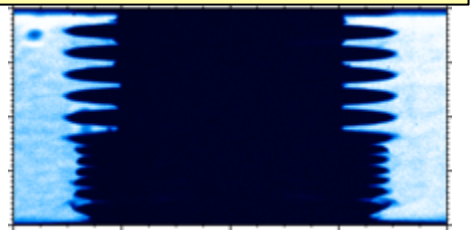

Magnetized MRT growth

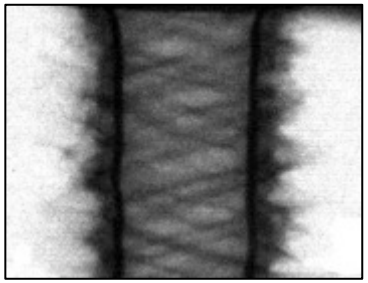

Experimental Data

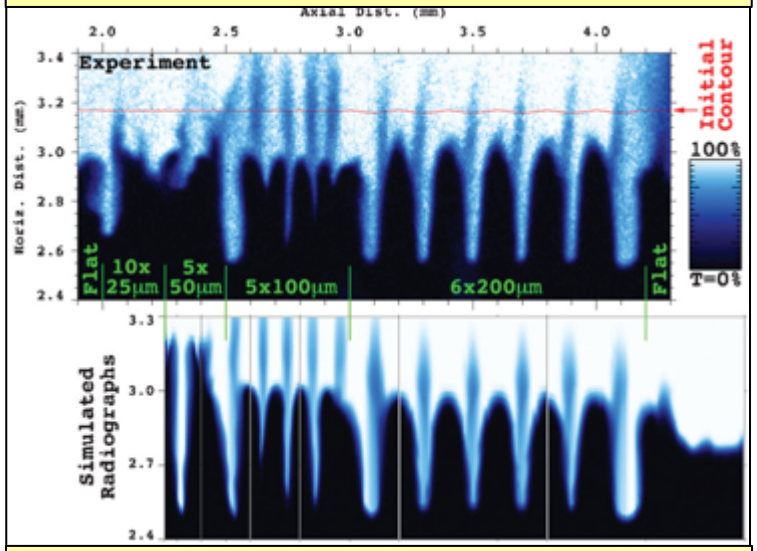

Simulated Data

Dielectric-coated Al liner implosion

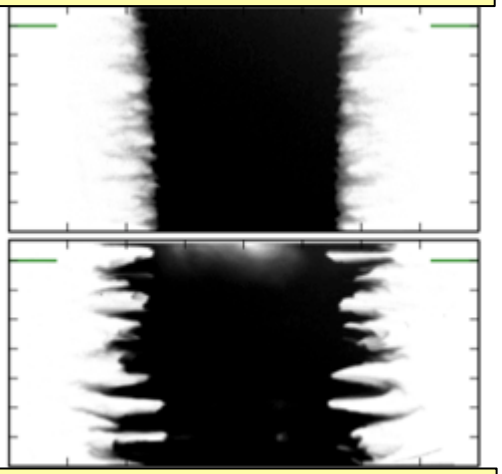

Uncoated

Magnetized & dielectric-coated Be (R_0/R_f~17)

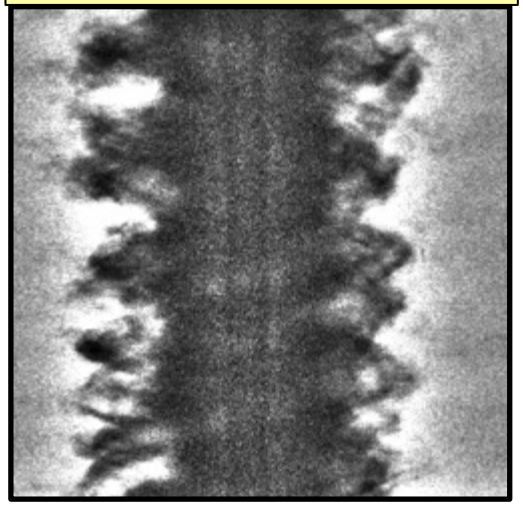

High-resolution 2D modeling can capture early growth down to the ~50-micron scale

D.B. Sinars *et al.*, Phys. Rev. Lett. (2010).
R.D. McBride *et al.*, Phys. Rev. Lett. (2012).
T.J. Awe *et al.*, Phys. Rev. Lett. (2013).
K.J. Peterson *et al.*, Phys. Rev. Lett. (2014).
T.J. Awe *et al.*, submitted (2015).

Z has the flexibility to drive loads with specific pulse shapes

- Isentropic drive pulses are routinely incorporated in dynamic material experiments
- Timing of magnetic diffusion wave must be considered
  - Material generally melts at diffusion front
- Constrained by max dI/dt and timescale of pulsed power
- **Not currently employed for MagLIF**

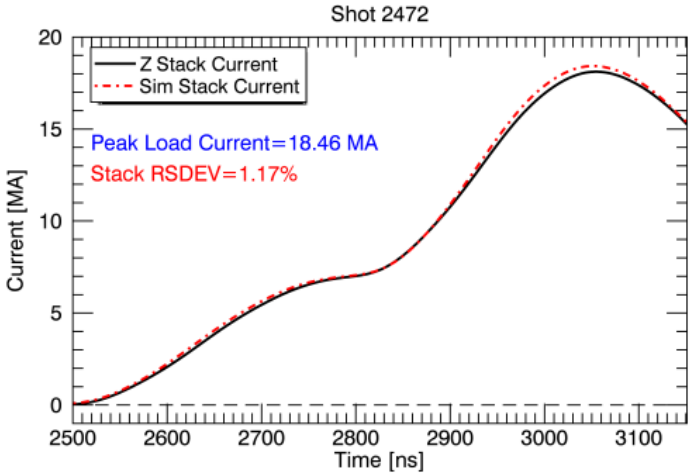

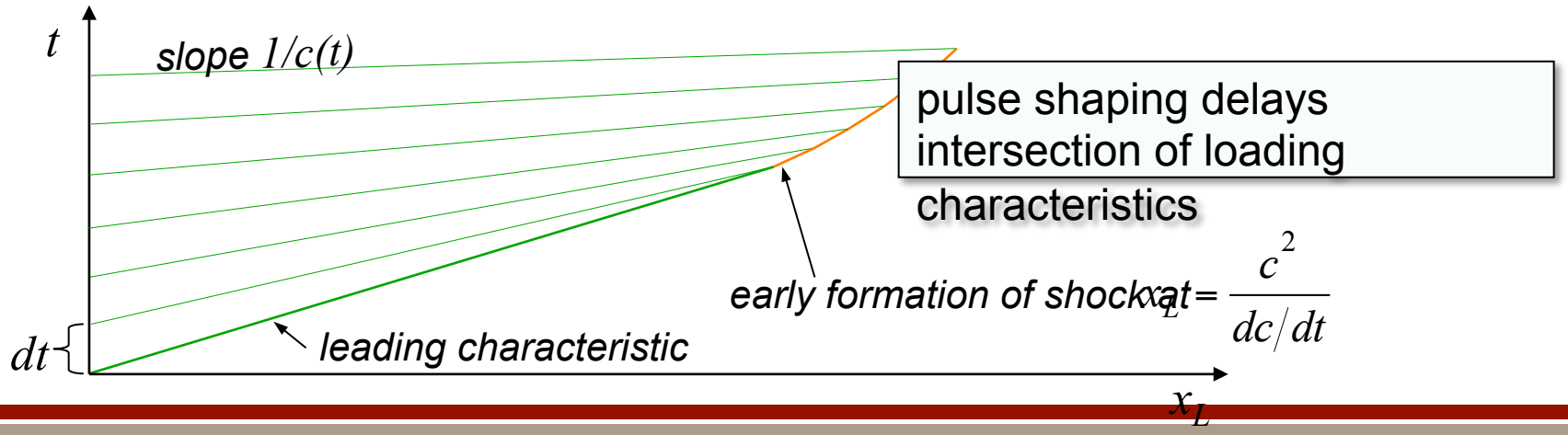

Sandia National Laboratories

MAGNETIZED INERTIAL FUSION

The presence of a magnetic field can strongly affect transport properties, e.g. electron heat conduction

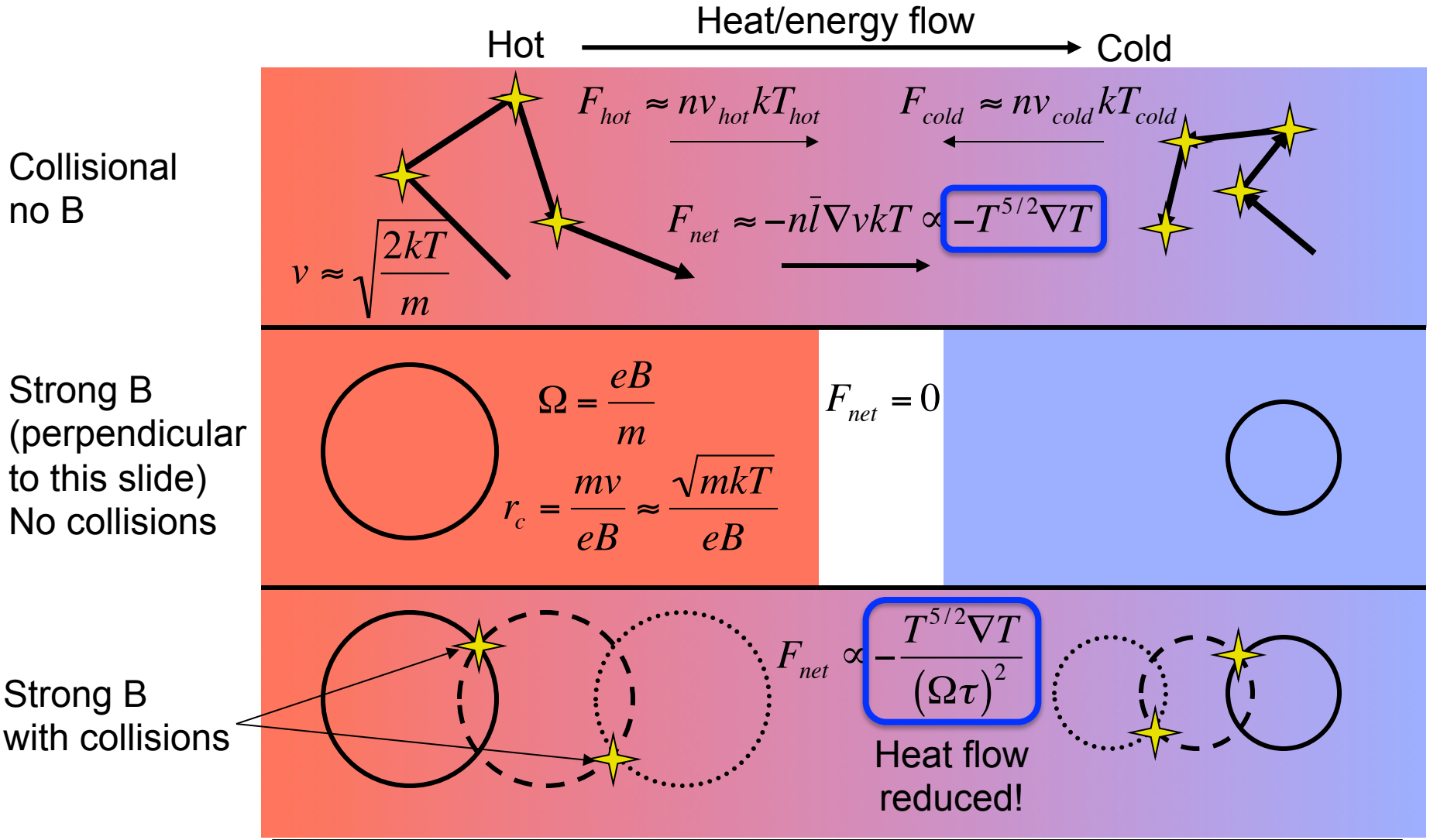

"Anomalous" heat transport can reduce the benefit of magnetic fields (e.g., in tokamaks) but there remains a significant benefit

Recent laser-driven spherical capsule implosions* showed higher temperatures (and yields) due to fuel magnetization

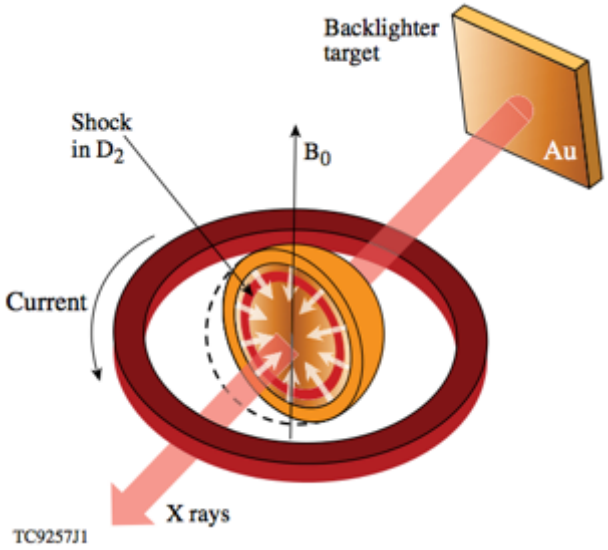

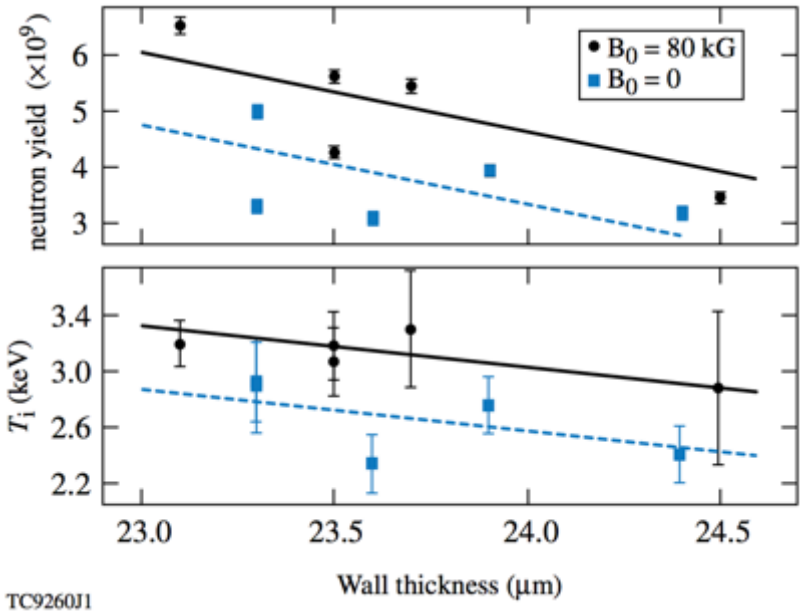

- Simple axial field used in a spherical implosion geometry
- Field suppressed electron heat conduction losses along one direction
- The resulting 15% increase in temperature and 30% increase in yield is consistent with estimates for transverse heat loss suppression
- This is an example of success with a target that produced fusion yield without magnetization—can we produce yield in targets that would not produce significant yield otherwise?

* P.Y. Chang *et al.*, Phys. Rev. Lett. 107, 035006 (2011).

Heating the fuel prior to compression can lower traditional ICF requirements on velocity and fuel convergence

Sandia National Laboratories

Simulation with:
- Constant velocity
- No radiation loss
- No conductivity loss

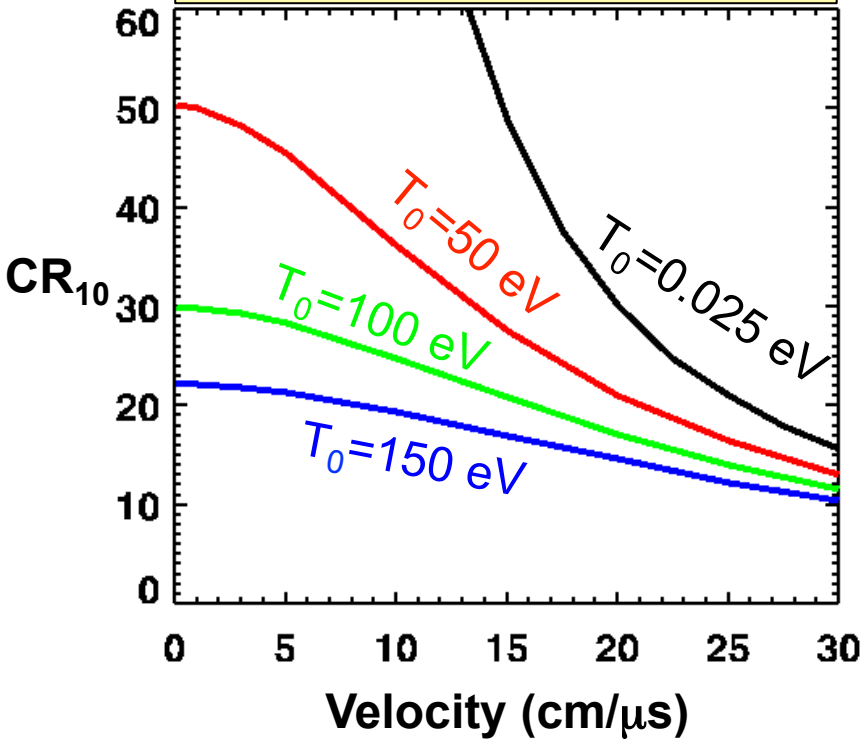

CR_{10} = Fuel Convergence Ratio (R_0/R_f) needed to obtain 10 keV

- **Laser heating of fuel (6-10 kJ) offers one way to reach pre-compression temperature of ~200 eV**
- **Detailed simulations suggest we can reach fusion temperatures at convergence R_0/R_f ~ 25**

If losses can be controlled, fuel preheat is advantageous.

Magnetization (*BR*) can be used to reduce ρR requirements and reduce electron heat losses, lower density also reduces bremsstrahlung radiation losses

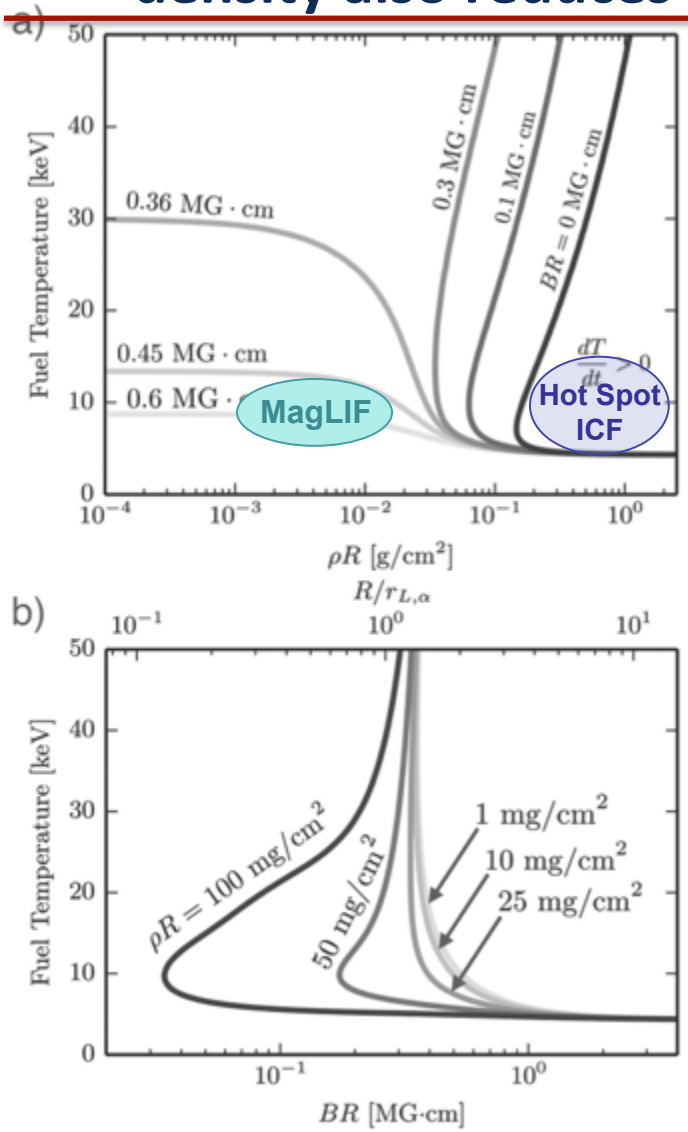

- **Initial 10-30 T field greatly amplified during the implosion through flux compression**
- **Too much field is inefficient—want to stagnate on plasma pressure, not magnetic pressure**

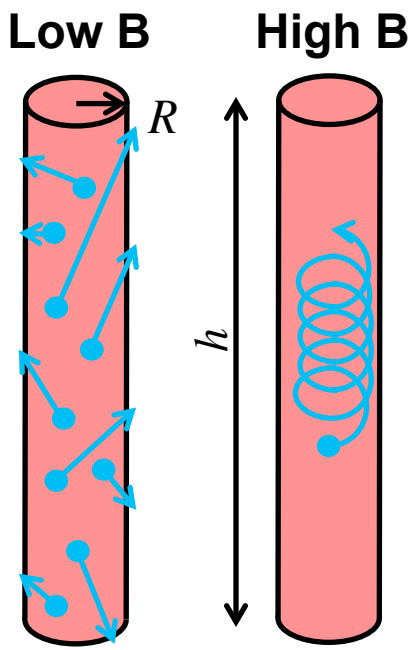

$$\frac{R}{r_\alpha} \approx 4BR\ [MG \cdot \mathrm{cm}]$$

- **Fraction of trapped tritons (or α's) a function of *BR***
- **Effects saturate at *BR* > 0.6 MG-cm**
- **Measurements to date suggest *BR* of 0.4 MG-cm**

Basko *et al*. Nuclear Fusion 40, 59 (2000); P.F. Knapp *et al.*, Phys. Plasmas (2015).

The Magnetized Liner Inertial Fusion (MagLIF) target design for Z leverages expertise from traditional ICF

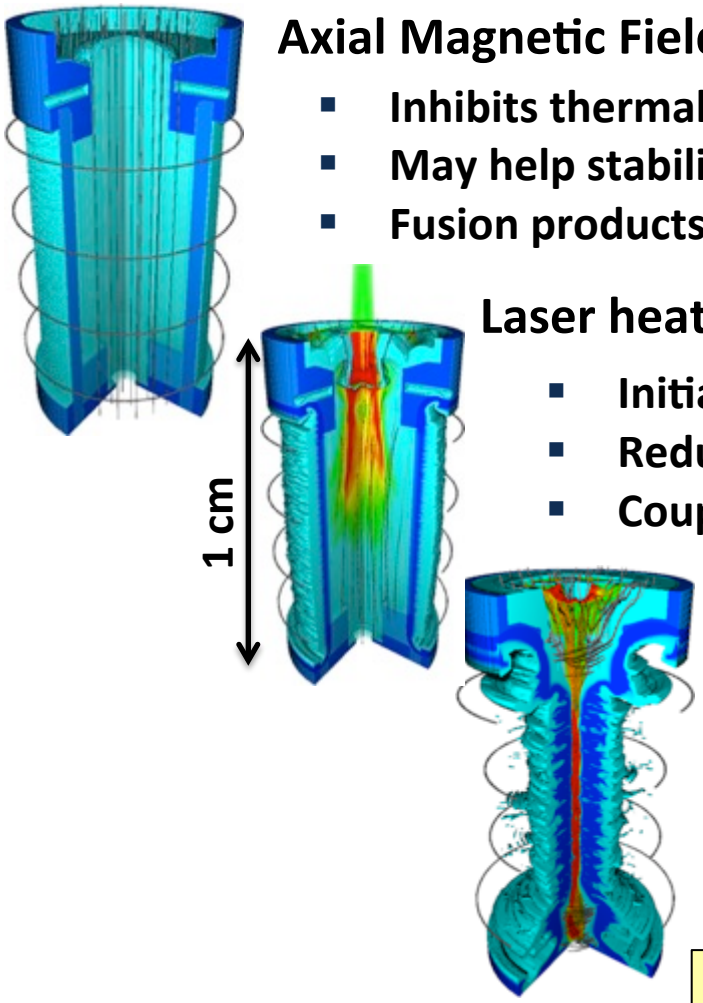

Axial Magnetic Field (10 T initially; 30 T available)

- Inhibits thermal losses from fuel to liner
- May help stabilize liner during compression
- Fusion products magnetized

Laser heated fuel (2 kJ initially; 6-10 kJ planned)

- Initial average fuel temperature 150-200 eV
- Reduces compression requirements (R_0/R_f ~ 25)
- Coupling of laser to plasma in an important science issue

Magnetic compression of fuel (~100 kJ into fuel)

- ~70-100 km/s, quasi-adiabatic fuel compression
- Low Aspect liners ($R/\Delta R$~6) are robust to hydrodynamic (MRT) instabilities
- Significantly lower pressure/density than ICF

Goal is to demonstrate scaling: $Y\,(B_{z0}, E_{laser}, I)$
DD equivalent of 100 kJ DT yield possible on Z

S.A. Slutz *et al.*, Phys Plasmas (2010); S.A. Slutz & R.A. Vesey, Phys Rev Lett (2012); A.B. Sefkow *et al.*, Phys Plasmas (2014).

Anatomy of a MagLIF Experiment

- **Field Coils**: Helmholtz-like coil pair produce a 10-30 T axial field w/ ~3 ms rise time. Current designs of 30T eliminate all diagnostic access
- **ZBL**: 1-4 kJ green laser, 1-4 ns square pulse w/ adjustable prepulse (prepulse used to help disassemble laser entrance window)
  - No phase plates were used in the initial experiments!

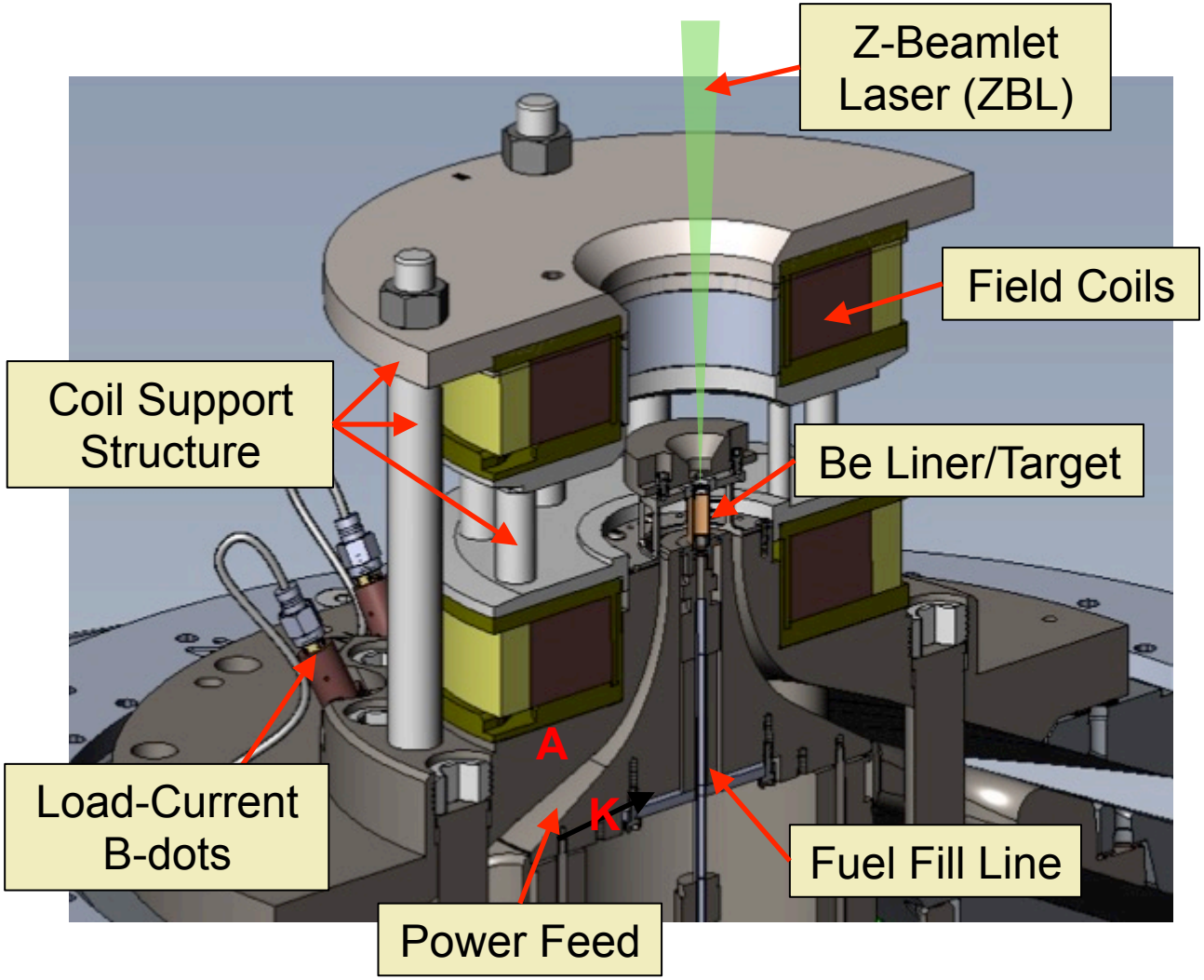

Anatomy of a MagLIF Target

- **Be Liner**: OD = 5.63 mm, ID = 4.65 mm, h = 5–10 mm
- **LEH Window**: 1-3 μm thick plastic window. Supports 60 PSI pure D2 gas fill.
- **Washer**: Metal (Al) washer supporting LEH window
- **Channel**: Al structure used to mitigate the wall instability (also referred to as a "cushion"). Also reduces LEH window diameter to allow thinner windows
- **Return Can:** Slotted for diagnostic access

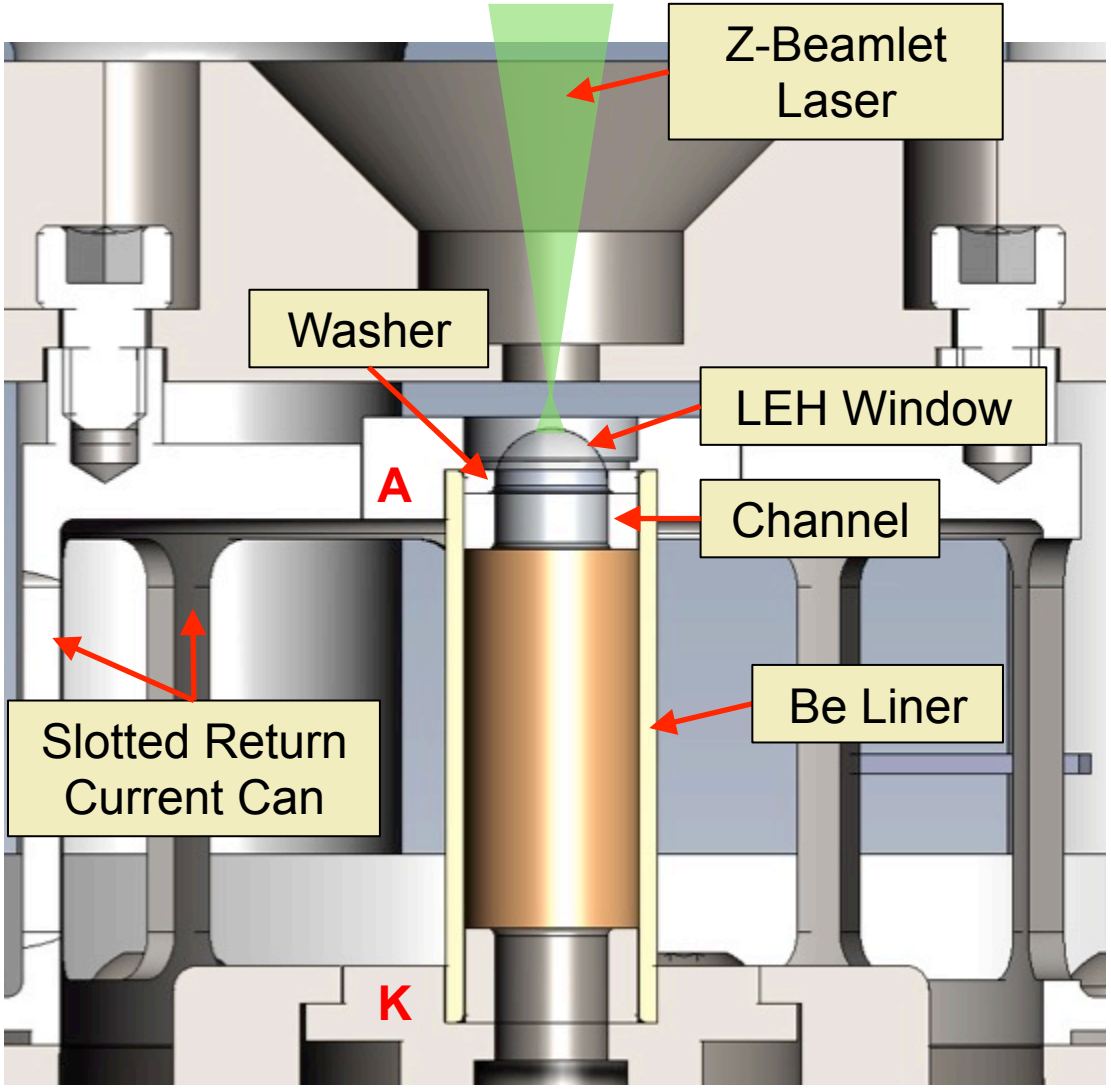

An example fully integrated 2D HYDRA calculation illustrates the stages of a MagLIF implosion

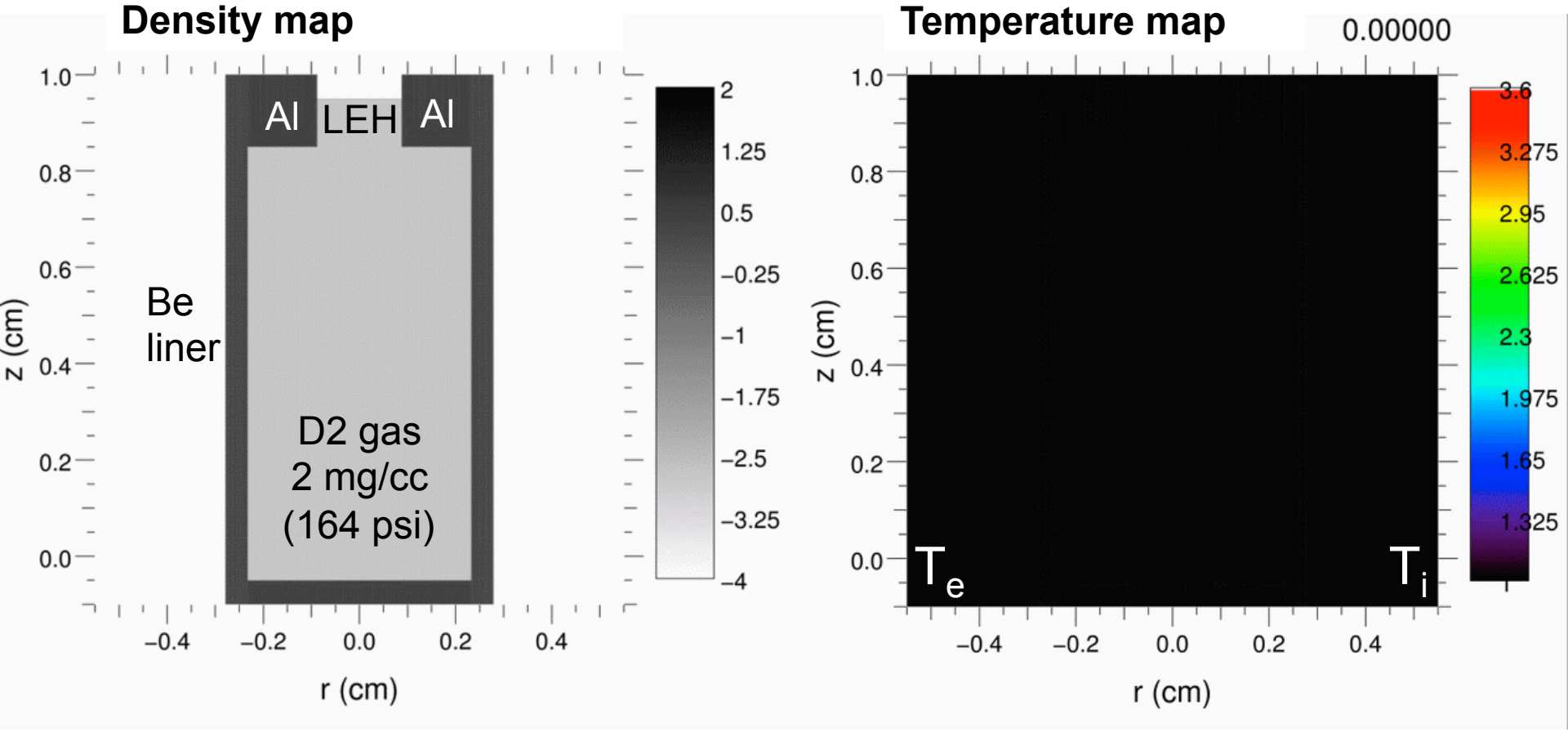

Example calculations by A.B. Sefkow: DD fuel, I=18 MA, B_Z=10 T, E_{LASER}=2.6 kJ

The fusion fuel is preheated using the Z-Beamlet laser after the liner begins to implode

Sandia National Laboratories

Density map

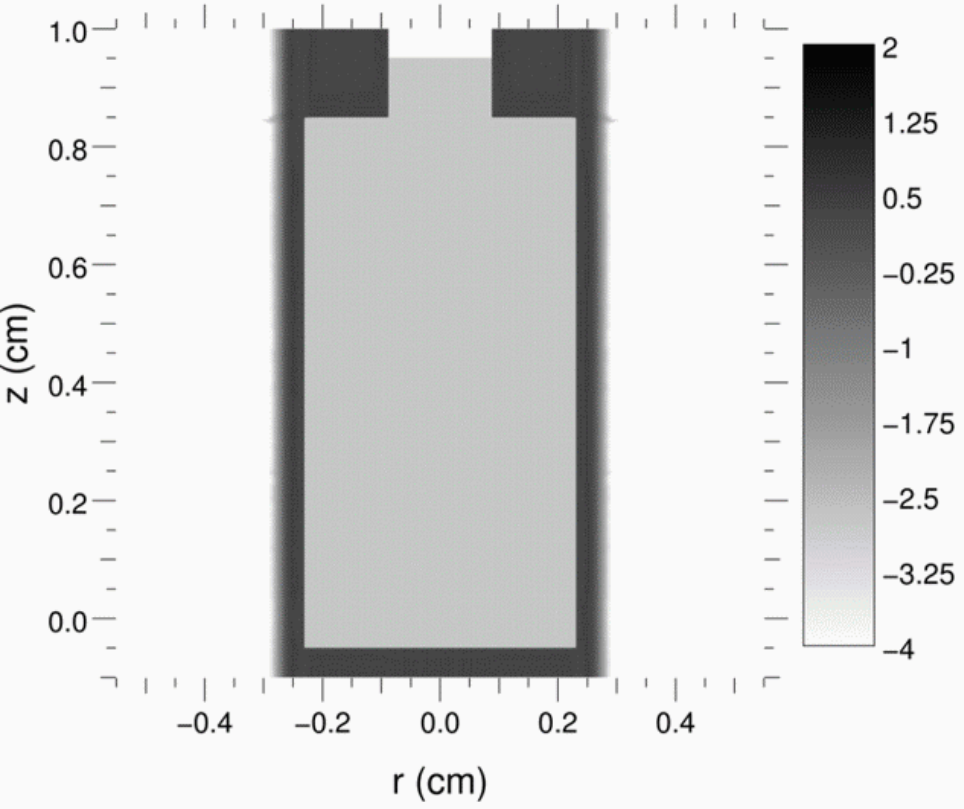

Temperature map

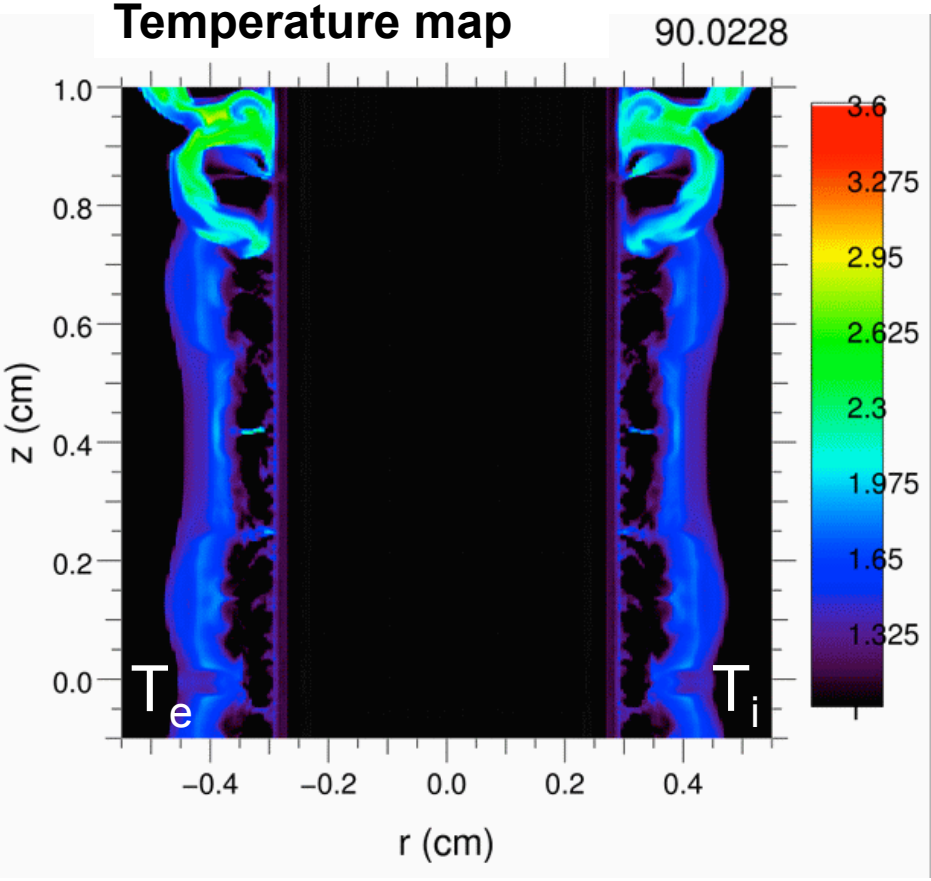

Example calculations by A.B. Sefkow: DD fuel, I=18 MA, B_Z=10 T, E_{LASER}=2.6 kJ

The fusion fuel is preheated using the Z-Beamlet laser after the liner begins to implode

Sandia National Laboratories

Density map

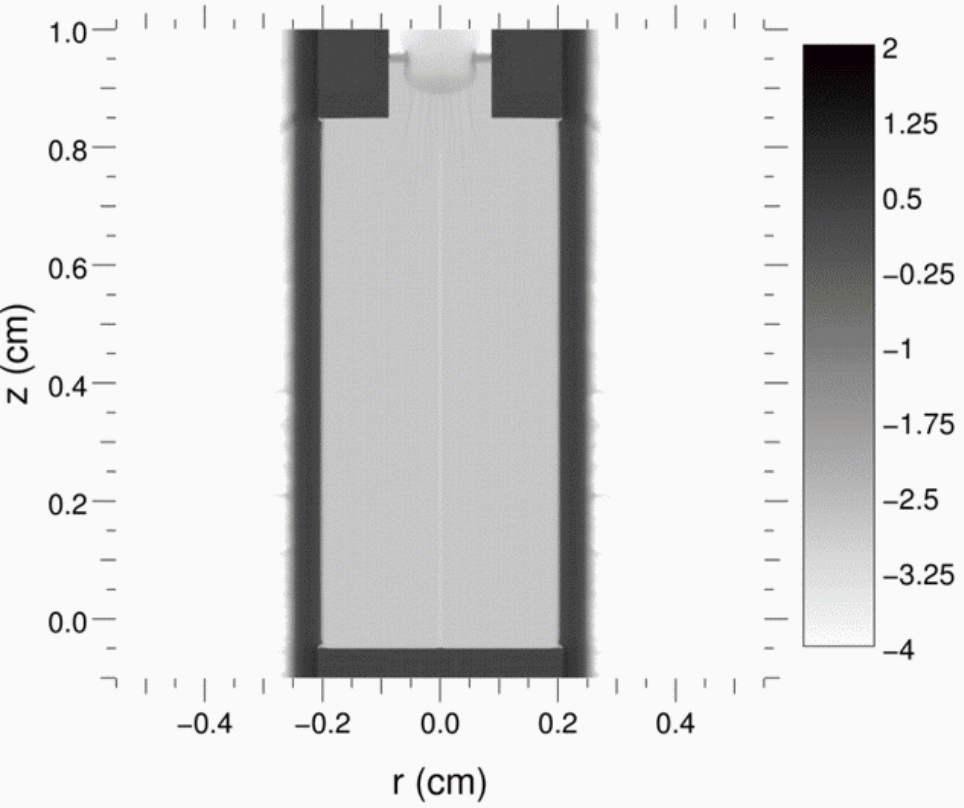

Temperature map

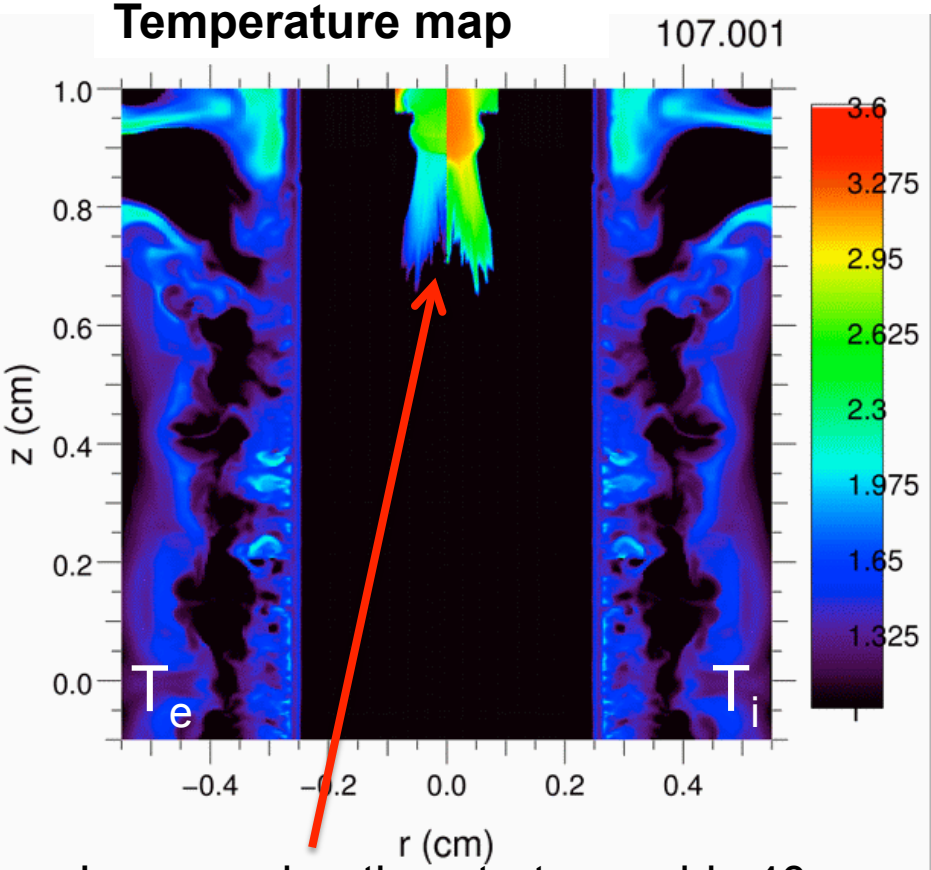

Laser preheating starts roughly 40 ns before the liner reaches the axis

Example calculations by A.B. Sefkow: DD fuel, I=18 MA, B_Z=10 T, E_{LASER}=2.6 kJ

The fusion fuel is preheated using the Z-Beamlet laser after the liner begins to implode

Sandia National Laboratories

Density map

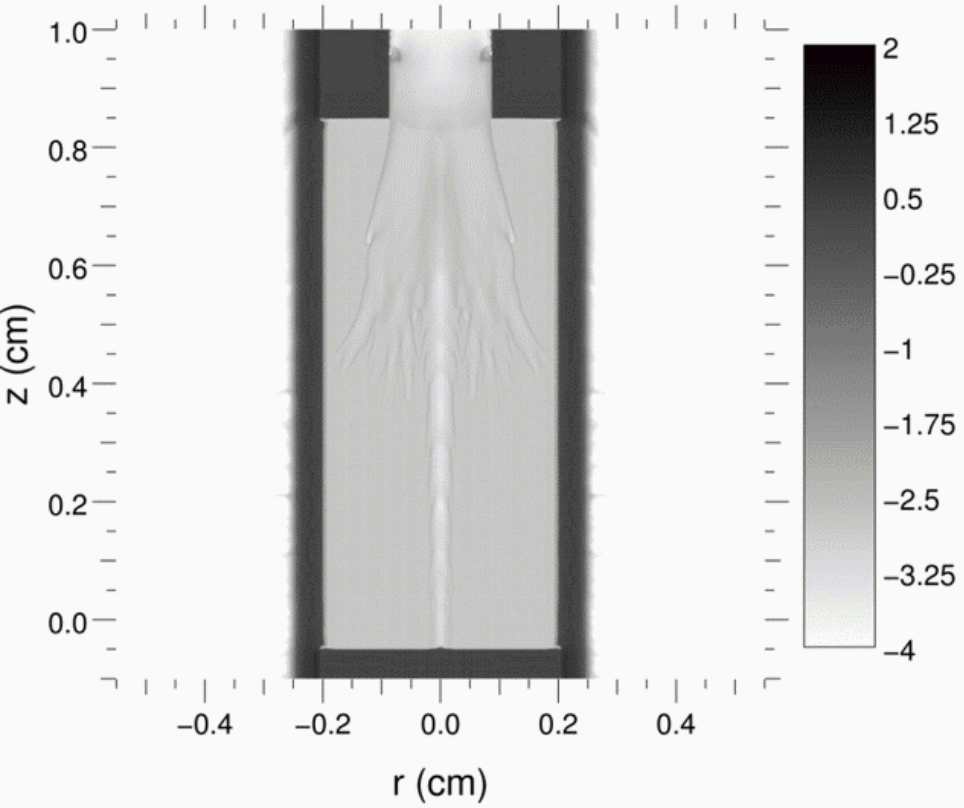

Temperature map

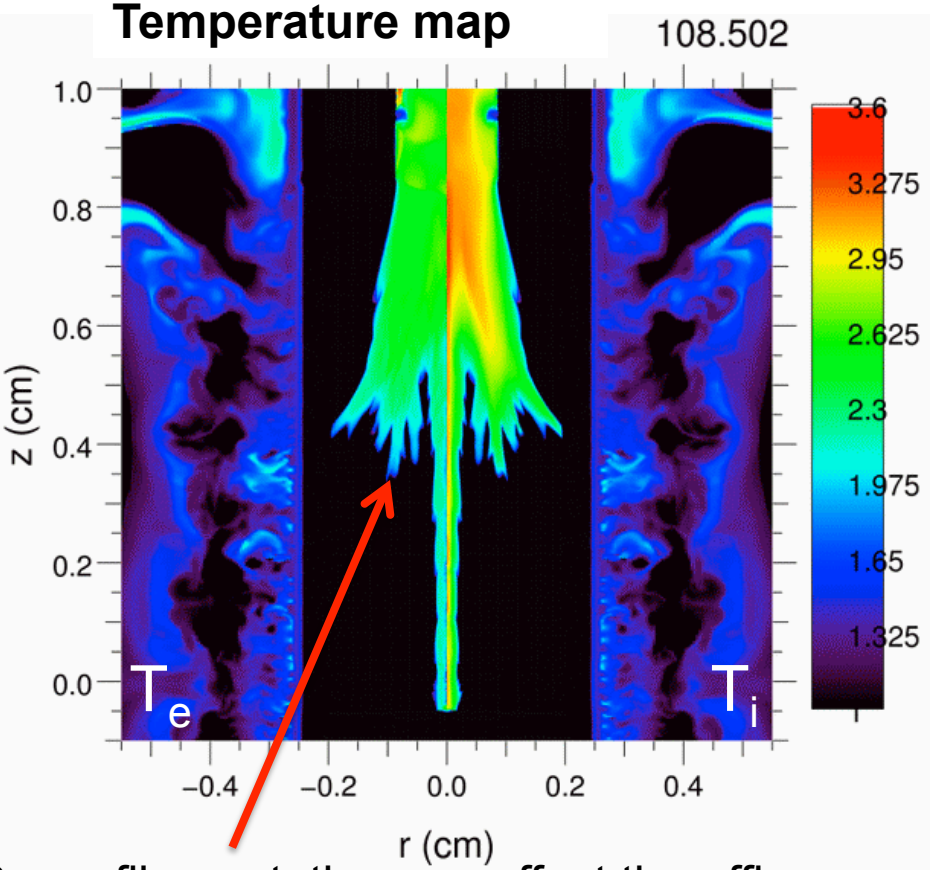

Beam filamentation can affect the efficacy and depth of laser coupling to the fuel

Example calculations by A.B. Sefkow: DD fuel, I=18 MA, B_Z=10 T, E_{LASER}=2.6 kJ

The preheated fuel is then compressed by the imploding liner, reducing the convergence required to reach fusion temperatures

Sandia National Laboratories

Density map

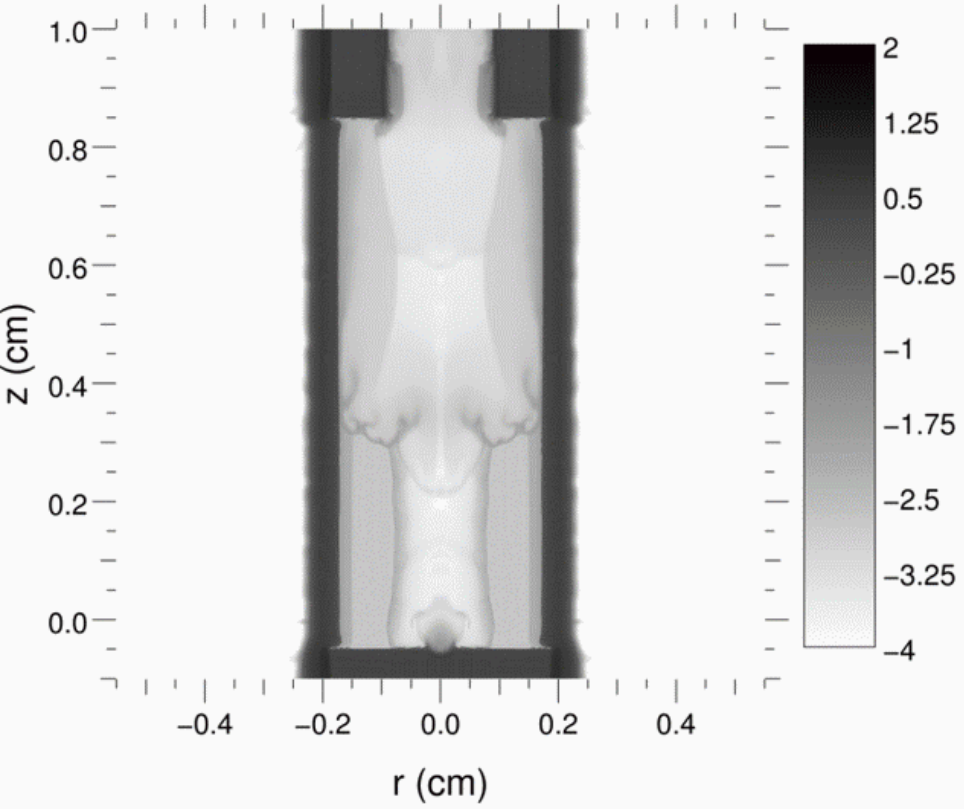

Temperature map

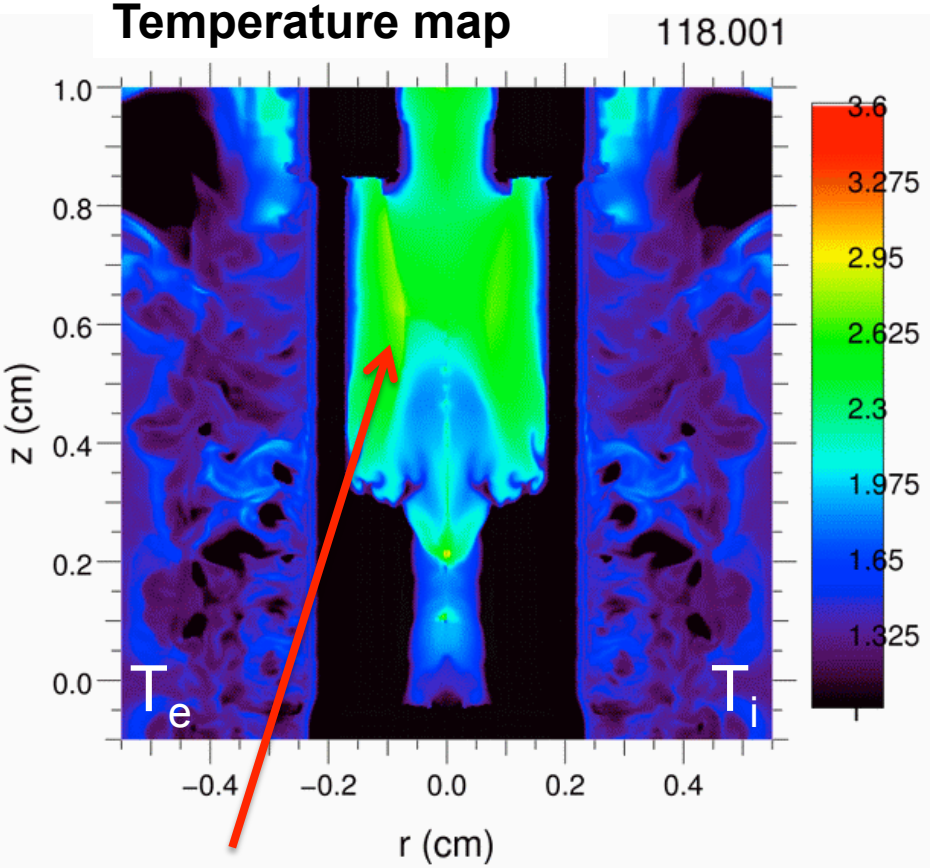

Initially high peak temperatures (~1 keV) relax to ~300 eV as the energy diffuses into the fuel

Example calculations by A.B. Sefkow: DD fuel, I=18 MA, B_Z=10 T, E_{LASER}=2.6 kJ

The preheated fuel is then compressed by the imploding liner, reducing the convergence required to reach fusion temperatures

Sandia National Laboratories

Density map

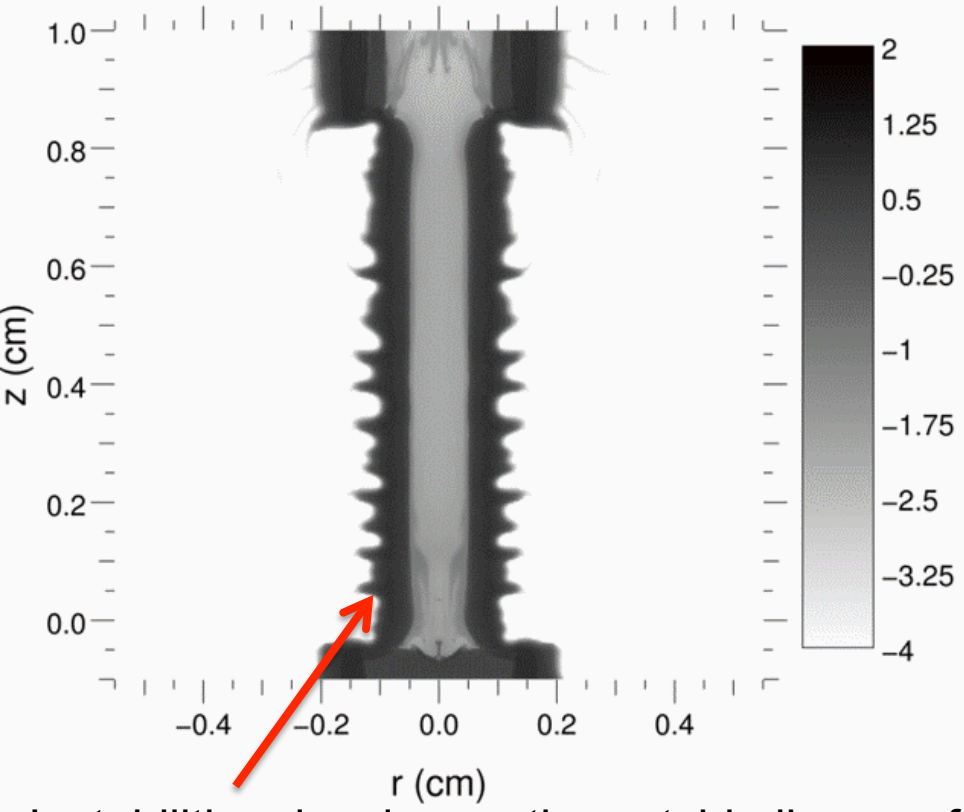

Temperature map

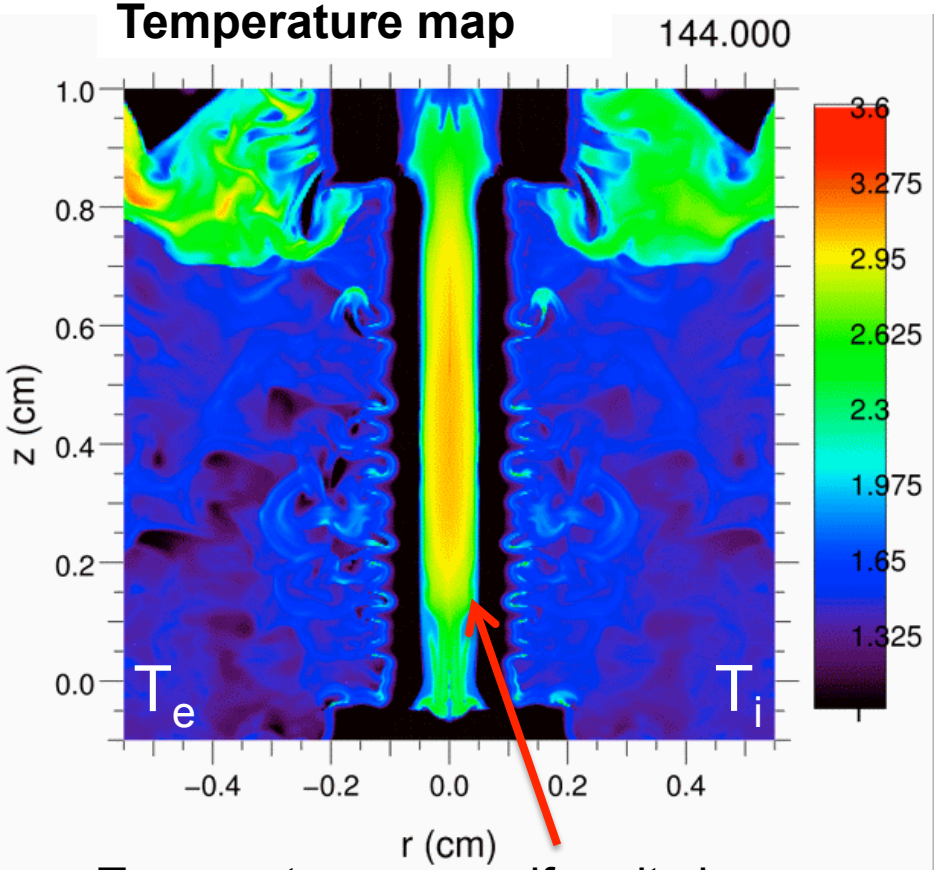

Instabilities develop on the outside liner surface, but impact on fuel mitigated by use of thick liner

Temperature non-uniformity is smoothed out during compression

Example calculations by A.B. Sefkow: DD fuel, I=18 MA, B_Z=10 T, E_{LASER}=2.6 kJ

The preheated fuel is then compressed by the imploding liner, reducing the convergence required to reach fusion temperatures

Sandia National Laboratories

Density map

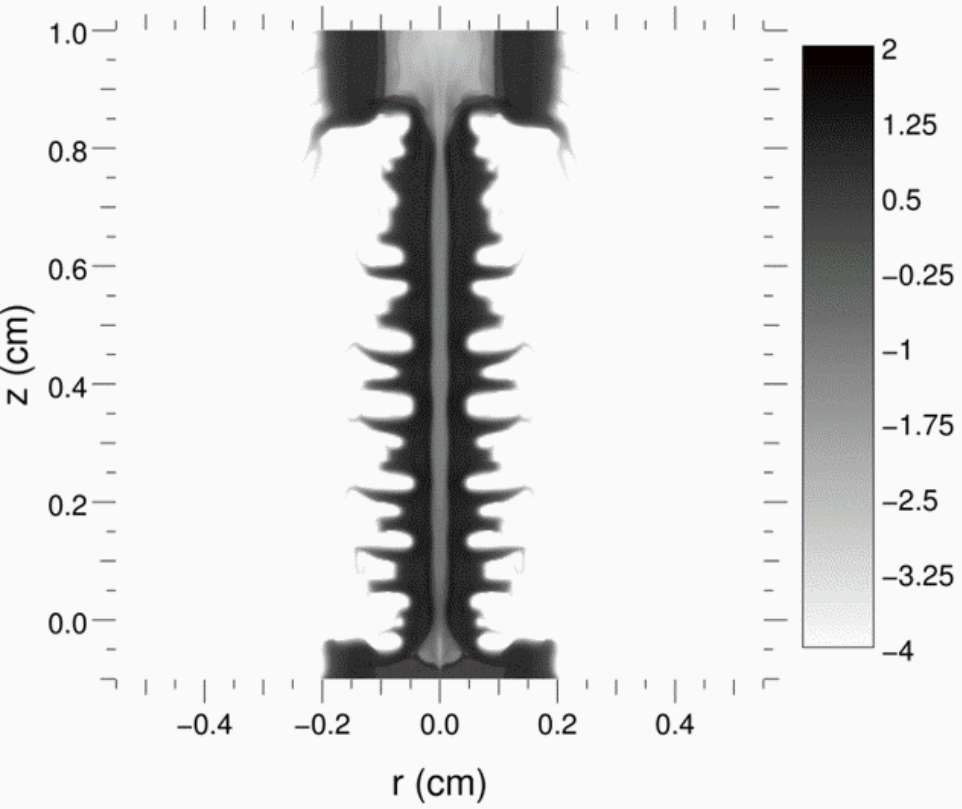

Temperature map

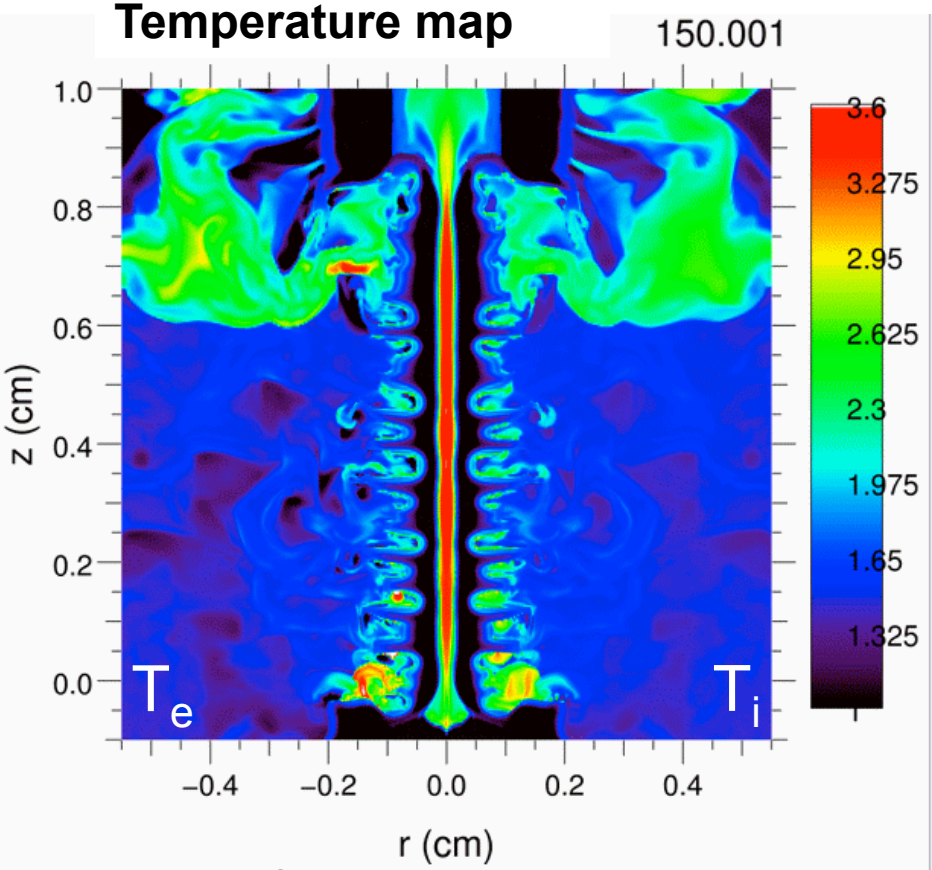

The axial magnetic field is compressed by the liner (some loss due to Nernst) and suppresses heat loss to the relatively cold liner

The preheated fuel is then compressed by the imploding liner, reducing the convergence required to reach fusion temperatures

Sandia National Laboratories

Density map

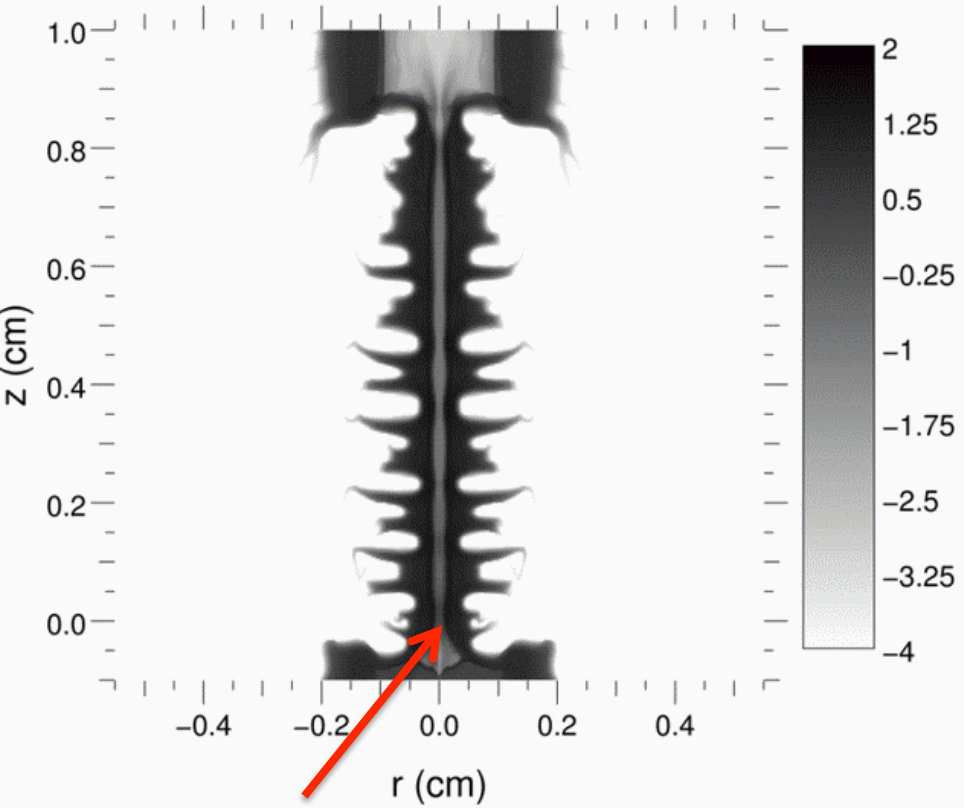

Final fuel density ~1 g/cc
Inertial confinement provided by liner

Temperature map

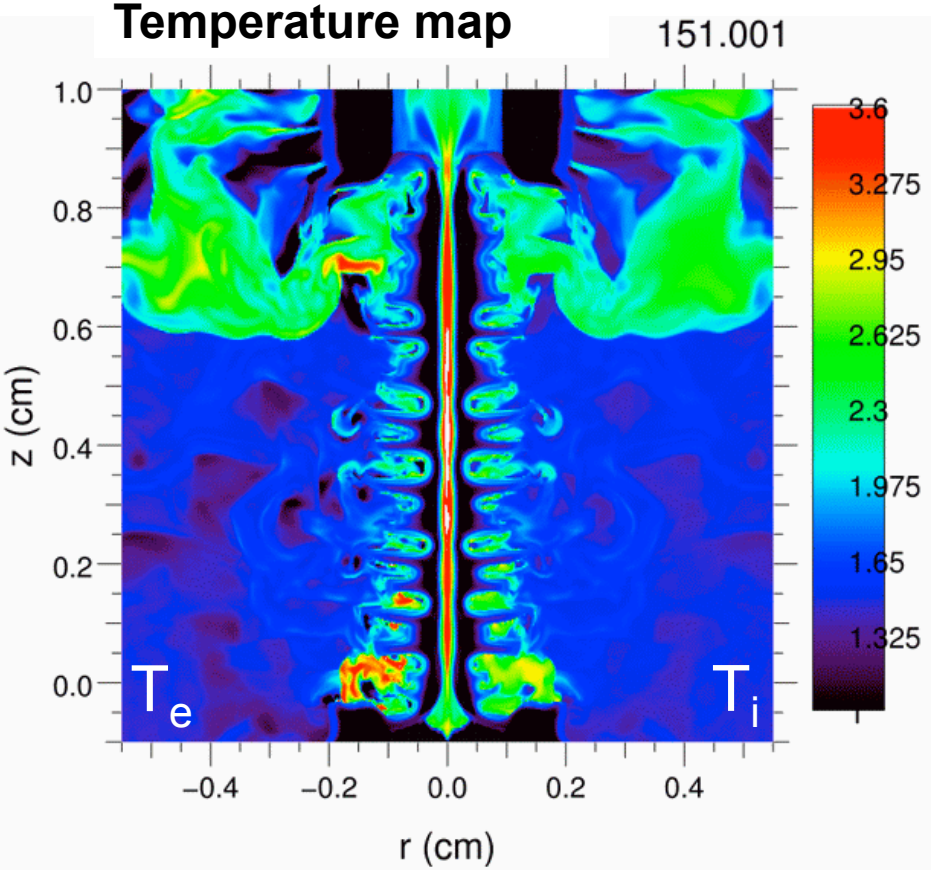

Final temperature ~8 keV
Peak Bfield >13000 T, Radial CR~23

Example calculations by A.B. Sefkow: DD fuel, I=18 MA, B_Z=10 T, E_{LASER}=2.6 kJ

The initial experiments used 10 T, 2.5 kJ laser energy, and a ~19 MA current to drive a D_2 filled (0.7 mg/cm^3) Be liner

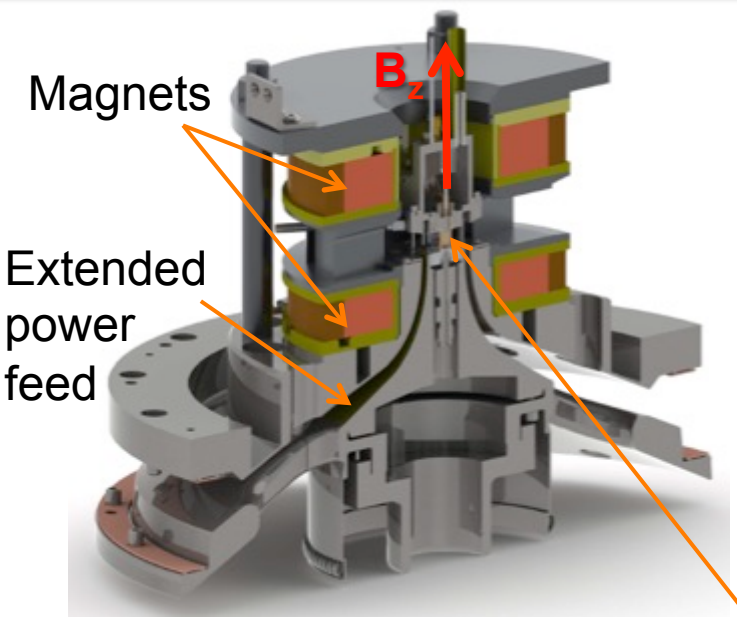

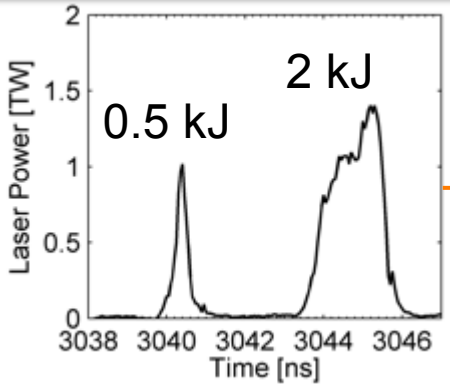

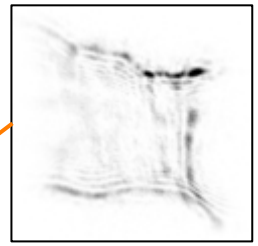

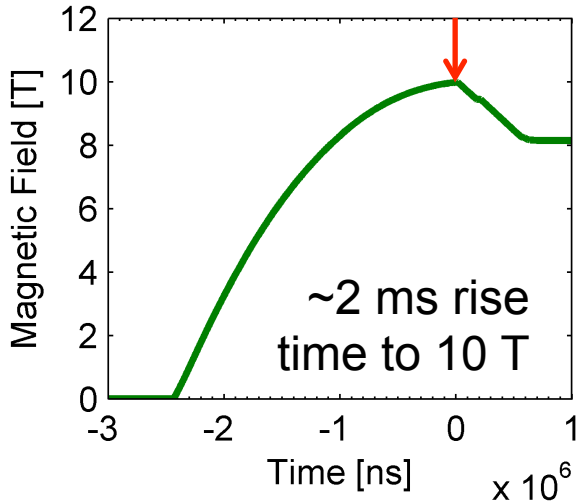

Target

We are taking a careful look at all stages of the target using multiple facilities and diagnostics

Sandia National Laboratories

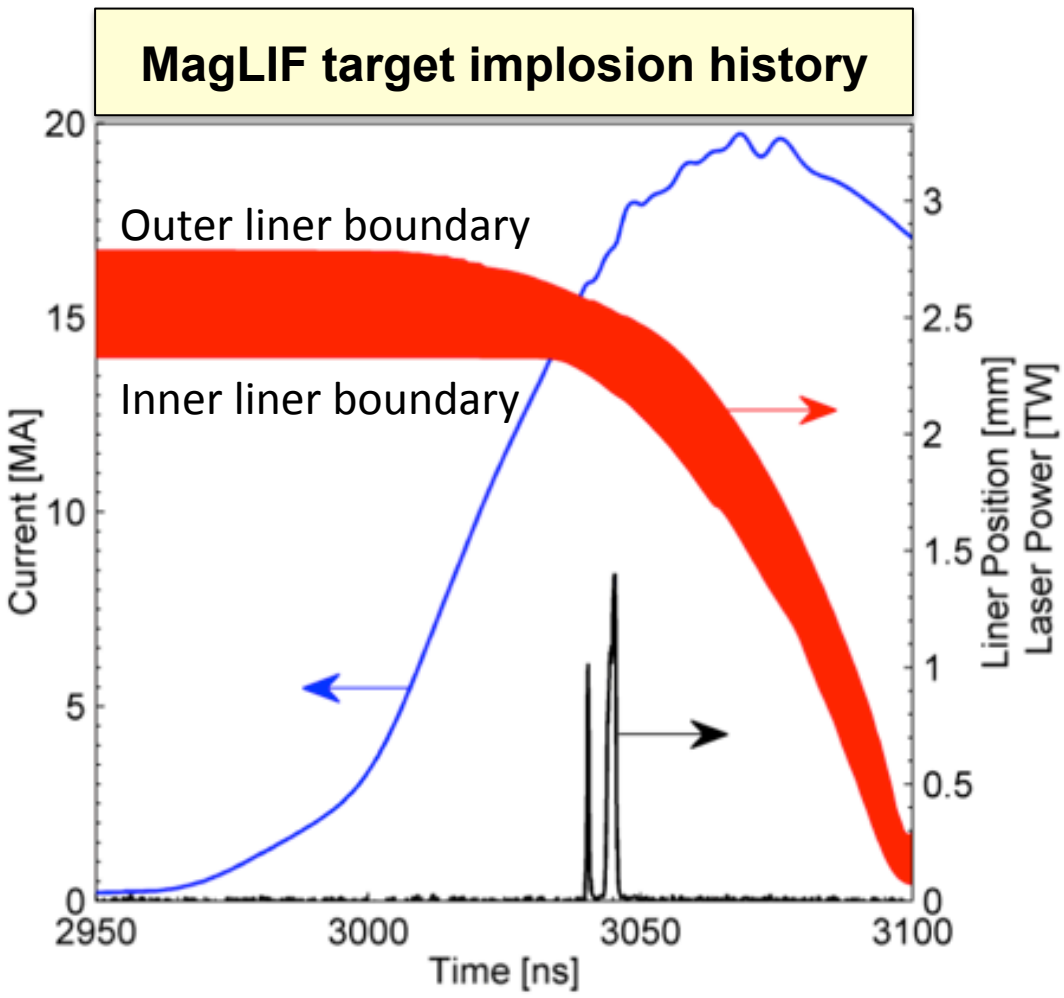

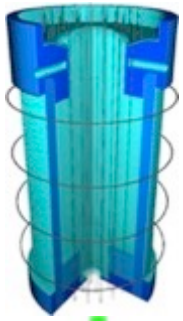

Initial Conditions
- Be liner
- ρ_{DT}~ 1-4 mg/cc
- B_{z0}~ 10-30 T (~0.1 MG)

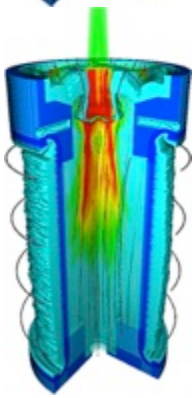

Laser Heating
- E_{laser} ~ 2-6 kJ @.53µm
- T_{DT} ~ 0.2 KeV
- ωτ ~ 2-5
- Research on Z, ZBL, Omega, Omega-EP

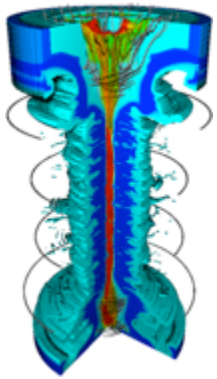

Implosion/stagnation
- V_{imp}~ 70-100 km/sec
- P_{DT} ~ 5 Gbar
- T_{ion} > 5 keV
- ωτ ~ 200 (B~100 MG)
- Research on Z, Omega

MagLIF has a very different compression methodology and stagnation parameters than traditional ICF

Metric	X-ray Drive on NIF	100 kJ MagLIF on Z
Characteristic Drive Pressure	~140-160 Mbar	26 MA at 1 mm is 100 Mbar
pdV work vs. Radius	Goes as R^2 (decreasing)	Goes as 1/R (increasing)
Peak velocity	350-380 km/s	70-100 km/s
Peak IFAR	13-15 (high foot) to 17-20	8.5
Hot spot R_0/R_f	35 (high foot) to 45	25
Volume Change	43000x (high) to 91000x	625x
Fuel (hot spot) ρR	>0.3 g/cm^2	~0.003 g/cm^2
Liner ρR	>0.7 g/cm^2 (main fuel)	>0.3 g/cm^2 (in Liner)
BR	n/a	>0.5 MG-cm
Burn time	0.15 to 0.2 ns	1 to 2 ns
T_ion	>4 keV	>4 keV
	Hot-spot ignition	Volumetric ignition

MagLIF could in principle provide high yield and gain[1] by burning an ice layer

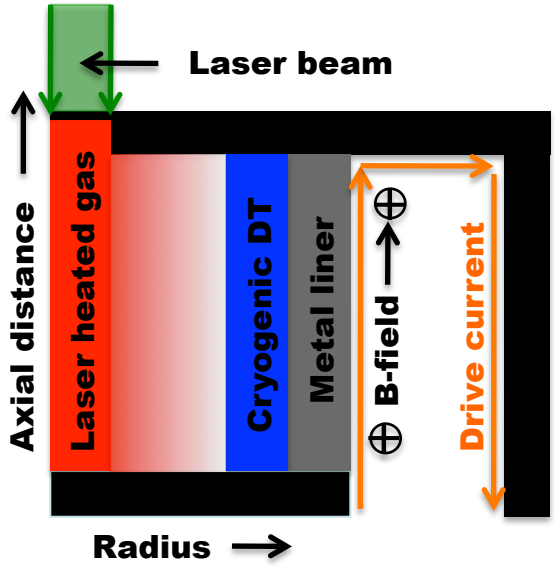

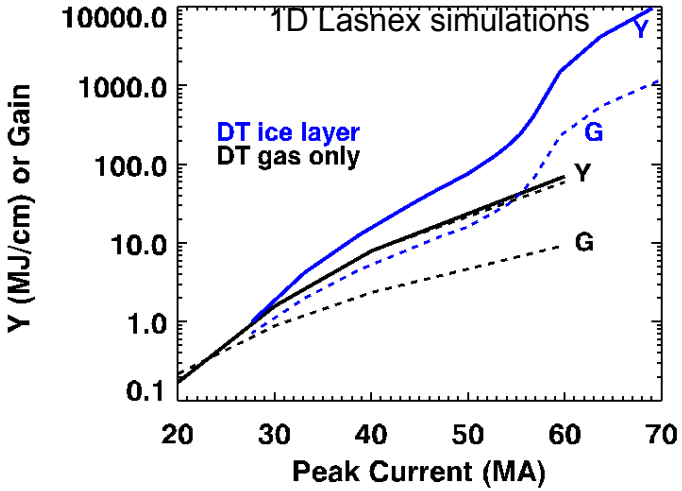

A 2D integrated Hydra simulation[2] produced ~ 6 GJ

L_{liner} = 10 mm, AR_{liner} = 6

ρ_{gas} = 5 mg cm^{-3}, B_z^0 = 8T

E_{laser} = 25 kJ, Peak drive current = 70 MA

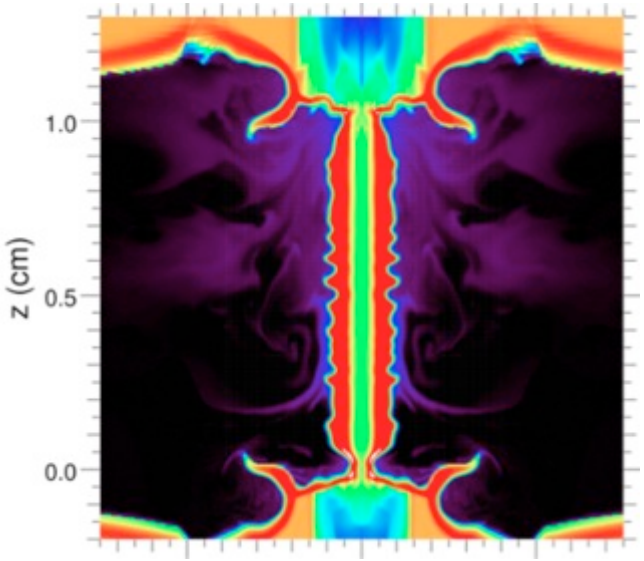

An intermediate regime exists wherein the B_z field is

- *strong enough* to reduce conduction losses, but
- *weak enough* not to inhibit the α deflagration wave

1 *Slutz and Vesey PRL 108, 025003 (2012)*

2 *Sefkow, Slutz, Koning et al. PoP 21, 072711 (2014*

We are currently debating three different plausible stagnation pictures

Sandia National Laboratories

- 1) Low coupling, low mix hypothesis
  - Very low (~10%) laser energy coupling
  - Little to no mix
  - Quasi-1D stagnation conditions
- 2) Moderate coupling, moderate laser induced mix
  - Reasonable (~50%) laser energy coupling
  - Moderate endcap/window/liner laser induced mix
  - Quasi-1D stagnation conditions when accounting for radiative loss
- 3) Moderate coupling, minimal laser induced mix
  - Reasonable (~50%) laser energy coupling
  - Minimal endcap/window/liner laser induced mix
  - 3D stagnation, inefficient thermalization

Stagnation picture could also depend on target parameters such as window thickness

Z data can be modeled by assuming lower than predicted coupling of laser energy and no mix and 200-300 J in fuel

Sandia National Laboratories

HYDRA Simulations

main pulse
2 ns, 2 kJ

main pulse
0.2 ns, 0.2 kJ

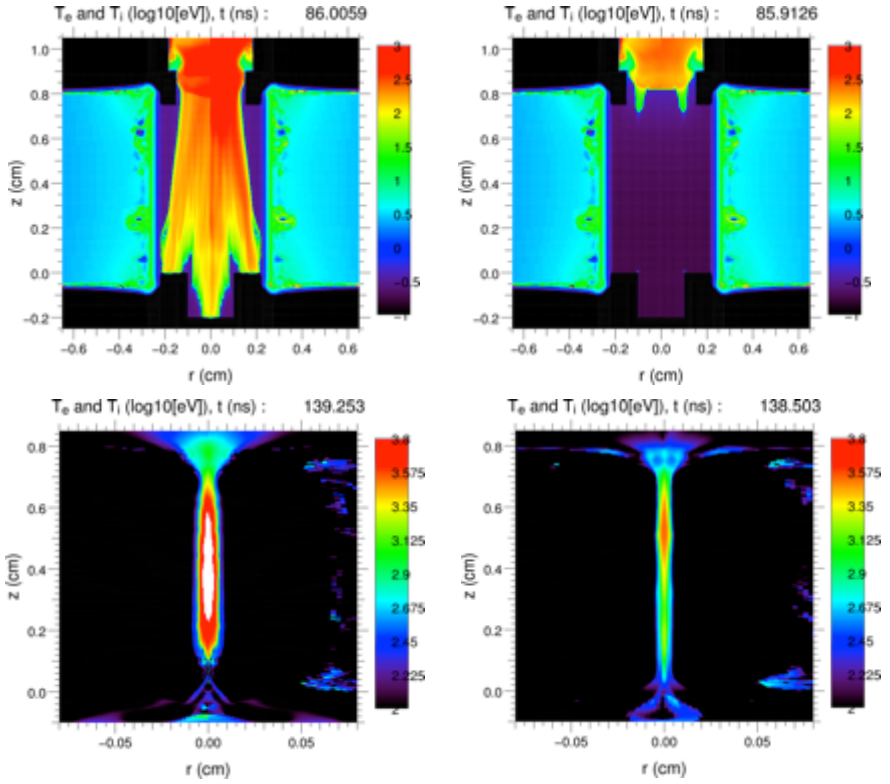

A.B. Sefkow *et al.*, Phys. Plasmas (2014).

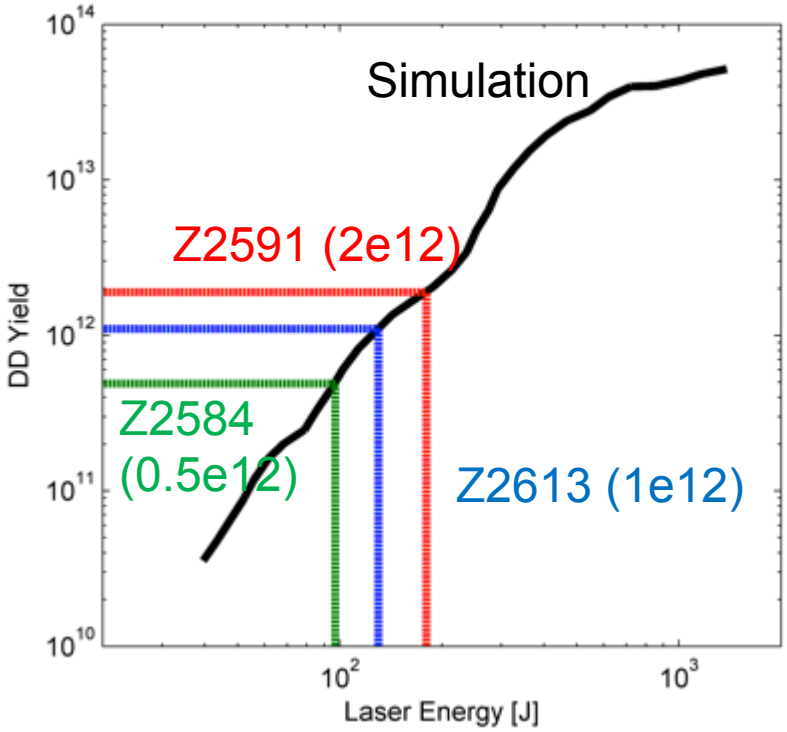

Simulations with 200 J match not only the yield, but other parameters measured in the experiments (temperature, shape, BR, etc.)

Excellent agreement is obtained between post-shot degraded (poor laser/gas Coupling) 2D & 3D simulations and experimental observables

Parameter	Measured/inferred [z2591]	Post-shot simulations
• I_{max}	19 ± 1.5 MA	19 MA
• t_{imp}^{5MA}	+90 ± 1 ns	+90 ns (~70 km/s)
• r_{laser}	450 ± 150 μm	450 ± 150 μm
• E_{gas}^{abs}	~100-300 J	200 ± 50 J
• r_{stag}^{hot}	44 ± 13 μm	40 μm (r_{stag}^{liner} 53 μm, CR_{2D}^{liner} 44)
• $\langle T_i \rangle^{DD}$, $\langle T_{i,e}^{spec} \rangle$	2.5 ± 0.75, 3.0 ± 0.5 keV	3.0 ± 0.5, 2.7 ± 0.5 keV
• ρ_{gas}^{stag} , m_{loss}	0.3 ± 0.2 g cm^{-3}, ~70%	0.4 ± 0.2 g cm^{-3}, 61%
• ρR_{gas}, ρR_{liner}^{stag}	2 ± 1, 900 ± 300 mg cm^{-2}	2.6 ± 1.0, 900 mg cm^{-2}
• $\langle P^{stag} \rangle$, E_{gas}^{stag}	1.0 ± 0.5 Gbar, 4 ± 2 kJ	1.5 ± 0.3 Gbar, 7 ± 2 kJ
• $\langle B_z^f r_{stag} \rangle$	(4.5±0.5)e5 G cm ($r_{stag}/r_{L,\alpha}$ 1.7)	4.8e5 G cm ($r_{stag}/r_{L,\alpha}$ 1.8) ($\langle B_z^f \rangle$ 91 MG)
• Y_n^{DD}	(2.0±0.5)e12	(2.5±0.5)e12
• Y_n^{DD}/Y_n^{DT}	40 ± 20	41-57
• DD, DT spectra	isotropic, asymmetric	isotropic, asymmetric
• t_{burn}^{FWHM}	2.3 ± 0.6 ns (x-rays) [z2591, Y_n^{DD}=2e12] 1.5 ± 0.1 ns (x-rays) [z2613, Y_n^{DD}=1e12]	1.6 ± 0.2 ns (neutrons and x-rays)
• Liner emission	bounce & peak emission: t_{stag}+5 ns	bounce & peak emission: t_{stag} +5 ns
• Δz_{burn} shape	5 ± 1 mm, asymmetric	Helical shape and liner attenuation
• mix	0 - 10 %, not ≥ 20%	0% (by design)

Laser-only experiments appear to confirm that laser-fuel coupling is a concern: Multiple measurements are consistent with low energy coupling (~10-20%)

Sandia National Laboratories

Blast Wave Data

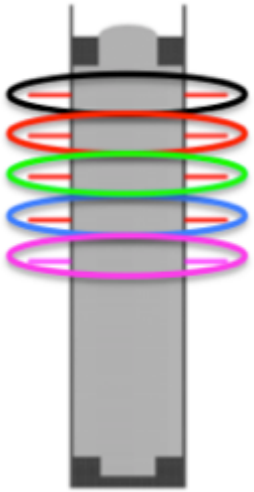

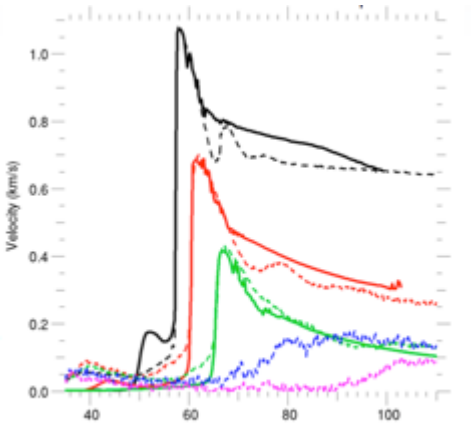

Ar imaging Data

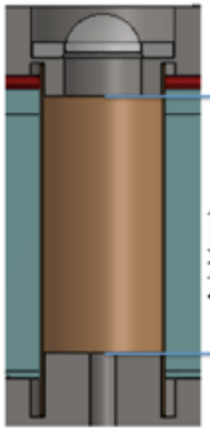

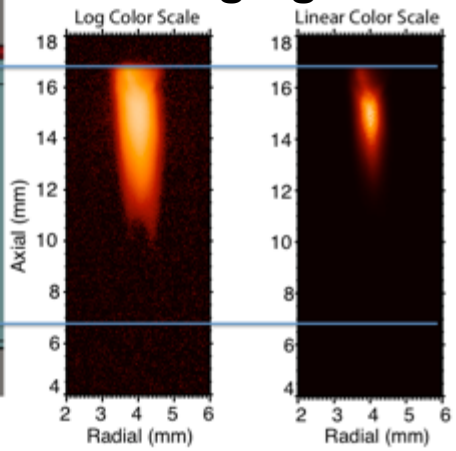

Calorimeter Measurements

Foil Transmission Data

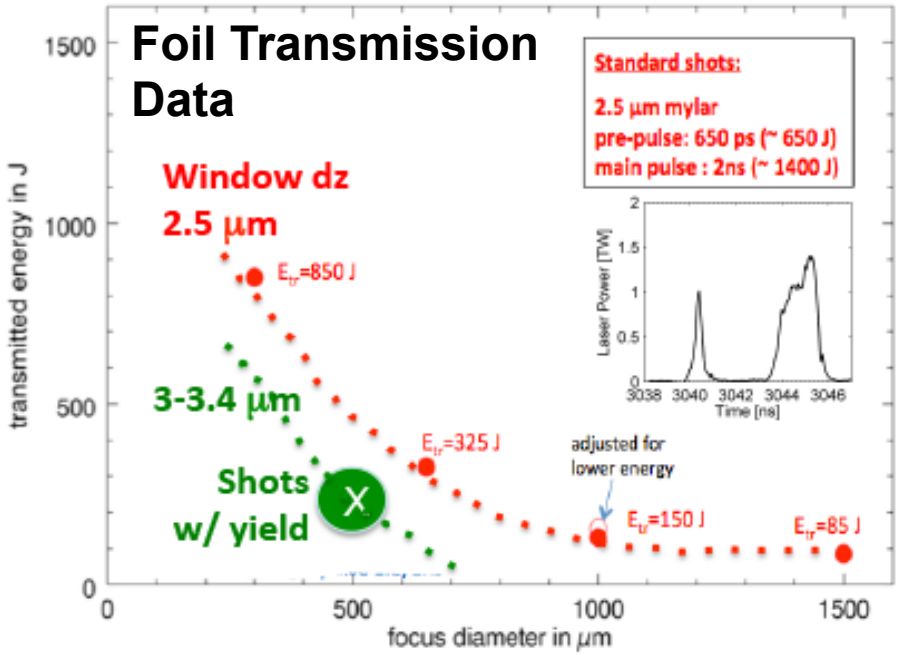

Shadowgraphy Data

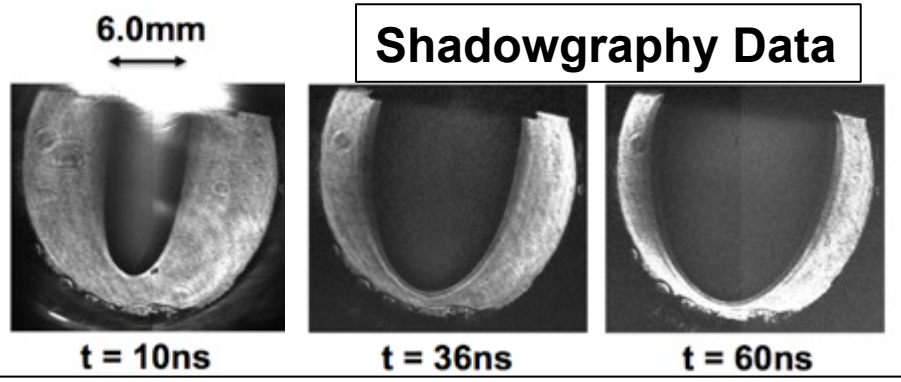

3D simulations suggest average stagnation quantities in current MagLIF implosions may be described by 1D

Early-time inner boundary *density*

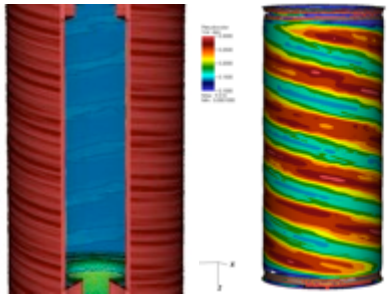

Long axial λ_z ~1 mm is from early-time feedthrough and imprints at the liner/gas interface

Since the interface is magneto-Rayleigh-Taylor stable, the gas is high β, and flux pile-up occurs there, λ_z also imprints on B_z

Inner boundary B_z

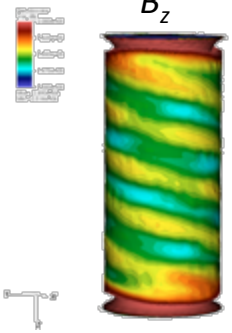

Late-time inner boundary *density* B_z

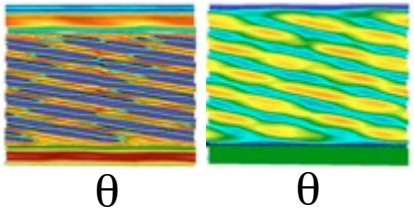

As in helical perturbation on rear side of liner, inner surface helix persists and grows as well

Exp Sim

Resulting structure does not strongly modify 2D physics

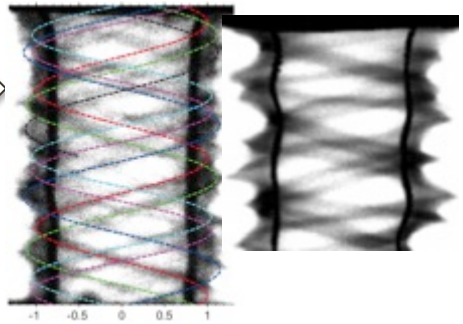

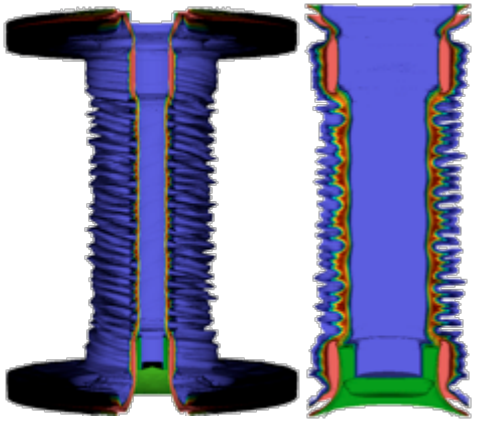

Resulting weakly helical (dr << dz) emitting stagnation column remains quasi-2D such that $P_{stag}^{exp} \sim P_{stag}^{3D} \sim P_{stag}^{2D} \sim 1$ Gbar

When not accounting for variations due to convergence as *f*(z), the averaged quantities may be approximately described even in 1D

A. B. Sefkow, et. al., *in preparation* (2015).

Variation in self-emission and liner opacity contribute to observed structure

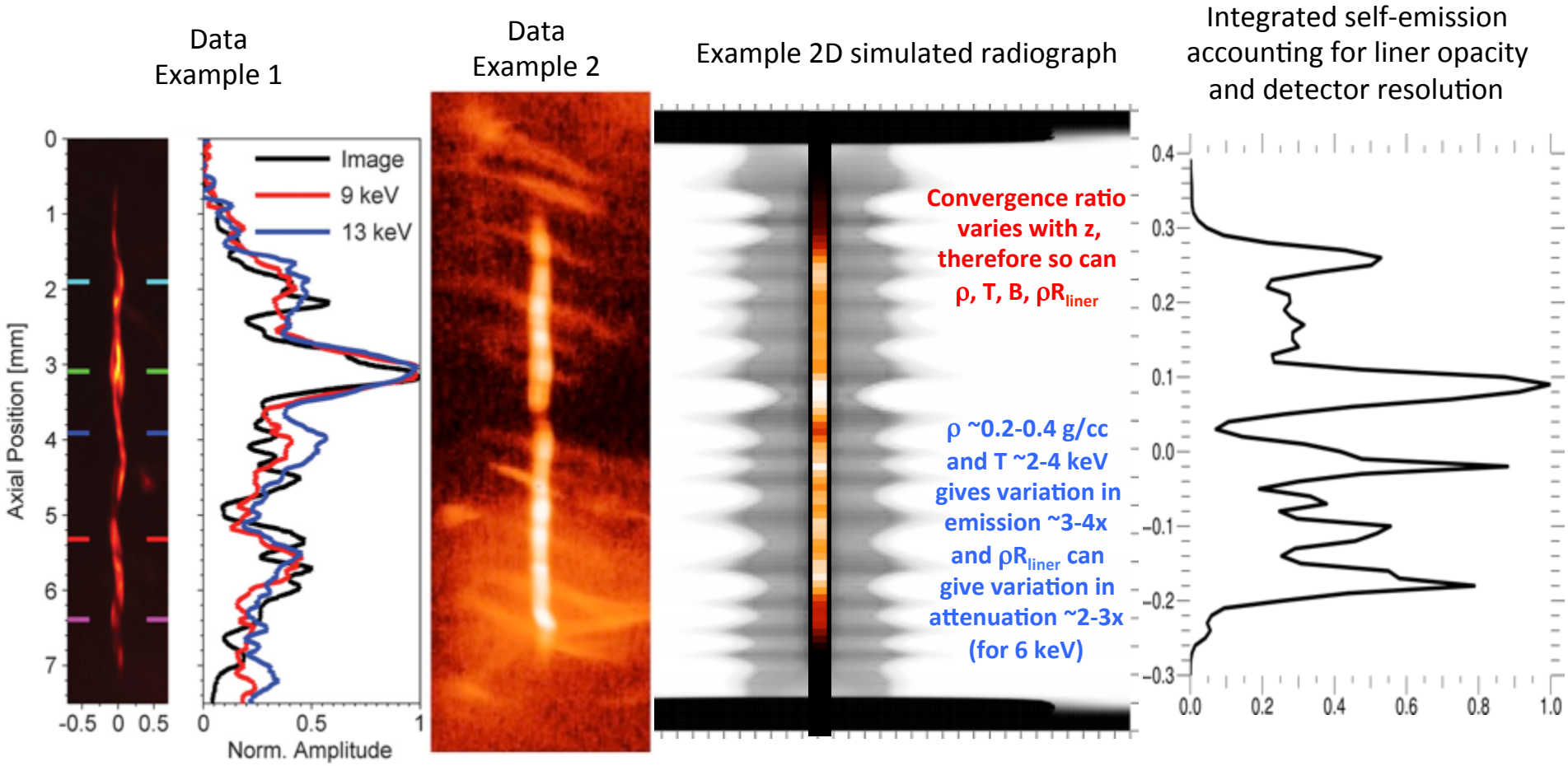

However, helical emission and radiographs require 3D simulations

A. B. Sefkow, et. al., *in preparation* (2015).

Full 3D with helical instability growth is needed to correctly simulate the stagnation column

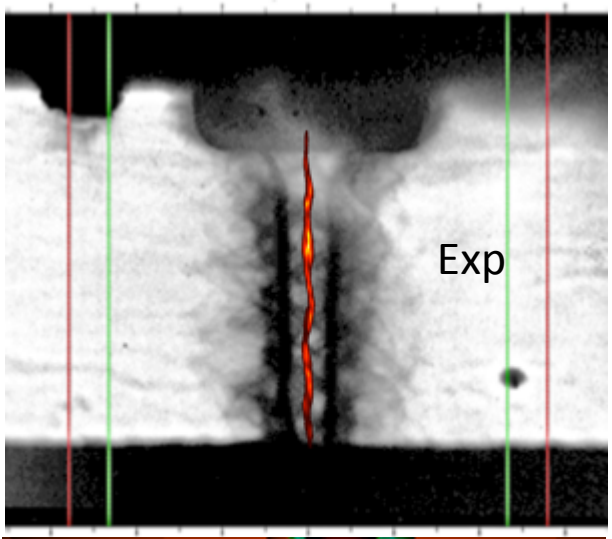

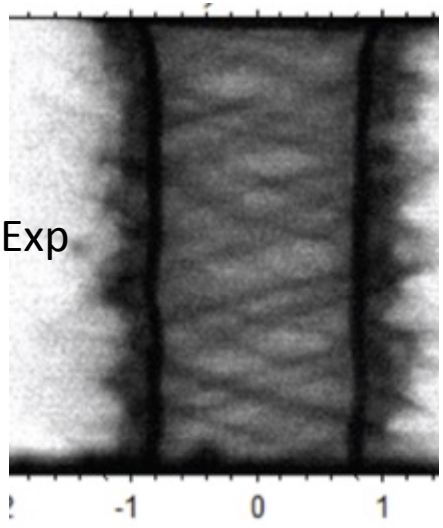

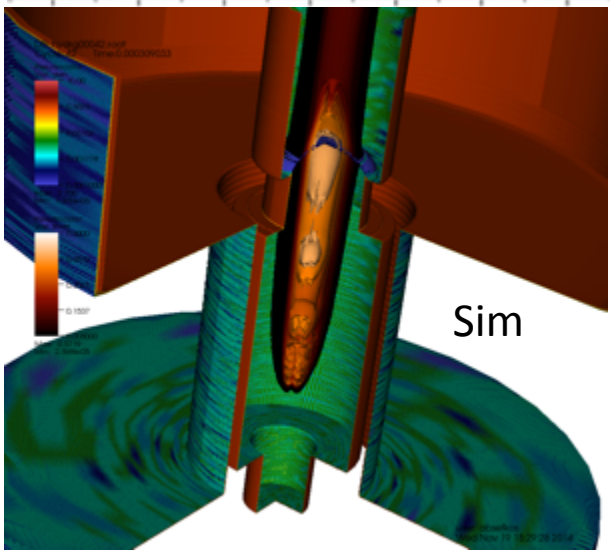

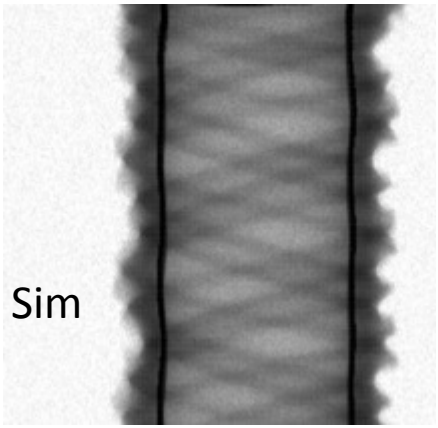

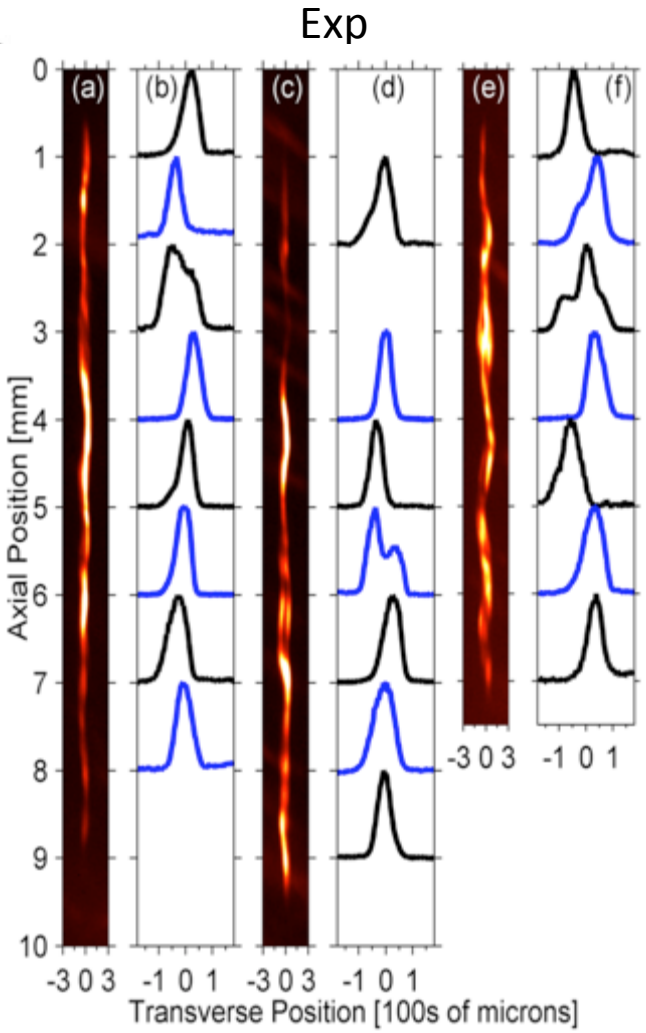

Implosion instabilities also have the potential to degrade neutron yield

Sandia National Laboratories

Density Profile at Peak Neutron Emission

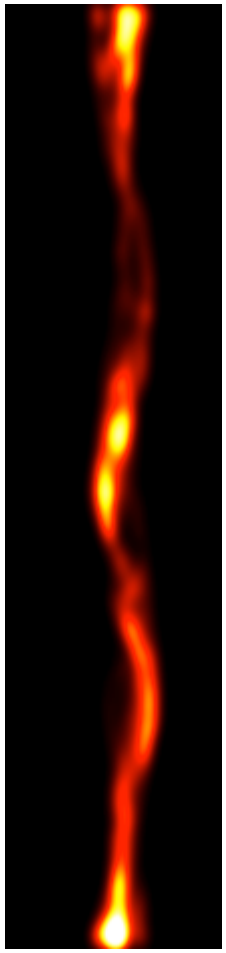

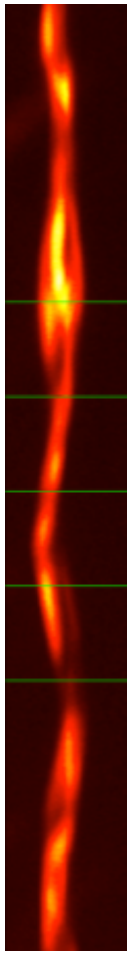

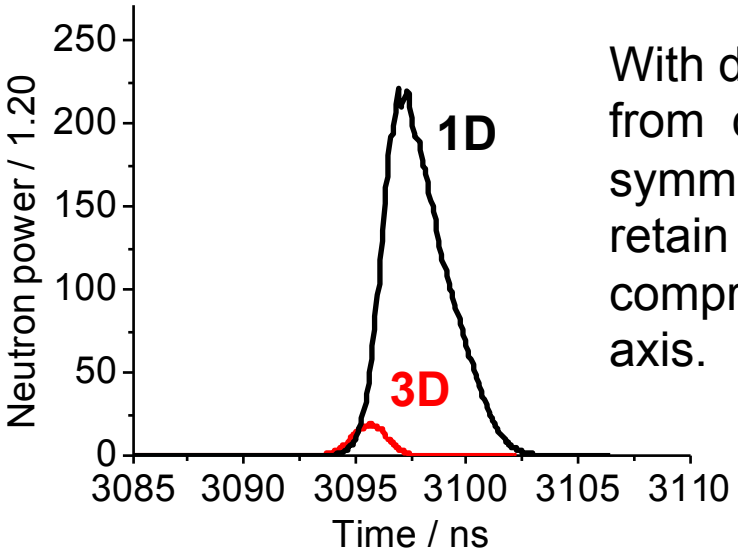

With departures from cylindrical symmetry we retain only initial compression on axis.

Yield vs Preheat Energy

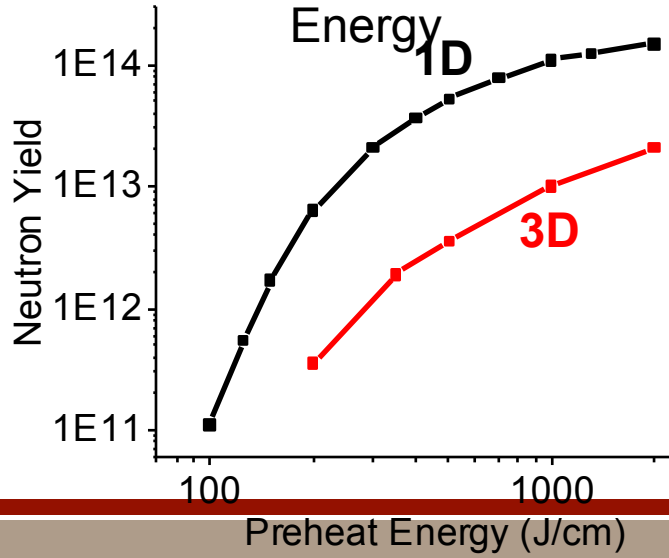

Yield still scales with increasing preheat energy, but magnitude lowered from 1D equivalent

Azimuthal liner structure is not effectively decelerated against compressed fuel.

Spikes of liner material can penetrate through fuel

- Reduces fuel compression (liner can decelerate against liner)
- Increases surface area to thermal losses.
- Mixes cold fuel and liner material into hot fuel.

Fuel volume can be bisected creating bifurcated structures evident is some of the Ar imaging

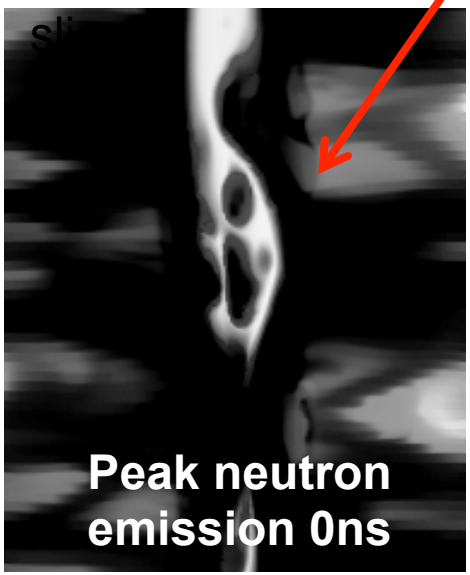

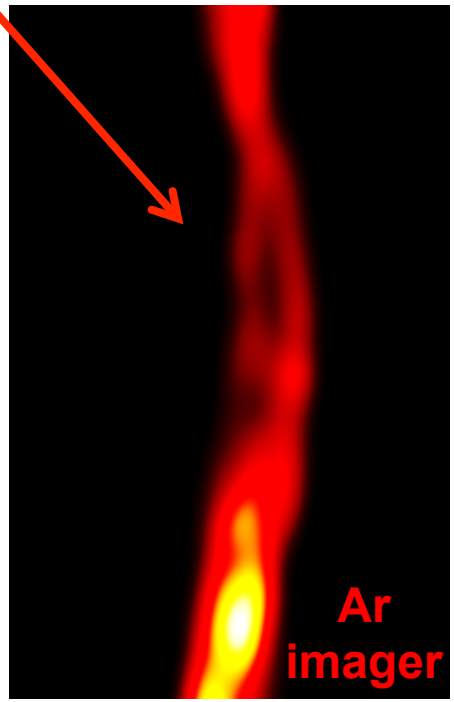

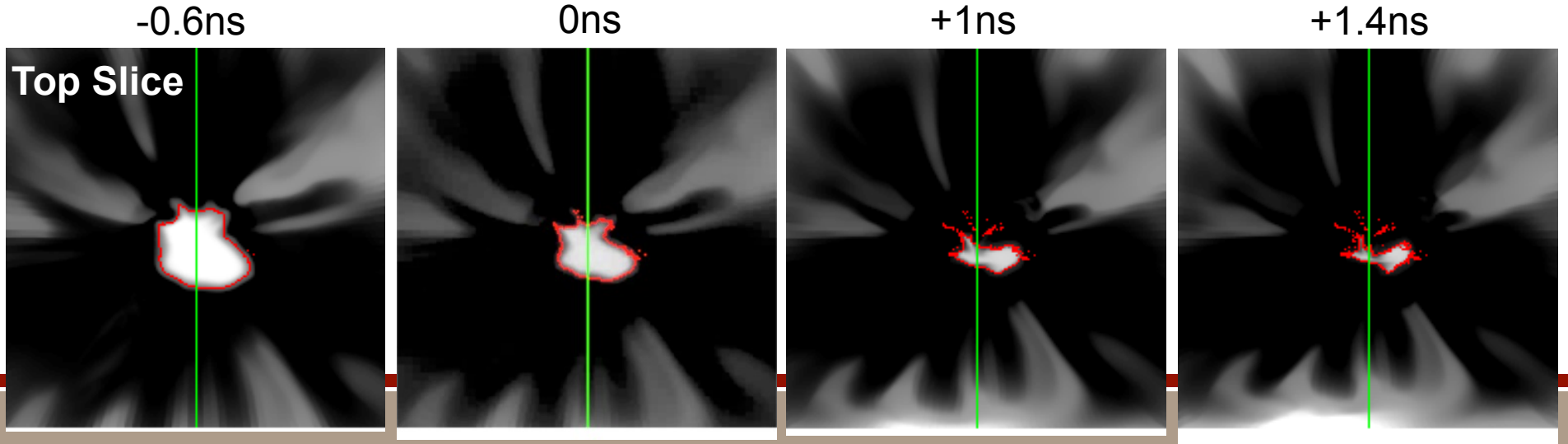

In the coming year, we plan to investigate the role of liner instabilities on stagnation performance

Dielectric coatings may reduce instability growth (Al liners - K. Peterson DZP)

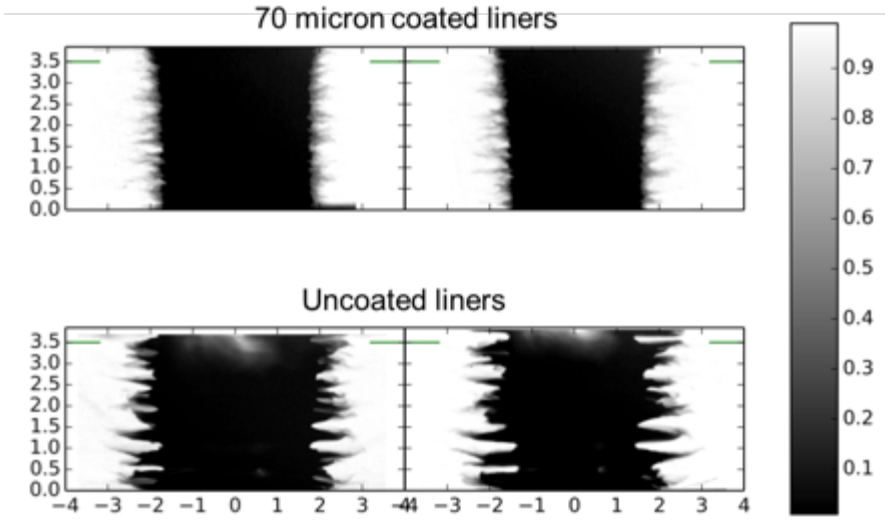

Increasing thickness of the liner by 40% reduces yield in 1D by ~40% (neglecting end losses). However thicker liner (lower aspect ratio) might be expected to reduce feedthrough of MRT instabilities. There might be a better compromise than AR 6

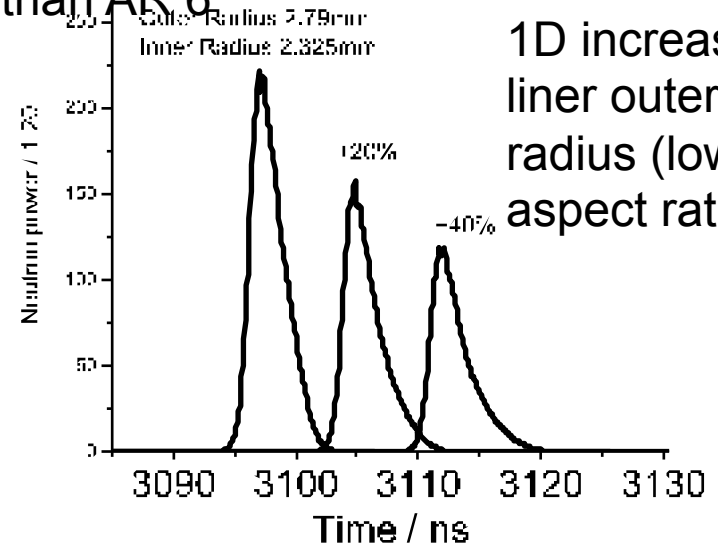

1D increase liner outer radius (lower aspect ratio)

Sandia National Laboratories

CODES AND MODELING

Our modeling and simulation strategy for magnetically driven implosions is currently under revision

Sandia National Laboratories

- Validated modeling is endemic to all of the other focus areas
- Our main fully integrated scaling and design tools for magnetic drive are codes developed and supported by LLNL
  - E.g., LASNEX (2D MHD), HYDRA (3D MHD), ARES (3D MHD)
  - "Workhorse" codes that allow design and scaling studies
  - Large user base helps "break in the code" so that they are robust and at least partially validated over a wide range of problems and scales
- Additional tools being used do some problems because they offer unique physics advantages
  - E.g., GORGON (3D MHD), ALEGRA (3D MHD), LSP (hybrid-PIC)
  - Each does some things particularly well, but unproven in others
  - Small user base for each
- A relatively small number of FTEs across the laboratories are currently using MHD-based code tools

There are known deficiencies in the way that widely-adopted MHD models treat low density plasmas

- All of the codes demonstrated today to be capable of fully-integrated calculations are based on fluid-based MHD models
  - Necessitates use of density and conductivity "floors"
  - In some cases, the results are shown to be sensitive to the choices of the values for these floors
  - Accounting for magnetic flux loss in liner implosions requires higher-order corrections to the standard MHD models (e.g., "Nernst" and "Ettinghausen" terms) that have seldom, if ever, been validated
- We are looking at a two-pronged strategy to address this
  - Incorporation of "extended MHD" models that include electron terms in generalized Ohm's Law that are usually neglected*, potentially allowing us to push MHD-based codes down to lower plasma densities
  - Improvement & testing of hybrid particle-in-cell codes that model the particle kinetics directly, allowing us to push these codes to the high plasma densities typical of magneto-inertial fusion (e.g., LSP)
  - "Test codes" and good test problems will be needed to justify these

* e.g., Seyler & Martin, Phys. Plasmas (2011).

We are engaging with multiple collaborators to help us improve our codes for magnetically driven implosions

- **Improving MHD modeling:**
  - **U. Rochester**: Collaboration on "mini-MagLIF" is expected to examine MHD modeling of magnetic flux loss
  - **LLNL**: A "code workshop" at LLNL planned for June to understand the issues with our LLNL-based workhorse codes and develop a path forward
  - **Universities** (e.g., Cornell): Actively developing extended MHD models and doing validation experiments to understand the importance of including this new physics
- **Improving PIC/Hybrid-PIC modeling:**
  - **Universities**: We are trying to get more groups involved in this effort, e.g., Princeton University, through our Fundamental Science program
  - **Voss Scientific**: Sandia is engaging with Voss Scientific to develop robust hybrid PIC models for MagLIF
  - **ASC Program**: Sandia will be engaging with ASC program to develop robust hybrid PIC models for MagLIF
- **Validation**:
  - **NRL**: Is constructing theoretical validation problems (e.g., MHD Noh, Nernst)
  - Concurrently collect data that can be used to validate the new models

Backups

Sandia National Laboratories

Exceptional service in the national interest

Sandia National Laboratories

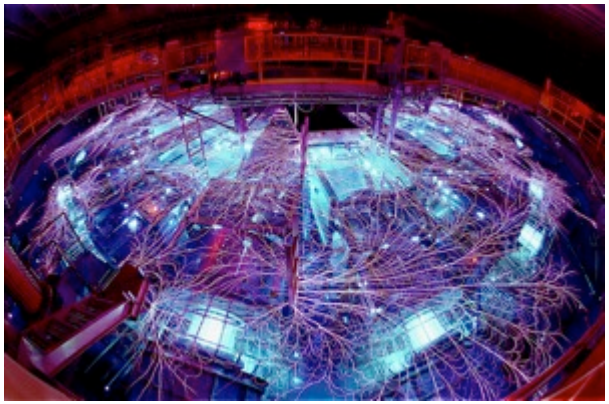

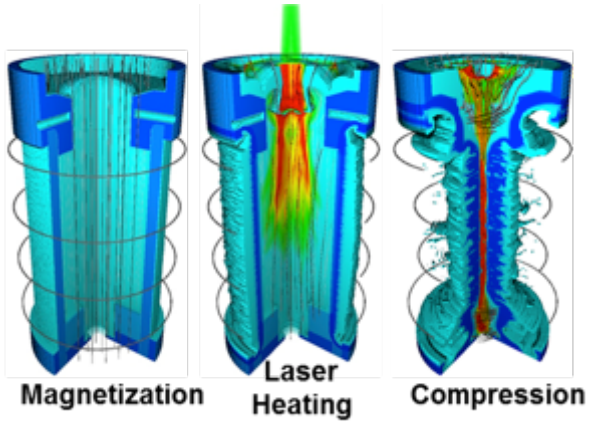

Diagnosing stagnation conditions in Magnetized Liner Inertial Fusion (MagLIF) Experiments

Matthew Gomez
for the MagLIF team
Sandia National Laboratories

National Implosion Stagnation Physics Group, Livermore, CA, October 27, 2015

U.S. DEPARTMENT OF ENERGY | NNSA

Sandia National Laboratories is a multi-program laboratory managed and operated by Sandia Corporation, a wholly owned subsidiary of Lockheed Martin Corporation, for the U.S. Department of Energy's National Nuclear Security Administration under contract DE-AC04-94AL85000.

A few key numbers for MagLIF

- Expected stagnation values:
  - Temperature: 2-4 keV
  - Density: 0.1-1 g/cc
  - Duration: 1-2 ns
  - Height: 5-10 mm
  - Radius: 50-100 µm
  - B field: 5-20 kT
  - Peak velocity: 70-100 km/s
- Note that fuel is D_2

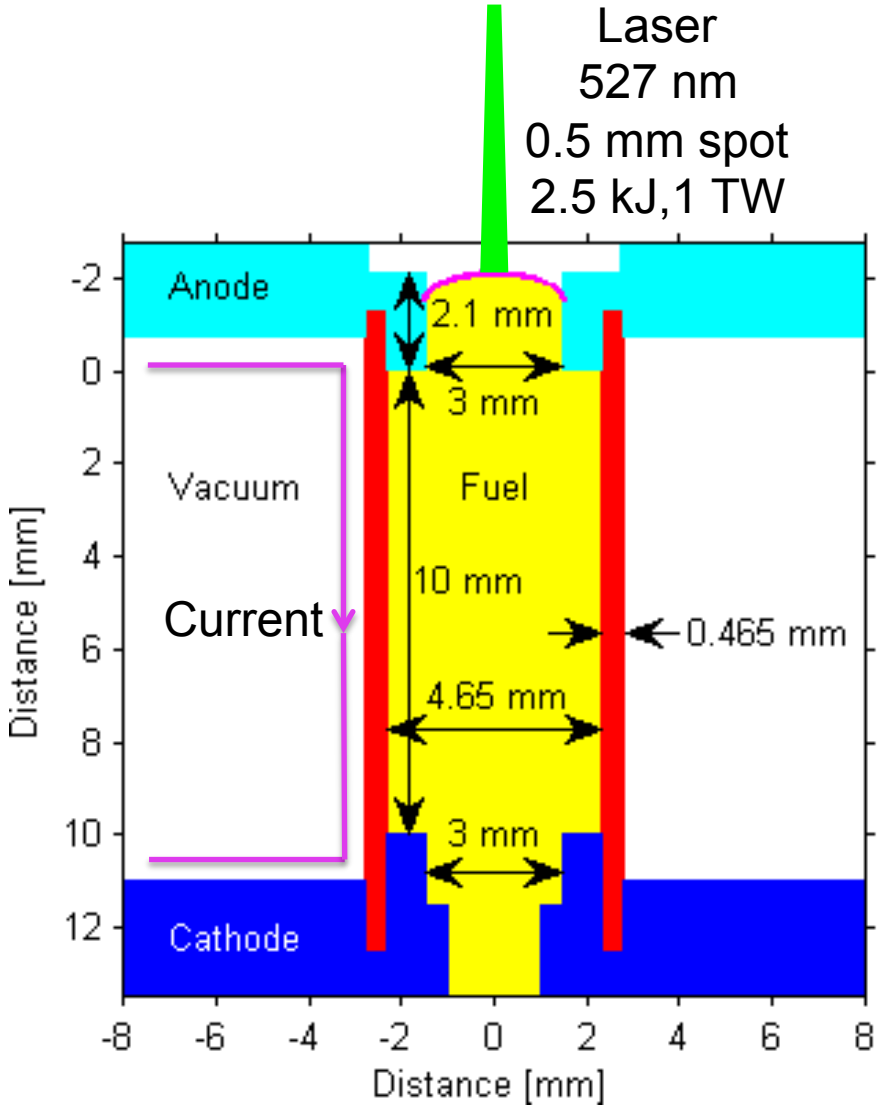

Experimental performance doesn't live up to simulation predictions

Sandia National Laboratories

- Several scenarios have been suggested to explain the discrepancy
  - If we assume 10% laser energy coupling to the fuel (as opposed to 50%) simulations match experimental observables with zero mix and essentially a 1D stagnation
    - ~10% laser transmission observed with 3 µm LEH window, so this may explain initial experiments
  - If we assume 50% laser coupling and allow for a few percent liner/endcap/window mix, the experimental observables can again be matched with a relatively 1D stagnation
    - 1.5 µm LEH windows allow more laser through, but performance goes down with Al endcaps (improves with Be endcaps)
  - If we assume 50% laser coupling and minimal mix, experimental observables can be matched assuming a relatively 3D stagnation

There are several stages in MagLIF each with diagnostic challenges

- In imploding MagLIF experiments, we only diagnose stagnation
  - We use separate experiments to investigate laser heating
  - There is a 50 ns window during which we do not know the conditions of the fuel
- Laser heating occurs near the start of the >50 ns implosion
  - A small amount of high Z material mixed in can substantially reduce the effective preheat energy
  - We have some evidence that the endcap material substantially affects stagnation conditions particularly when the coupled laser energy is high

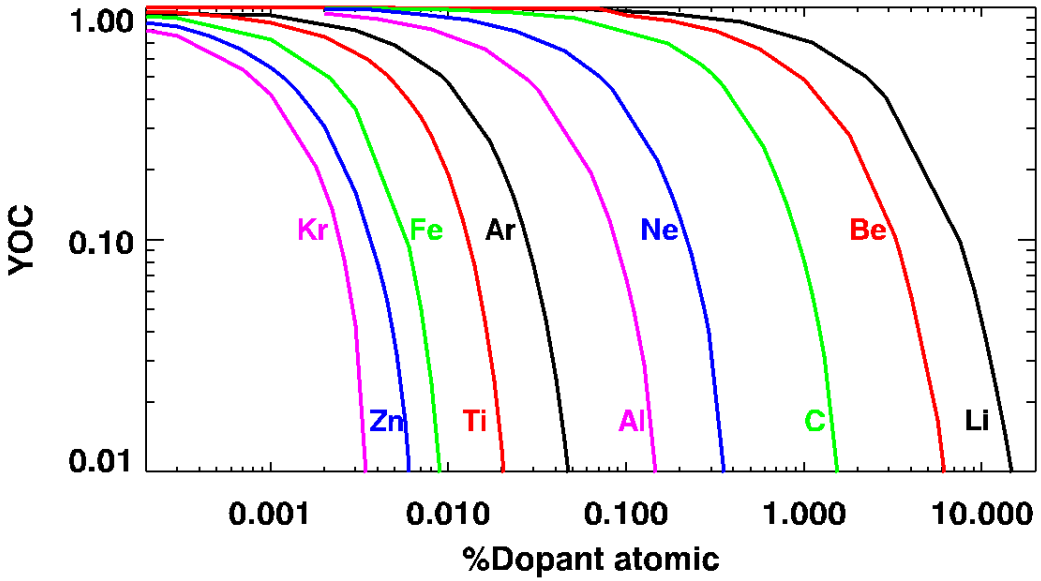

Table of diagnostics and measured quantities

Measurement goal	Diagnostic/observed quantity	In use / improvements
Electron temperature	8-20 keV x-ray spectrum - Continuum emission slope	Yes - Time resolved
	6-8 keV x-ray spectrum - Impurity line ratios	Yes - Time resolved
	Filtered x-ray images - Image intensity ratios	Yes - Time resolved
Ion temperature	Neutron time of flight spectrum - Width of neutron peak	Yes - Space resolved
	Recoil spectrometer - Neutron tracks	No - Need DT
Morphology	Time-resolved imaging - intensity variation	Yes - resolution
	Neutron imaging - intensity variations	No - need DT
	Spherically-bent crystal imaging - intensity variations	Yes - time resolved
Plasma density	6-8 keV x-ray spectrum - Width of impurity line	Yes - Time resolved
	Filtered x-ray diodes - Absolute x-ray power	Yes - Space resolved
Burn duration	Gamma reaction history	No - need DT
Liner opacity	Neutron time of flight spectrum – down scatter ratio	Yes - collimation
	6-8 keV x-ray spectrum - depth of K edge	Yes - S/N
Magnetic field	Neutron time of flight spectrum - secondary shapes	Yes - S/N
	Activation samples – DD to DT ratio	Yes - more samples

We applied the majority of the Z diagnostic suite to assess stagnation

Sandia National Laboratories

- Most of these diagnostics were already available on Z and were designed to measure ~100 kJ x-ray yields from wire arrays not the ~10 J x-ray yields in MagLIF
  - Time-integrated, axially-resolved spectroscopy
    - Added a high-resolution, high-sensitivity, 6-8 keV spectrometer
  - Time-resolved, spatially-integrated x-ray power
  - Time-integrated self-emission imaging
    - Added a high-resolution, monochromatic bent crystal imager
  - Time-resolved self emission imaging
- Neutron diagnostics at Z consist of
  - Neutron time of flight spectroscopy
  - Neutron activation samples
  - Neutron imaging
    - We do not have sufficient yield for this to work yet

The Z machine creates a relatively harsh environment for diagnostics

Sandia National Laboratories

- Shrapnel routinely damages diagnostics
  - We combat this by increasing distance and shielding
  - This reduces diagnostic sensitivity
- There is a lot of electromagnetic noise
  - Limits the use of streak cameras
- Multi-MeV gammas generated through Bremsstrahlung emission
  - Create background on x-ray diagnostics
  - Produce false counts on neutron activation samples
  - Can saturate NTOF detectors at early times

These experiments utilize deuterium gas as the fusion fuel

- **Primary reactions**

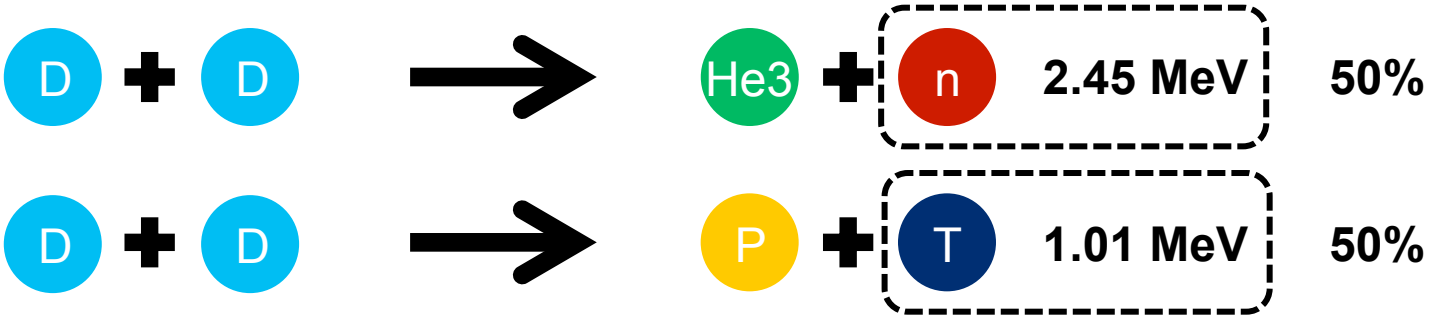

- **Secondary reaction**

Burn-averaged ion temperatures at stagnation reach 2.5 keV

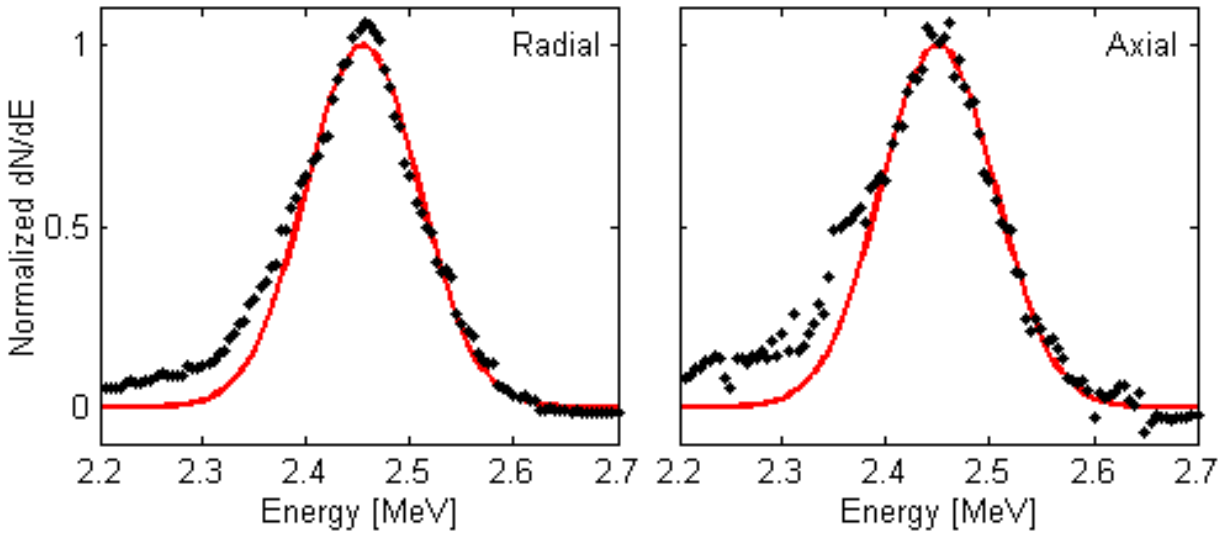

- Inferred ion temperature is a burn-weighted average
  - This is a spatially- and temporally-integrated measurement
- Axial and radial NTOF signals are consistent with one another
- The NTOF signal constrains the burn duration to less than 5 ns
- Experiments that produce the highest yields also have the highest ion temperatures
  - Temperatures range from as low as 1 keV up to 2.5 keV
- Primary DD NTOF signals used to determine neutron bang time

Stagnation duration is determined using time-resolved x-ray diagnostics

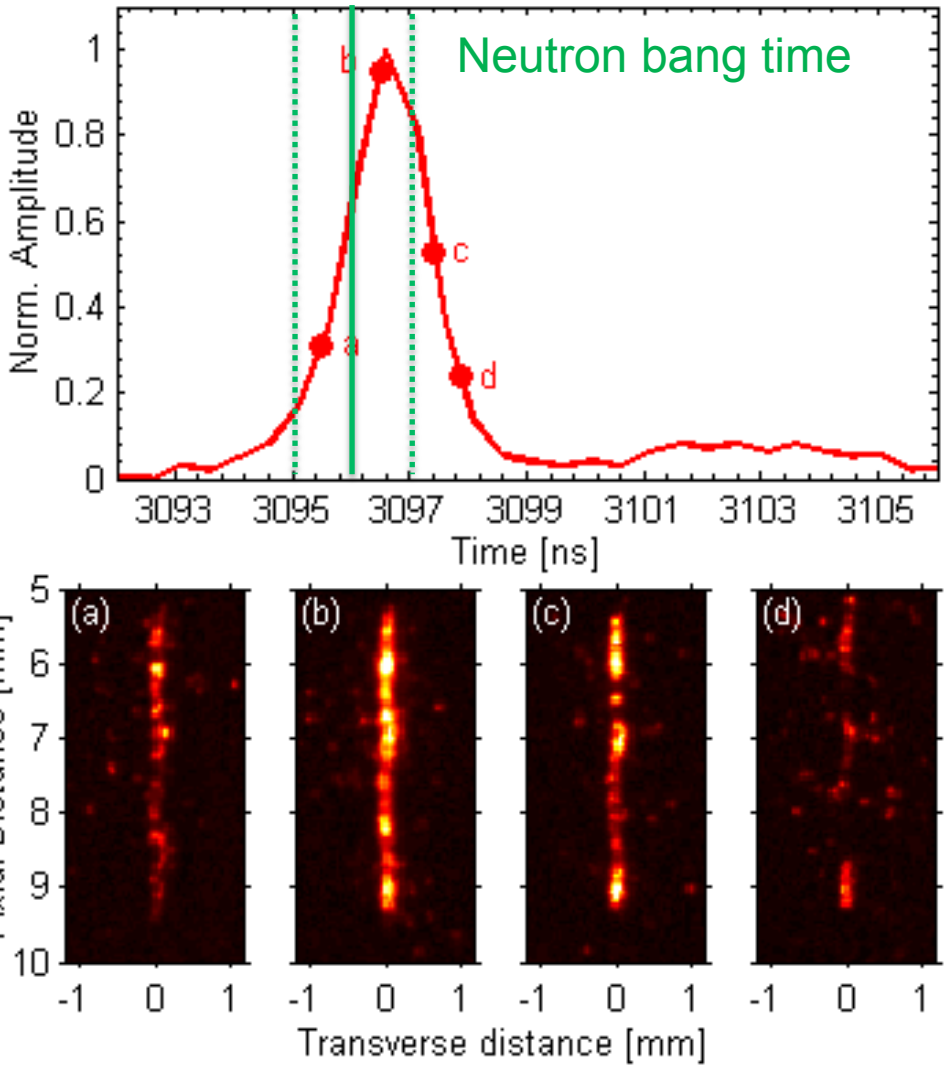

- Based on the NTOF signals we calculate the neutron bang time to within +/- 1ns
- At the same time:
  - we observe a 2 ns FWHM peak on the x-ray diode traces
  - a narrow stagnation column is recorded on a time-resolved, filtered, x-ray pinhole camera

- From this we infer that the x-ray emission and the neutrons are coming from the same location
- Neutron imaging and a burn history diagnostic would help confirm this assertion

Determination of time-integrated electron temperature

- We use the slope of the continuum emission (8-20 keV) to determine the electron temperature
  - The signal is axially-resolved, but integrated over the radial dimension
  - Typical values are between 2 and 4 keV (bright spots are cooler)
  - The signals are weak, and appear to get weaker as we remove sources of higher Z mix
  - Diagnostic is time-integrated so late time emission can affect the signal
  - In the future we could use the Hybrid-CMOS to eliminate this issue

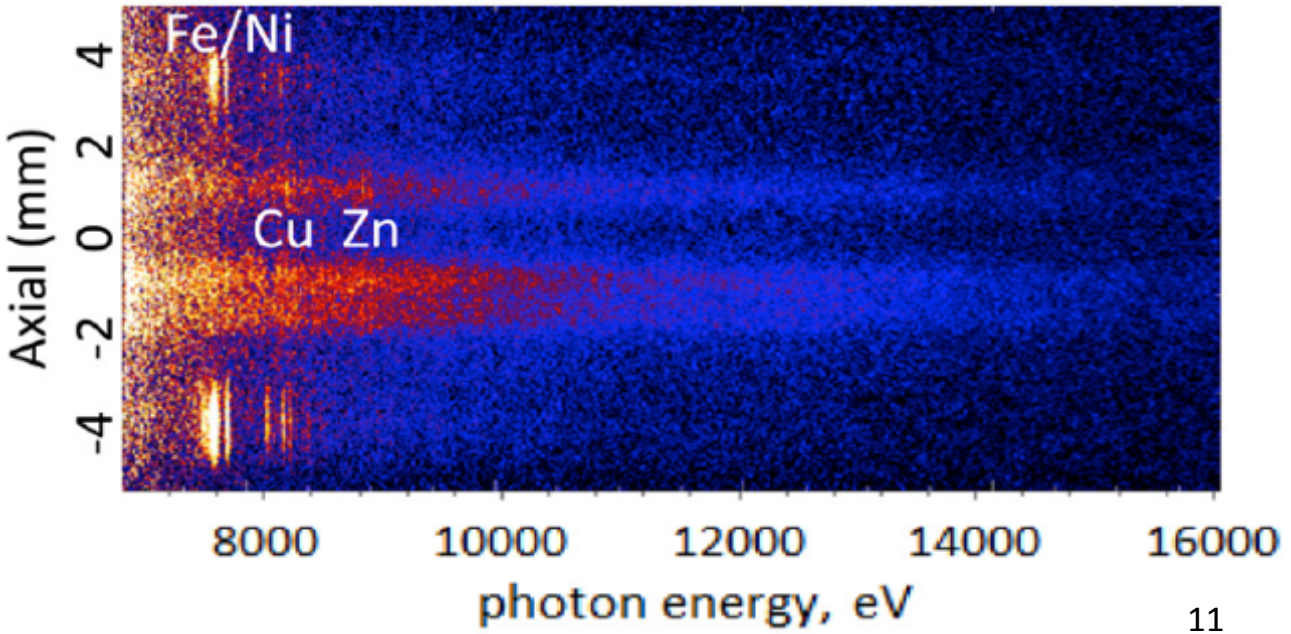

Different electron and ion temperatures can be explained with the same toy model

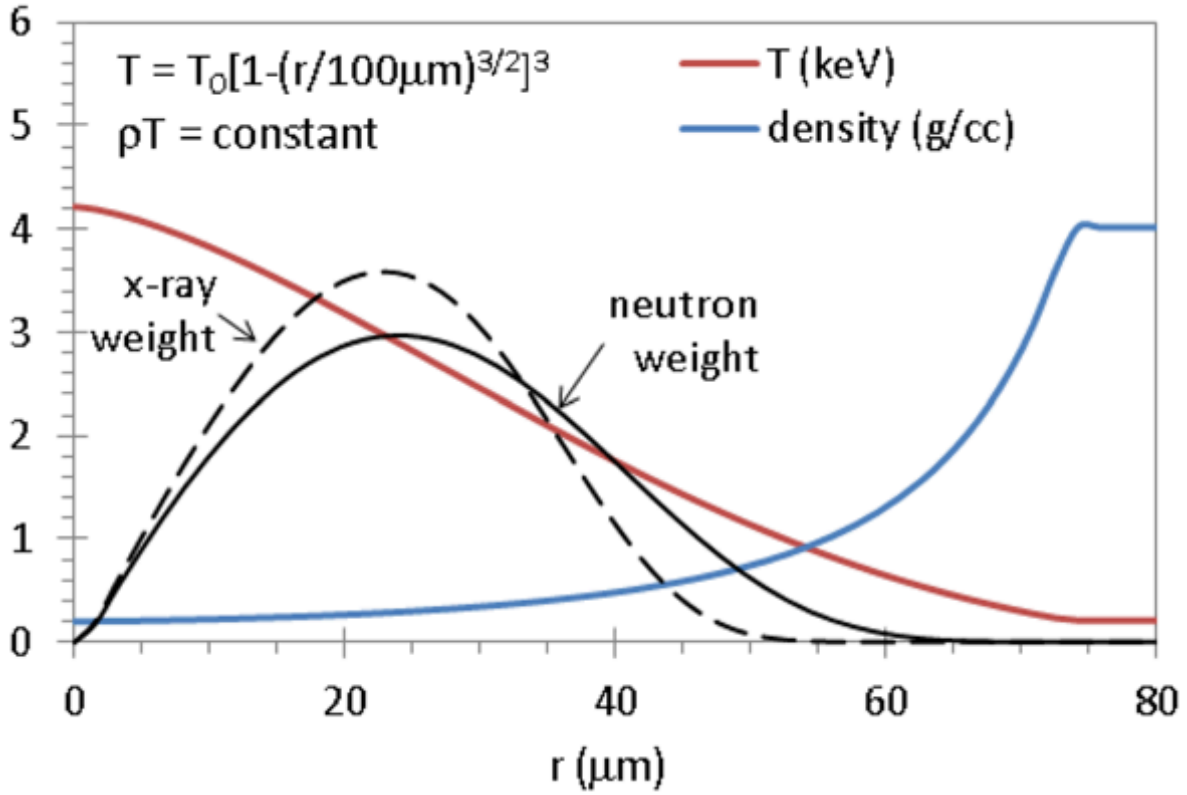

- Isobaric model of radial-dependence of temperature and density
- Emissivity-weighted electron temperature samples hotter region of plasma than burn-weighted ion temperature

Electron temperature also derived from contaminant line ratios

- 6-8 keV spectrometer observes emission lines from Fe and Ni
  - S65 beryllium contains ~100 PPM Fe and ~20 PPM Ni
  - Contaminants appear to be relatively uniformly distributed in Be
- Signal is axially-resolved, but radially-integrated
- Diagnostic is only sensitive in regions where there is Be mix and it is hot enough to produce He-like Fe
- Observed temperature range is 1-2 keV

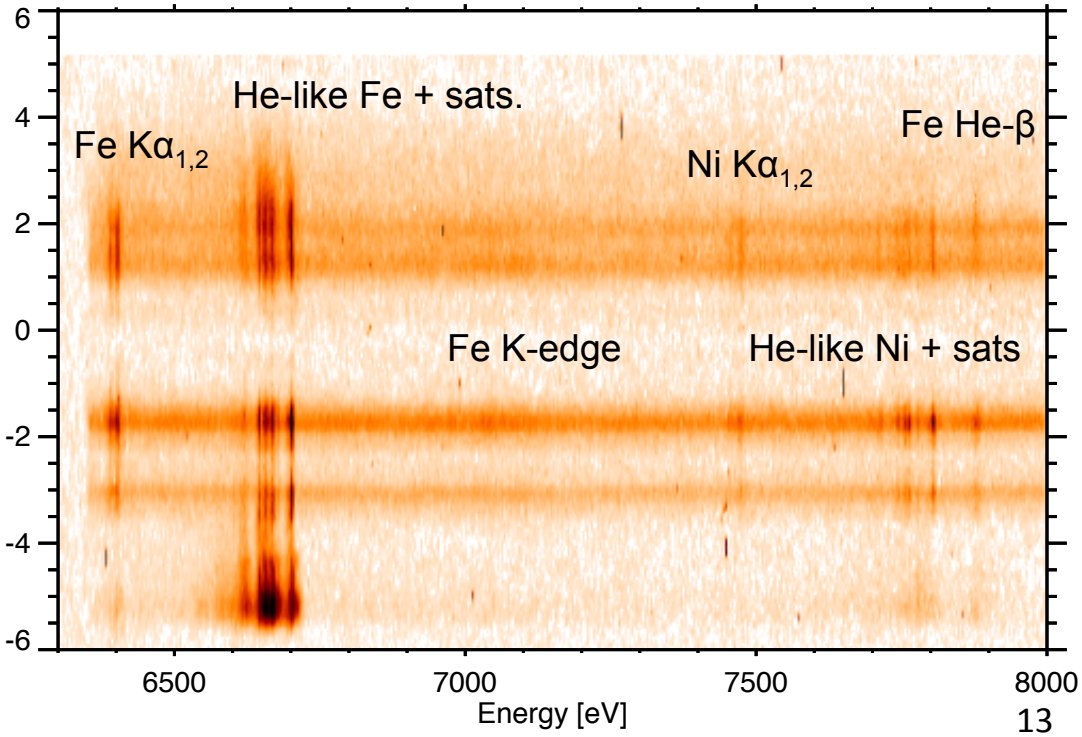

Our cartoon picture of stagnation consists of 3 regions

- We observe inconsistent measurements of the stagnation temperature
- This cartoon picture shows a possible scenario that explains this discrepancy
- The hot core produces radiation >10 keV, producing continuum slope
- The surrounding mix region is cooler and contains Fe(Be) which produces the line emission

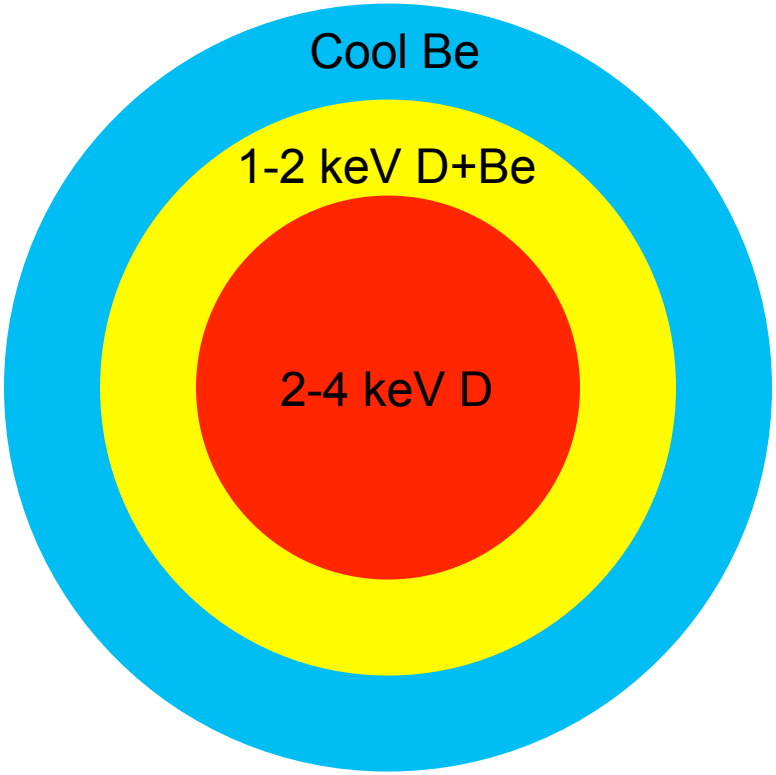

The local density is determined from the Fe line spectra

- The line width of the He-beta line gives the local electron density
  - Values are typically around 1-2e23 cm^{-3}
  - This is 0.15-0.3 g/cm^3 assuming approximately 1% Be mix
- This density is representative of the location with Fe mix

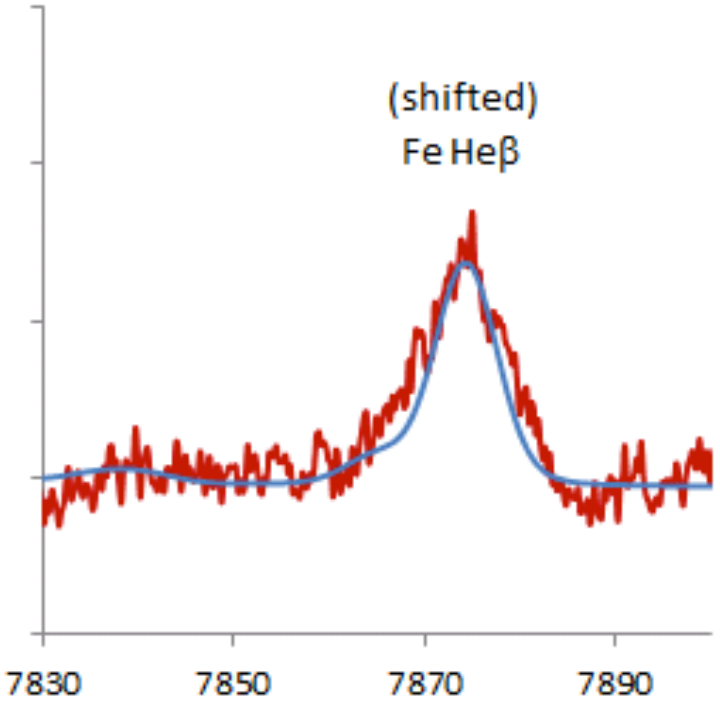

We also infer liner opacity and Be mix fraction from the Fe line spectra

- Be liner opacity inferred from Fe K-edge assuming uniformly distributed 100 PPM Fe
  - GA is working on characterizing contaminants in each target
- Be mix fraction inferred from Fe line intensity relative to continuum intensity

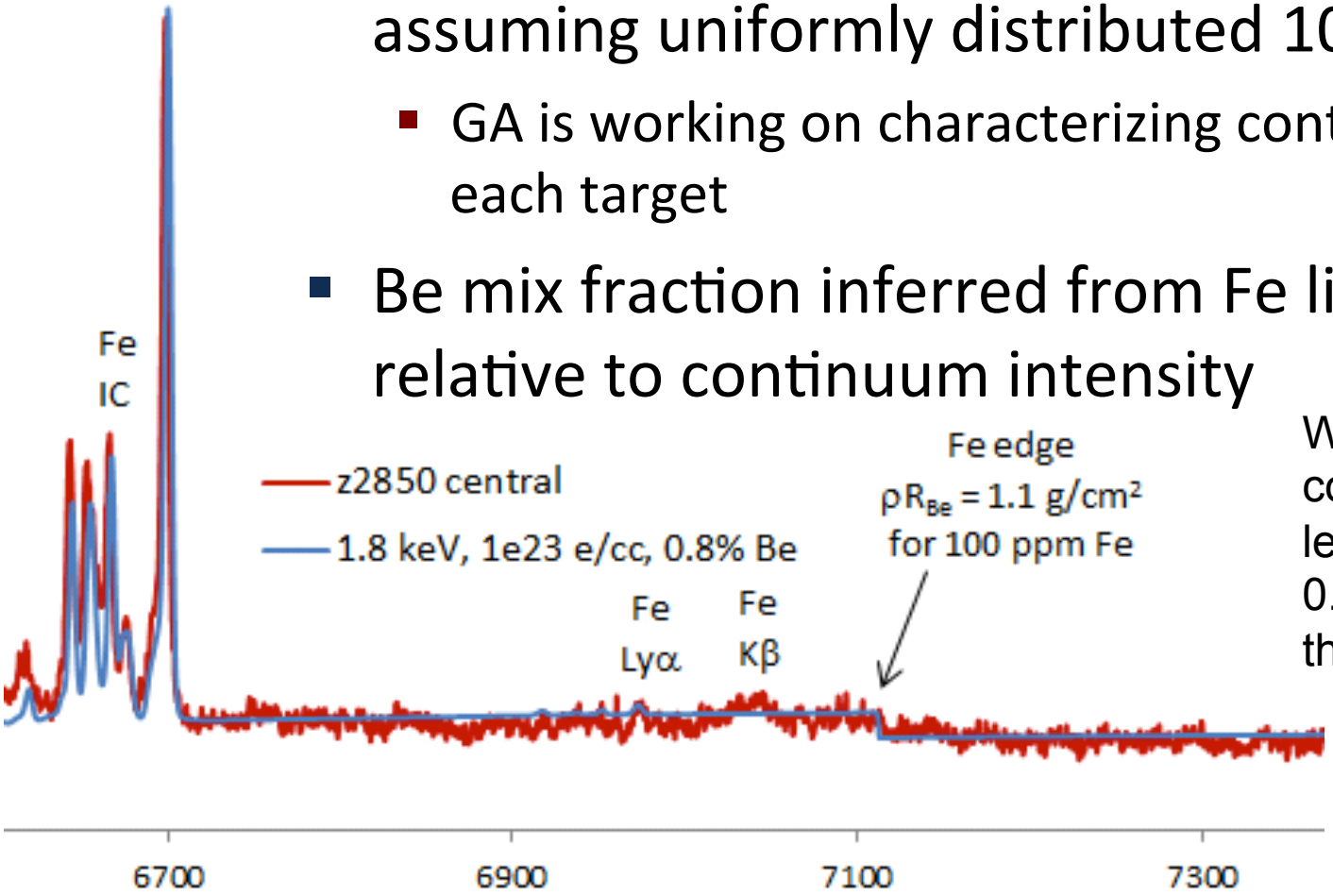

We believe the hot core has significantly less mix than the 0.8% inferred from this measurement

The hot fuel volume is determined using spherically bent crystal imaging

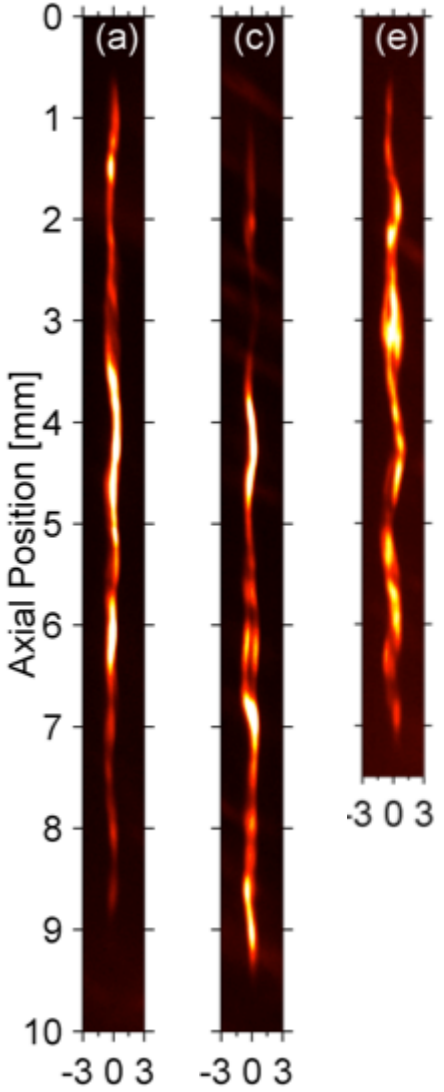

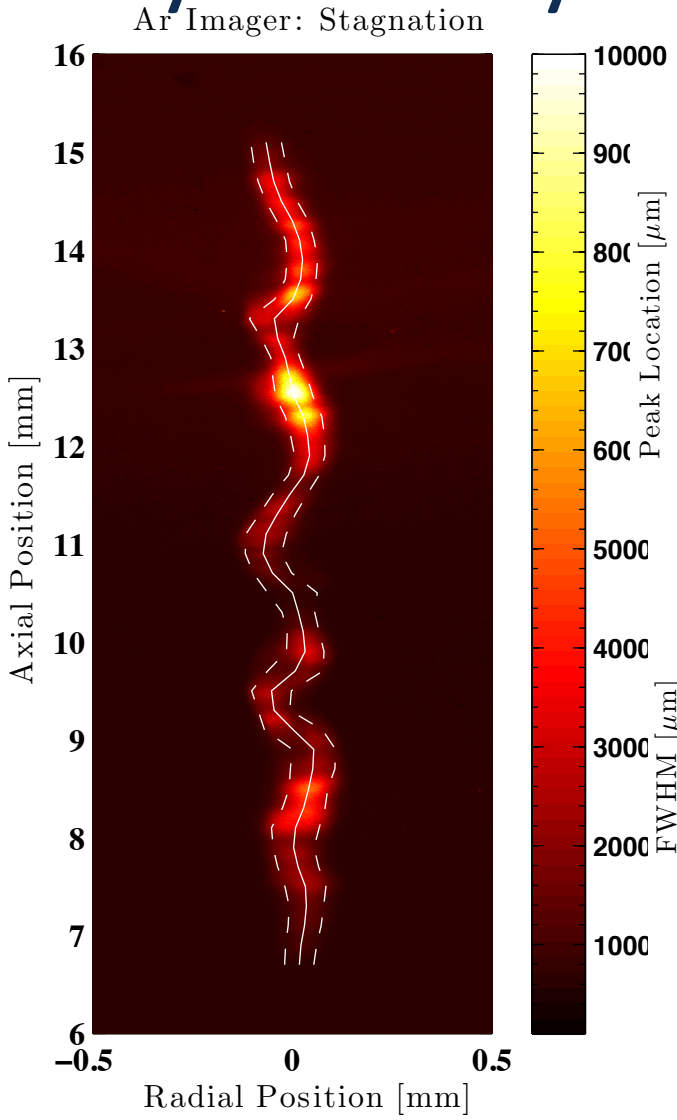

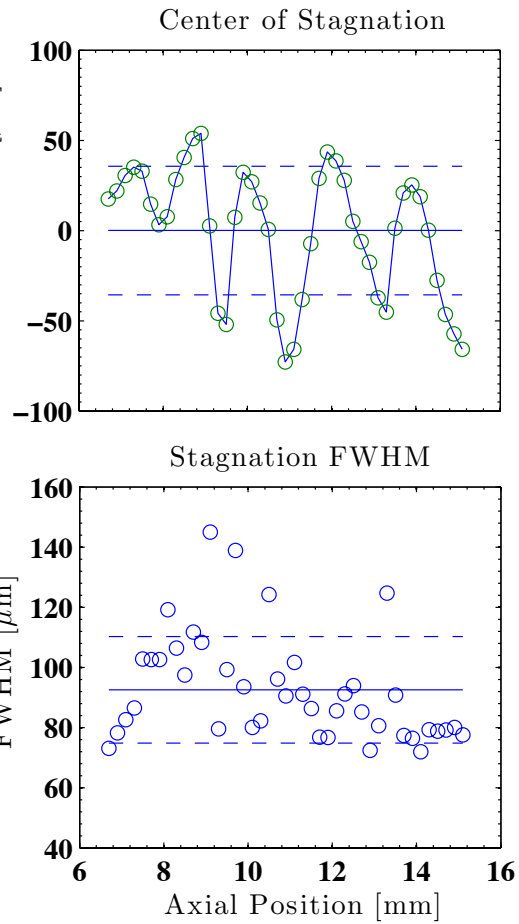

We are developing a high-resolution, time-resolved imaging diagnostic

Sandia National Laboratories

- Spatial resolution better than 30 μm
  - 3-5 resolution elements across the stagnation column
  - Hundreds of resolution elements along the stagnation column
- Temporal resolution of 250 ps using NSTec Gen-2 MCP
  - Up to 8 frames during stagnation
- We believe that this diagnostic will be instrumental in determining the degree of 3D behavior in MagLIF
- We anticipate fielding this diagnostic on experiments in CY16

Five color pinhole imaging demonstrates consistency in temperature and opacity inferences

Sandia National Laboratories

Image 1 Ti 22 μm | Image 2 Fe 24 μm | Image 3 Ni 20 μm | Image 4 Zn 20 μm | Image 5 Ti 101 μm

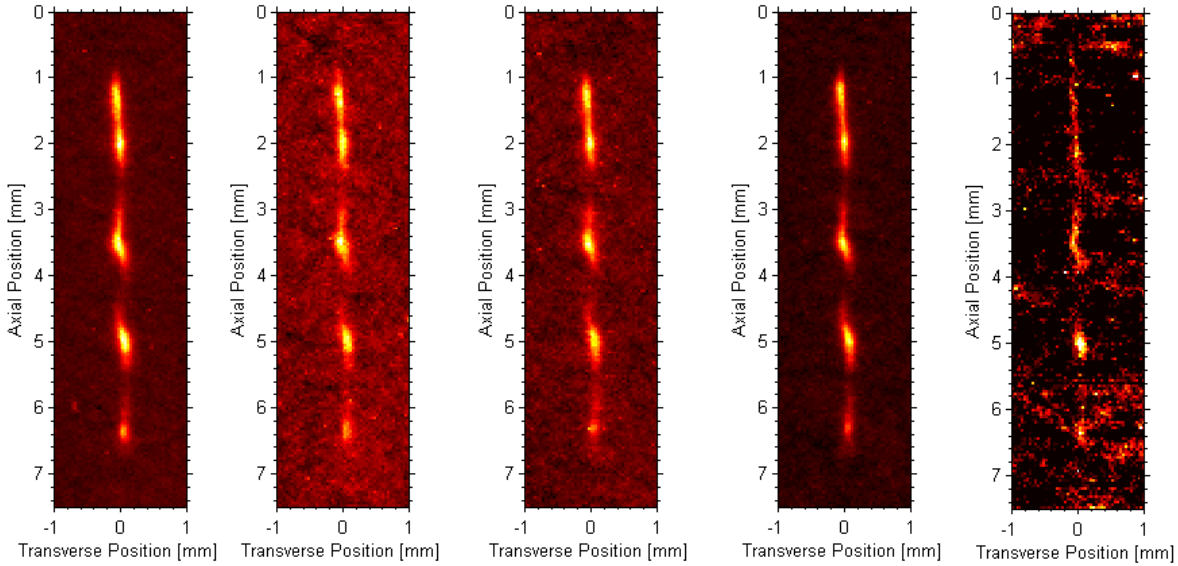

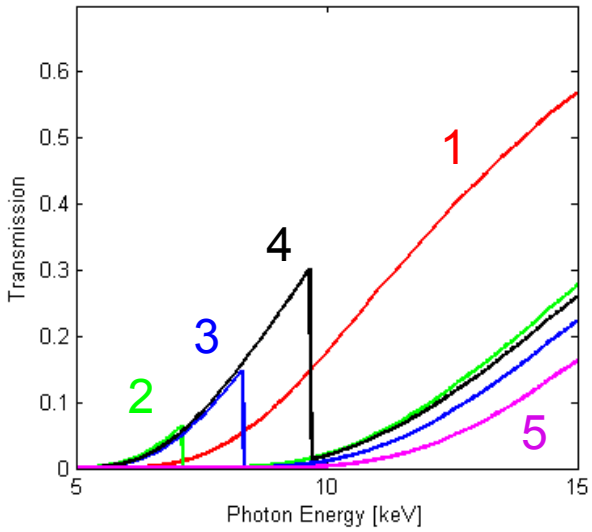

- Expected signal values for each filter are calculated assuming temperatures ranging from 0 to 8 keV and Be opacities ranging from 0 to 3 g/cm^2
- The ratio of the calculated signals are compared to the ratio of the measured signals at each axial location to find the best fit
- Temperatures range from 2 to 4 keV with an average of 3.1 keV
- Be opacities range from 0.3 to 2 g/cm^2 with an average of 1.2 g/cm^2

Absolute x-ray yield is also used to determine stagnation density

Sandia National Laboratories

- For a given volume, fuel temperature, liner opacity, and mix fraction, the average fuel density can be estimated from the absolute x-ray yield
  - Signals from calibrated PCDs and silicon diodes with various layers of Kapton filtration are used to determine the x-ray yield in different photon energy bands
  - Typically the unfolded density is approximately 0.3 g/cm^3
- Assuming our cartoon picture of stagnation, this measurement is associated with the hot core
  - The value is relatively similar to the inferred density of the D + Be mix region
- The x-ray yields correlate with neutron yield for similar targets
  - Note that variations in target materials can impact this comparison

Table of diagnostics and measured quantities

Measurement goal	Diagnostic/observed quantity	In use / improvements
Electron temperature	8-20 keV x-ray spectrum - Continuum emission slope	Yes - Time resolved
	6-8 keV x-ray spectrum - Impurity line ratios	Yes - Time resolved
	Filtered x-ray images - Image intensity ratios	Yes - Time resolved
Ion temperature	Neutron time of flight spectrum - Width of neutron peak	Yes - Space resolved
	Recoil spectrometer - Neutron tracks	No - Need DT
Morphology	Time-resolved imaging - intensity variation	Yes - resolution
	Neutron imaging - intensity variations	No - need DT
	Spherically-bent crystal imaging - intensity variations	Yes - time resolved
Plasma density	6-8 keV x-ray spectrum - Width of impurity line	Yes - Time resolved
	Filtered x-ray diodes - Absolute x-ray power	Yes - Space resolved
Burn duration	Gamma reaction history	No - need DT
Liner opacity	Neutron time of flight spectrum – down scatter ratio	Yes - collimation
	6-8 keV x-ray spectrum - depth of K edge	Yes - S/N
Magnetic field	Neutron time of flight spectrum - secondary shapes	Yes - S/N
	Activation samples – DD to DT ratio	Yes - more samples

Extra slides

Sandia National Laboratories

Magnetic flux compression demonstrated through secondary neutron yield and spectra

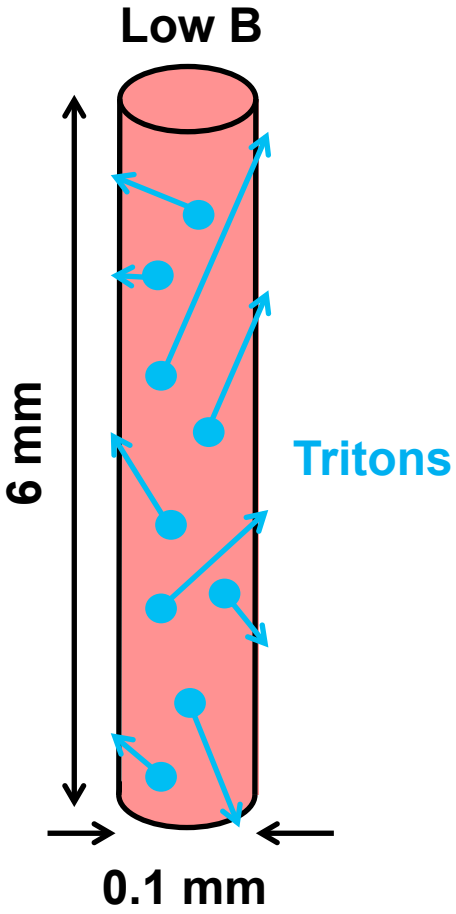

$\rho R \sim 2$ mg/cm^2
$\rho Z \sim 200$ mg/cm^2

In a high aspect ratio cylinder the effective areal density of the fuel is approximately the radial areal density

For $\rho R \sim 2$ mg/cm^2

DD/DT yield ratio > 1000

Magnetic flux compression demonstrated through secondary neutron yield and spectra

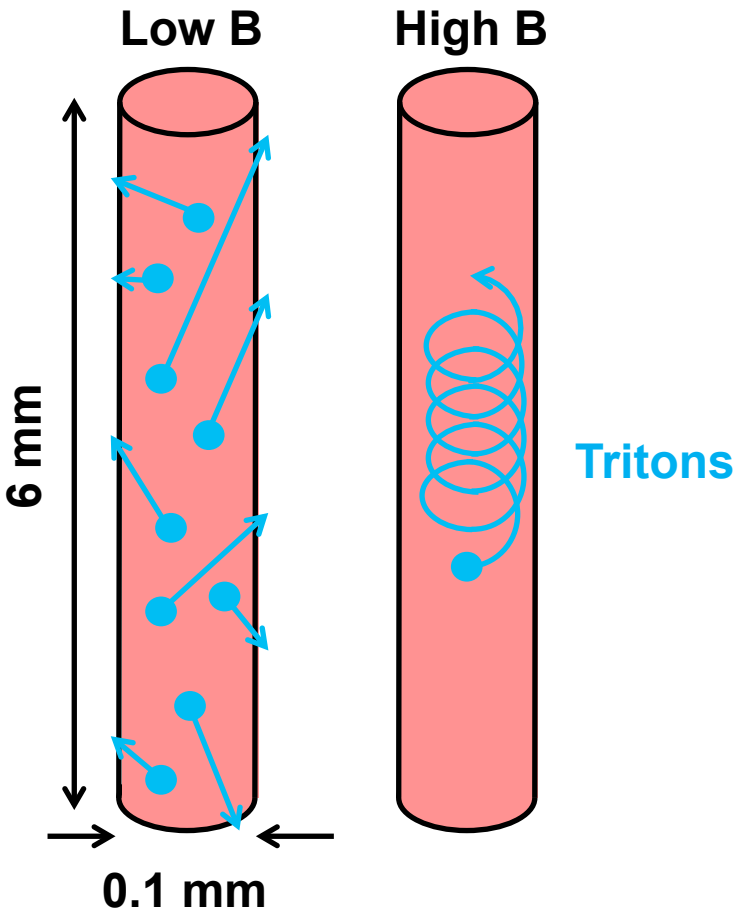

$\rho R \sim 2$ mg/cm^2
$\rho Z \sim 200$ mg/cm^2

In a highly magnetized cylinder the effective areal density of the fuel becomes much larger because the tritons cannot escape radially.

$\rho R \Rightarrow \rho Z \sim 200$ mg/cm^2

DD/DT yield ratio < 100

We observed DT yields as high as 5e10
DD/DT ~ 50-100

Magnetic flux compression demonstrated through secondary neutron yield and spectra

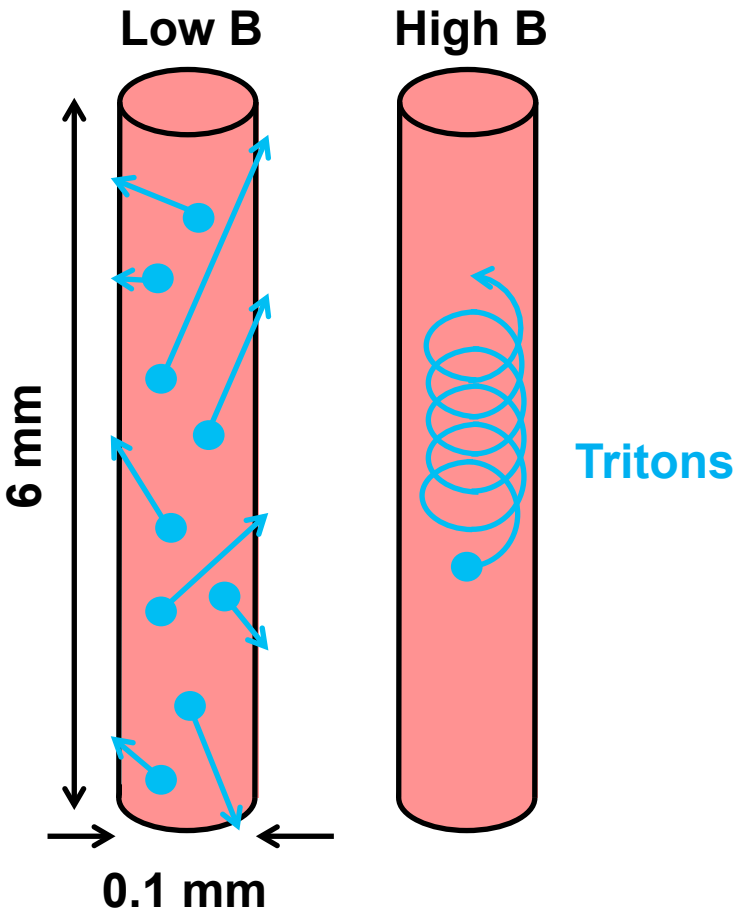

DT spectra are very sensitive to BR in this regime

As BR increases the distance between peaks in the axial spectra decreases

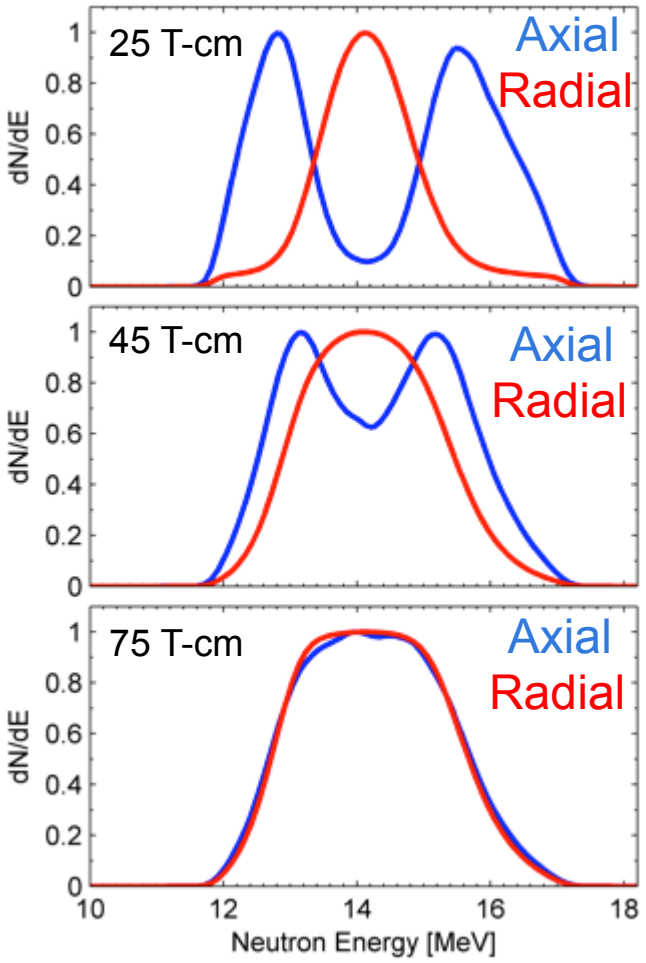

Our DT/DD yield ratio and DT spectra are consistent with BR ≈ 40 T-cm

Offline measurements confirm relatively low transmission with thick windows

Sandia National Laboratories

Transmission as a function of foil thickness for several laser spot sizes

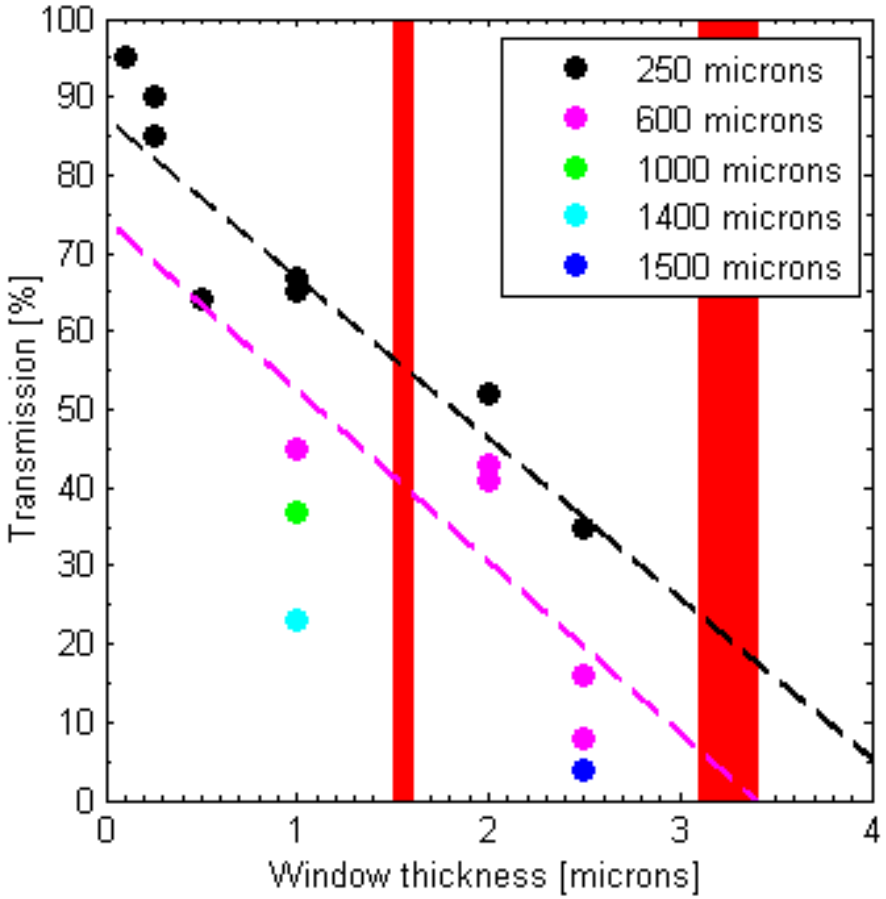

400-500 micron spot size

>3 micron thick foil

5-20% transmission

(100-400 J)

400-500 micron spot size

1.5 micron thick foil

40-60% transmission

(0.8-1.2 kJ)

Note: effects of magnetic field, fill pressure, and foil curvature not included

Energy coupled to fuel was less than expected in laser heating experiments

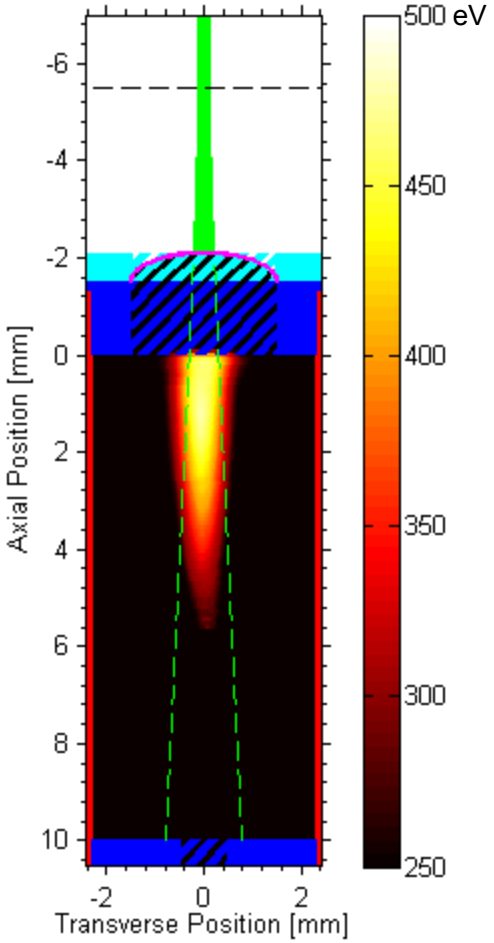

- **Measured energy is not 50% of delivered laser energy as expected**
  - **Measured energy is only 200 J**
- **Diagnostic is not sensitive to regions below 250 eV**
  - **There could be 100s of J hidden**
  - **New target and diagnostic designs to access lower temperature regions**
- **There is also unmeasured energy in the laser entrance channel**

Data with >3 micron LEH window not collected yet

We are investing in phase plates to improve our understanding of laser coupling

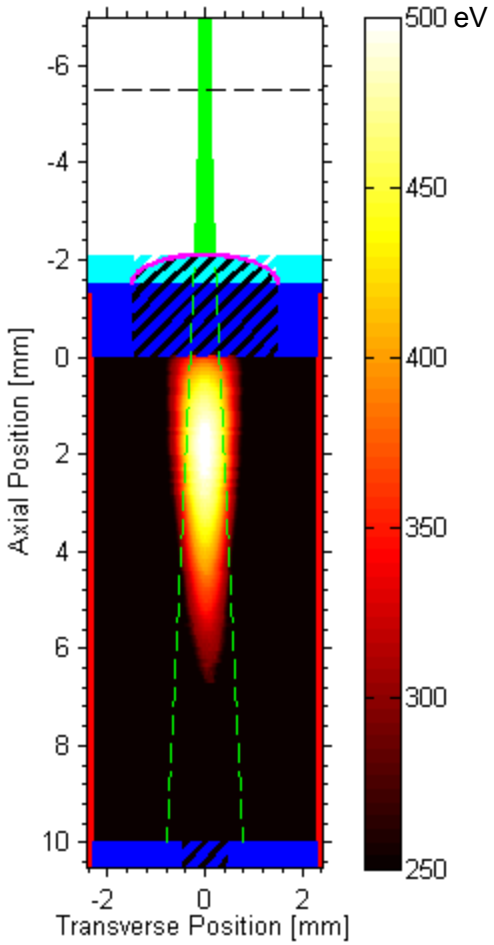

- **These efforts are expected to improve laser heating in MagLIF experiments**
- **Phase plates on loan from LLE have demonstrated improved energy deposition in laser heating experiments**
- **We have obtained our own phase plates and are starting to test them**

Neutron bang time was determined using neutron time of flight signals

Sandia National Laboratories

Neutron velocity

$$v = L_b - L_a / t_b - t_a$$

Five neutron time of flight (NTOF) detectors were located at five different distances from the source

Neutron bang time

$$t_0 = L_b t_a - L_a t_b / L_b - L_a$$

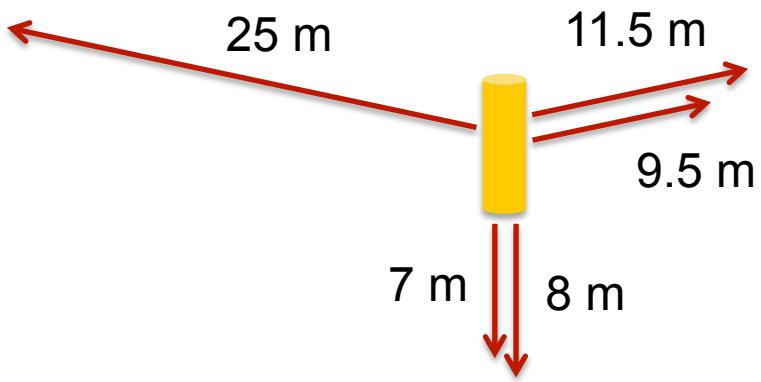

L is the detector distance
t is the arrival time

Using each permutation of pairs of detectors, the neutron bang time was determined typically to within 1 ns

Stagnation duration is determined using time-resolved x-ray diagnostics

Sandia National Laboratories

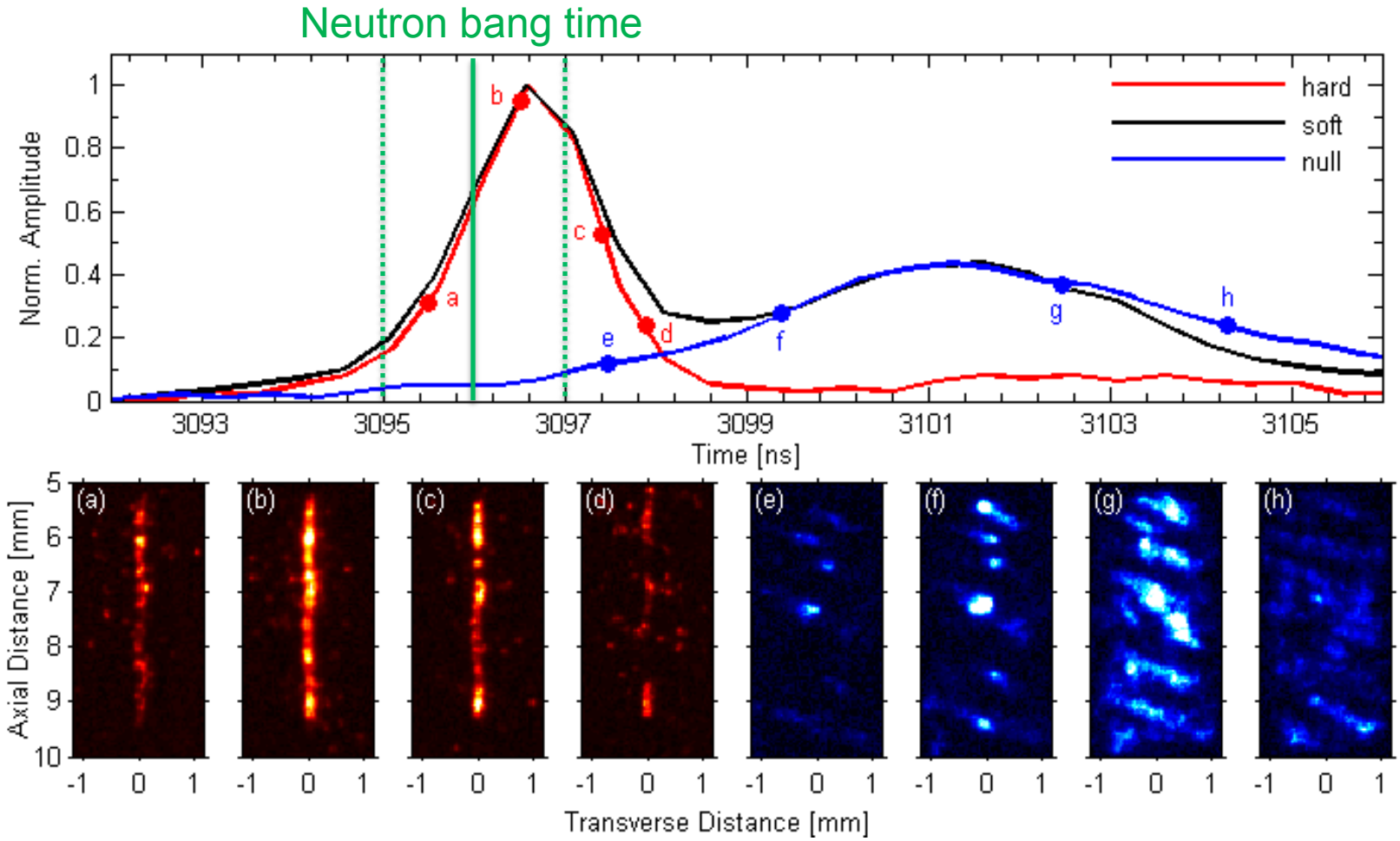

Narrow x-ray emission column observed at neutron bang time

THE PHYSICS OF STAGNATION IN MAGNETICALLY DRIVEN IMPLOSIONS AT Z

Patrick Knapp

Exceptional service in the national interest

Sandia National Laboratories

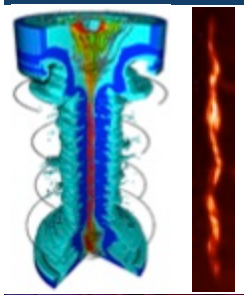

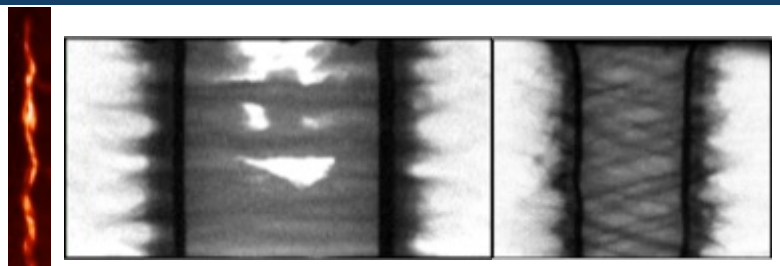

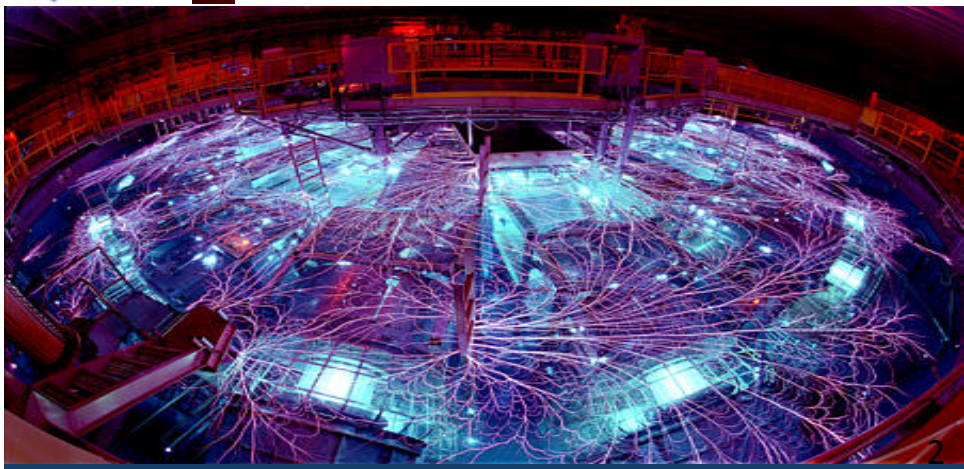

U.S. DEPARTMENT OF ENERGY

NNSA

Sandia National Laboratories is a multi-program laboratory managed and operated by Sandia Corporation, a wholly owned subsidiary of Lockheed Martin Corporation, for the U.S. Department of Energy's National Nuclear Security Administration under contract DE-AC04-94AL85000.

As always, many people contributed to this talk….

Matt Gomez[1], Stephanie Hansen[1], Paul Schmit[1], Kelly Hahn[1], Dean Rovang[1], Gordon Chandler[1], Eric Harding[1], Chris Jennings[1], Steve Slutz[1], Adam Sefkow[1], Dan Sinars[1], Kyle Peterson[1], Mike Cuneo[1], Ryan McBride[1], Tom Awe[1], Matt Martin[1], Carlos Ruiz[1], Gary Cooper[1], Bill Stygar[1], Mark Savage[1], Mark Herrmann[3], Gregory Rochau[1], John Porter[1], Ian Smith[1], Matthias Geisel[1], Patrick Rambo[1], Jens Schwarz[1], Brent Blue[2], Kurt Tomlinson[2], Diana Schroen[2], Robert Stamm[4], Ray Leeper[5], Charlie Nakleh[5]

… And many many more

[1]Sandia National Laboratories, Albuquerque, NM
[2]General Atomics, San Diego, CA
[3]Lawrence Livermore National Laboratory, Livermore, CA
[4]Raytheon Ktech, Albuquerque, NM
[5]Los Alamos National Laboratory, Los Alamos, NM

Nuclear diagnostics are extremely challenging on Z due to the unique environment

- Challenges of diagnosing neutrons on Z
- Primary DD neutrons and down-scatter
- Secondary DT neutrons and magnetic field

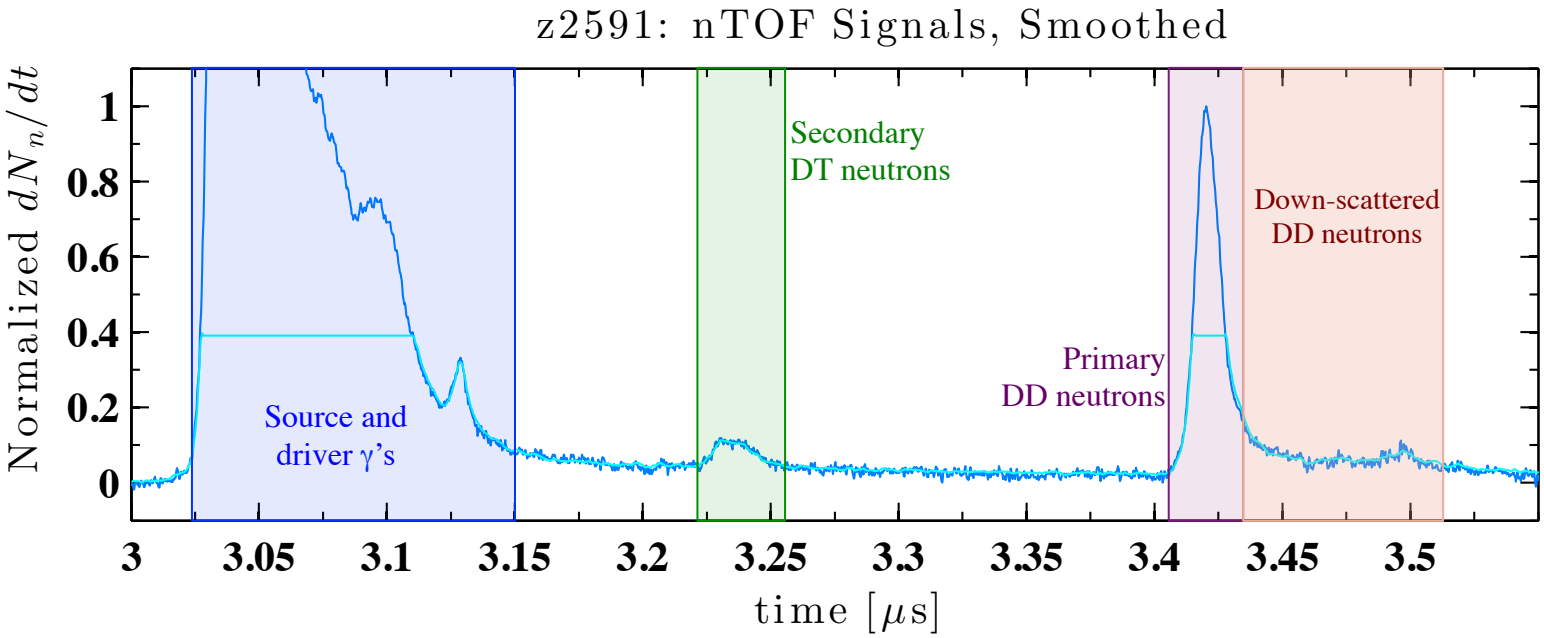

Z produces copious background radiation, resulting in high sensitivity floors

In MagLIF experiments, we can distinguish between a single source occurring near the x-ray pulse, and multiple sources with ~5ns separation

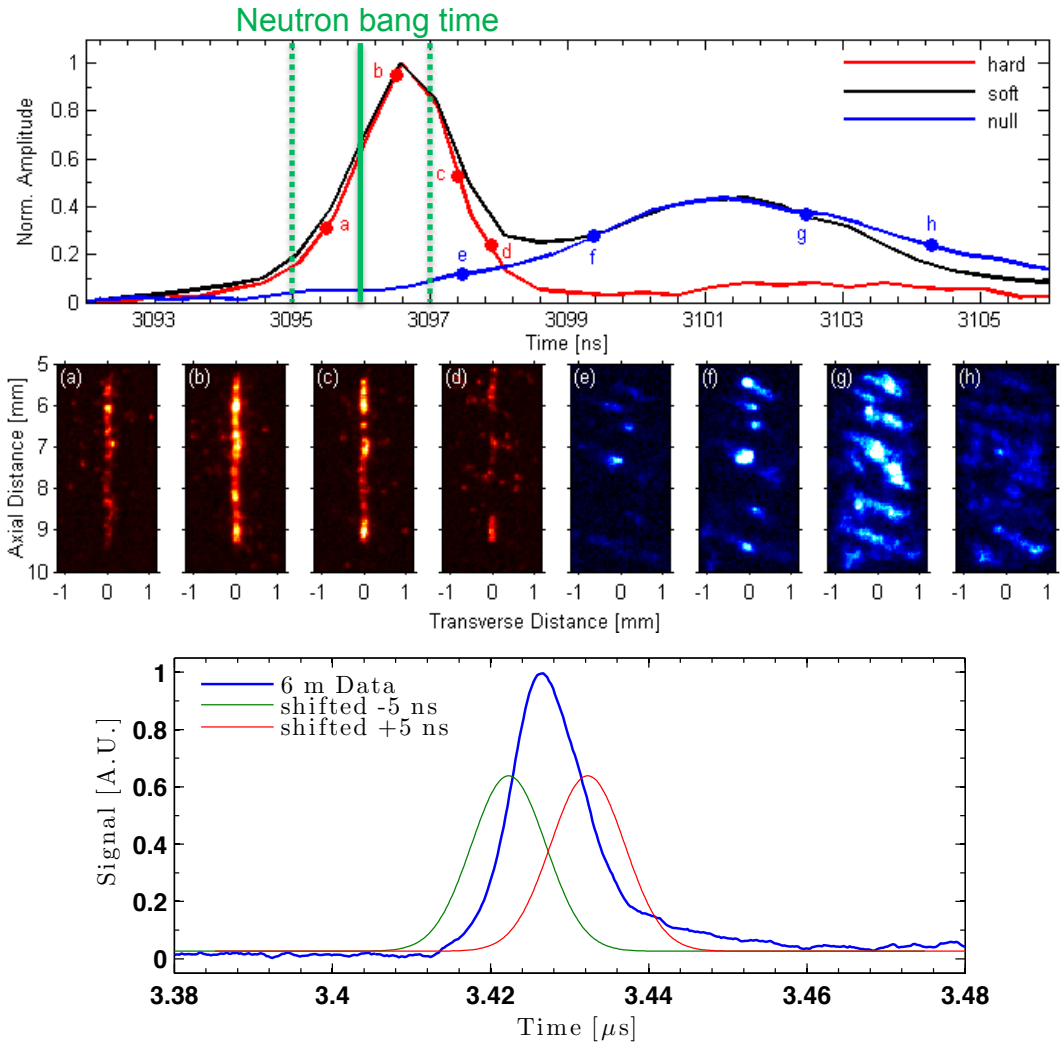

- Our closest nTOF is 6 m from the source, located underneath
- With 2-3 keV ion temperatures we could easily tell if additional neutrons were being produced post-stagnation
- If temperatures get much higher, a time-integrated spectrometer and burn history diagnostic would prove invaluable

Primary DD neutrons to date inform us of yield and ion temperature

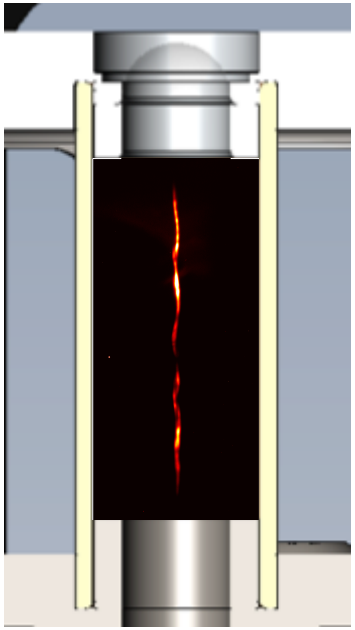

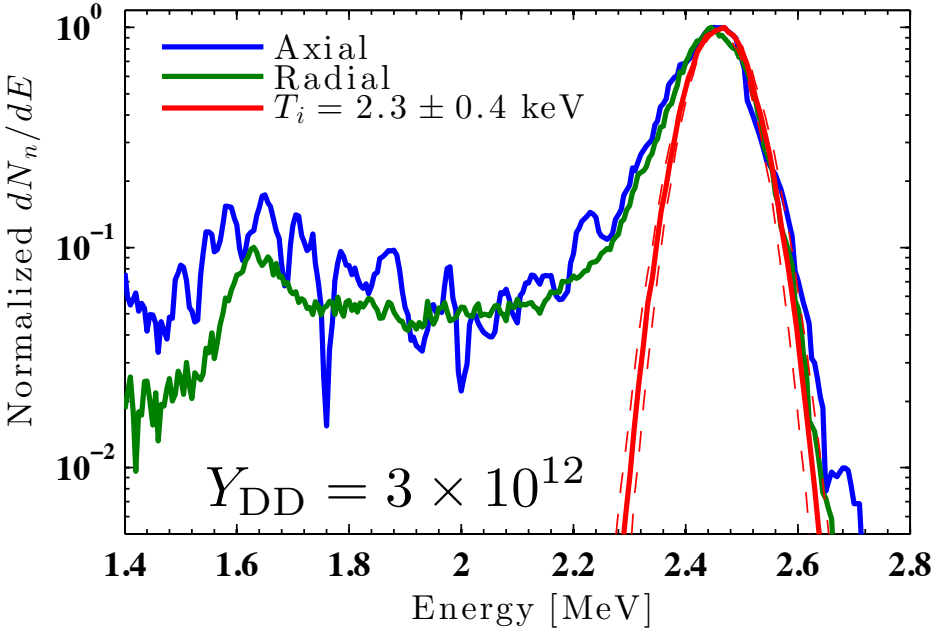

Don't have an absolute energy scale from nTOF's

This would be helpful for understanding residual motion

- Highly isotropic primary yields and spectra
- Ion temperatures are generally ~1-3 keV, generally scale with yield
- Uncertainties are large due to low SNR
- Down scatter can tell us about liner areal density, but scattering in the Z environment is significant and poorly quantified

Preliminary modeling of Be down-scatter shows trends, but does not include "environmental" scattering

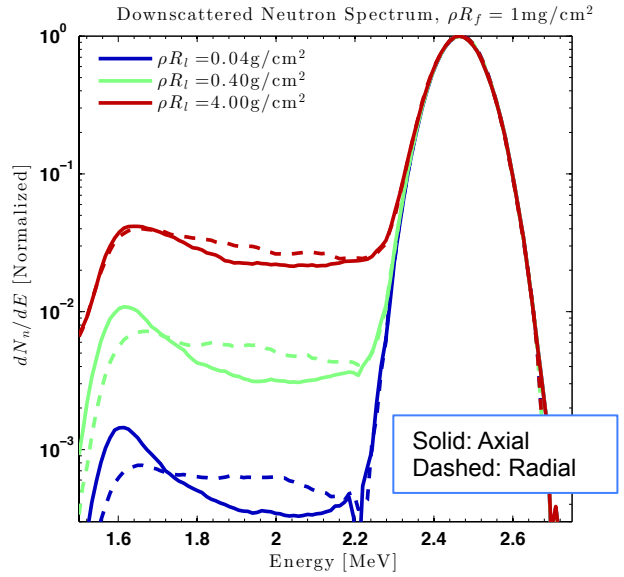

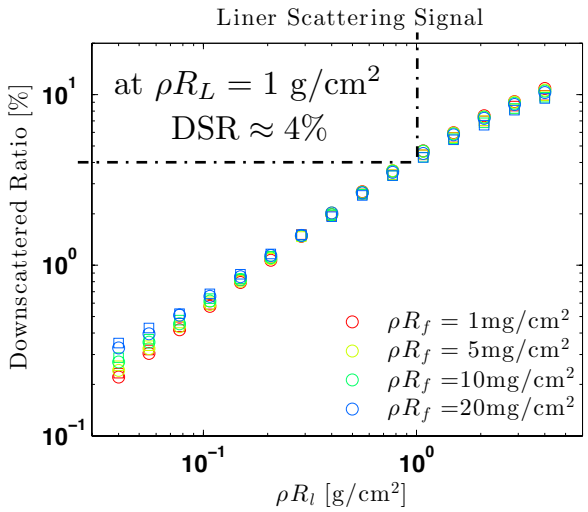

- Liner provides inertial confinement during burn
- DSR is ~linear with liner ρR
- Weak Dependence on fuel
- The viewing direction doesn't appreciably affect the integrated DSR because on average neutrons see same liner ρR, regardless of your viewing direction
- Spectrum does change:
  - Axial view is more "peaky" at the Be peak than the radial view and has a more pronounced dip
  - Dip is more pronounced because the differential cross-section prefers scattering at 0 or 180 degrees

$$DSR \equiv \frac{\int_{1.5}^{2.2} dN_n/dEdE}{\int_{2.2}^{\infty} dN_n/dEdE}$$

Magnetization ("BR") reduces ρR requirements for α deposition and minimizes electron heat losses

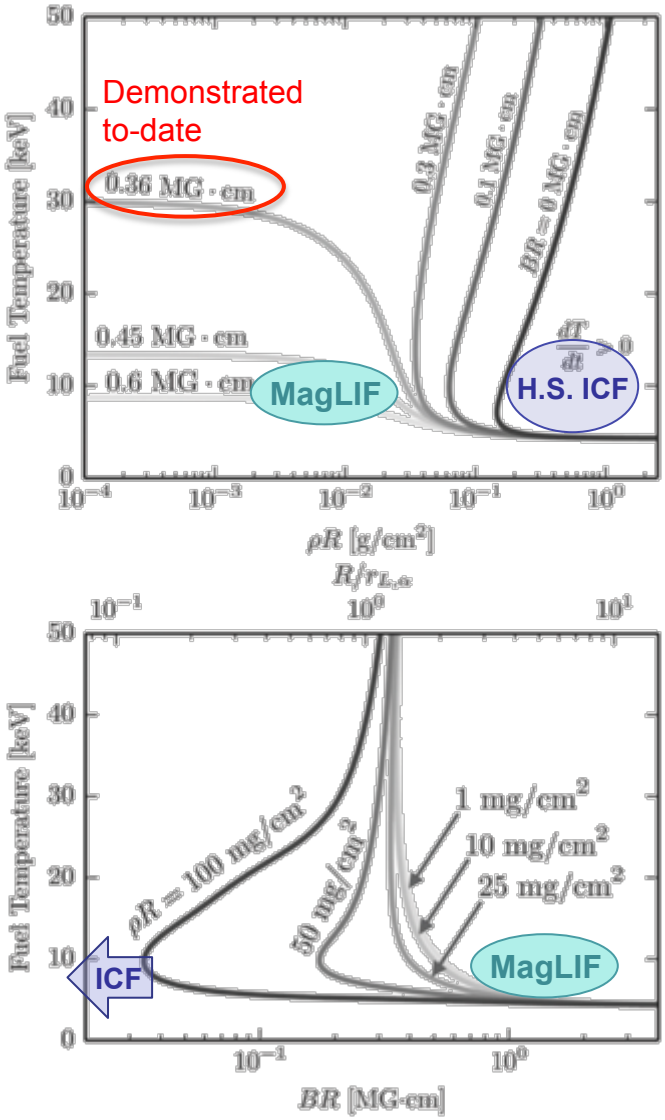

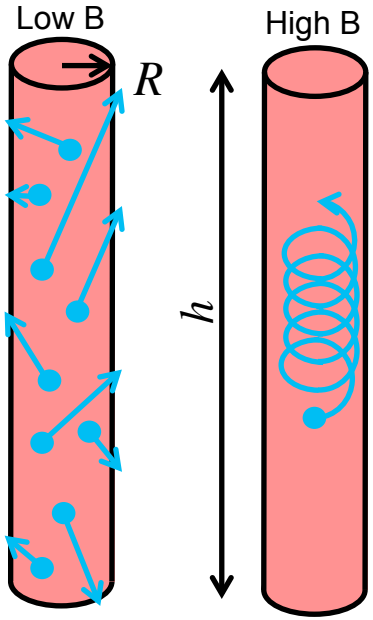

- Fraction of trapped a's (tritons) is a function of ***BR*** only*
- At BR>0.5 MG-cm the effects saturate (particles are well confined).
- Areal density responsible for ranging out α's is ρh, no ρR
- Measurements to date suggest >0.3 MG-cm!

$$\frac{R}{r_\alpha} = \frac{BR\ [T\cdot\mathrm{cm}]}{26.5} = \frac{BR\ [G\cdot\mathrm{cm}]}{2.65e5} \approx 4BR\ [MG\cdot\mathrm{cm}]$$

Pressing need to measure compressed flux at stagnation, but familiar techniques like proton probing don't work

$$B_\theta \gtrsim 50\ \mathrm{MG} \qquad r_g^{1\ \mathrm{MeV}} \approx 200\mu\mathrm{m}$$

*P.F. Knapp *et al.*, Phys. Plasmas **22**, 056312(2015)

Secondary DT neutrons can inform us about the compressed magnetic flux at stagnation

DD Fusion Reaction Branches

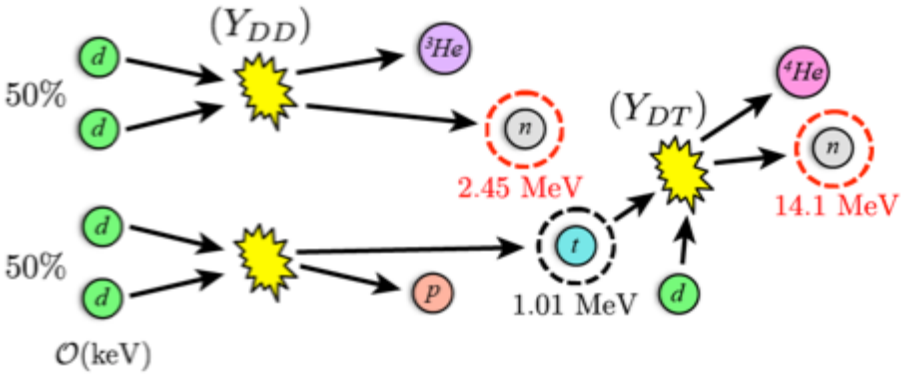

- In limit of low ρR, increasing BR serves primarily to extend triton path length
- Magnetizing tritons effectively modifies the geometry they "see" as they travel through the fuel

Probability of a triton reacting with a background deuteron:

$$P_i(\ell) = \int_0^{\ell} n_d(s)\sigma_{DT}(v_i(s))ds \approx n_d\sigma_{DT}\ell$$

Unmagnetized

$$\frac{Y_{2n}^{DT}}{Y_{1n}^{DD}} \propto \rho R$$

Magnetized

$$\frac{Y_{2n}^{DT}}{Y_{1n}^{DD}} \approx f(BR, \rho R)$$

Triton reactions are modeled using a combination fully kinetic LFP model and MC reaction kinetics

Kinetic Model[5,6]

- Landau-Fokker-Planck model, **No** stopping power models used
- Election-ion **AND** ion-ion collisions captured
- Ions are tracked accurately in magnetic field
- 1D isobaric fuel profiles w/ non-uniform *B*
- Can use spheres or cylinders
- No B_ϕ or axial variations

MonteBurns[6,7] **Reaction Modeling**

- Calculates neutron spectra and reaction probability for each triton quasi-particle
- ENDF differential cross-section data used
- Calculate spectra from multiple viewing angles

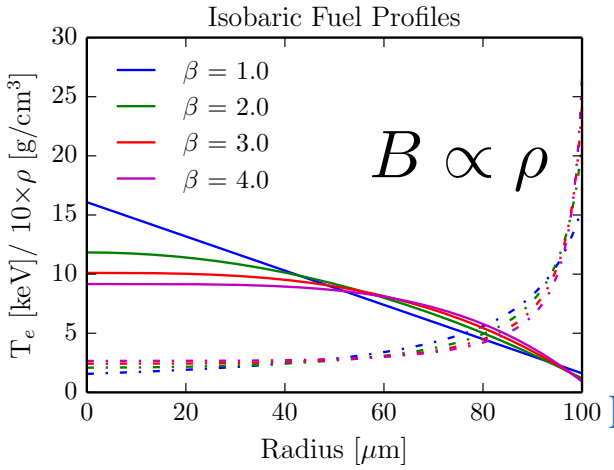

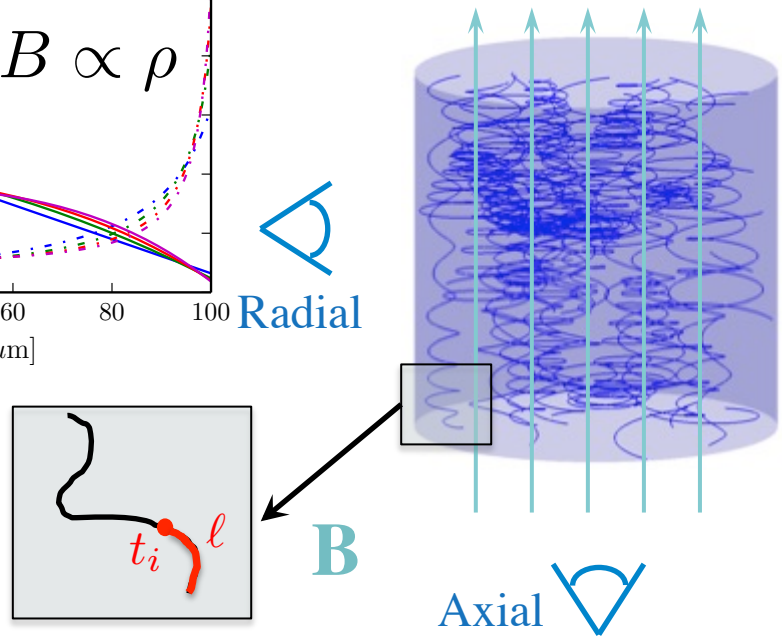

$$P_i(\ell) = \int_0^\ell n_d(s)\sigma_{DT}(v_i(s))ds \approx n_d\sigma_{DT}\ell$$

[5] P.F. Schmit, P.F. Knapp *et al*. Phys. Rev. Lett. **113**, 155004 (2014)
[6] P.F. Schmit *et al.*, Phys. Plasmas **20**, 112705 (2013)
[7] P.F. Knapp *et al.,* Phys. Plasmas **20**, 062701 (2013)

Magnetizing the tritons modifies their trajectories, imprinting on DT spectrum

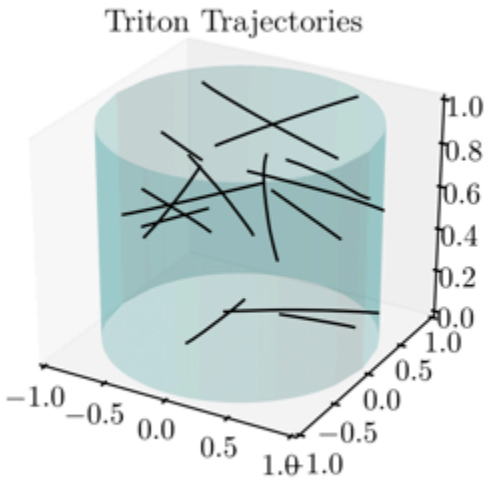

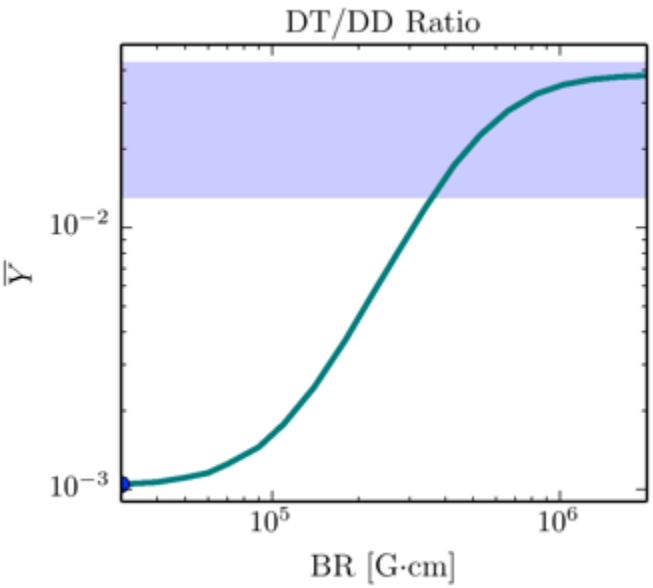

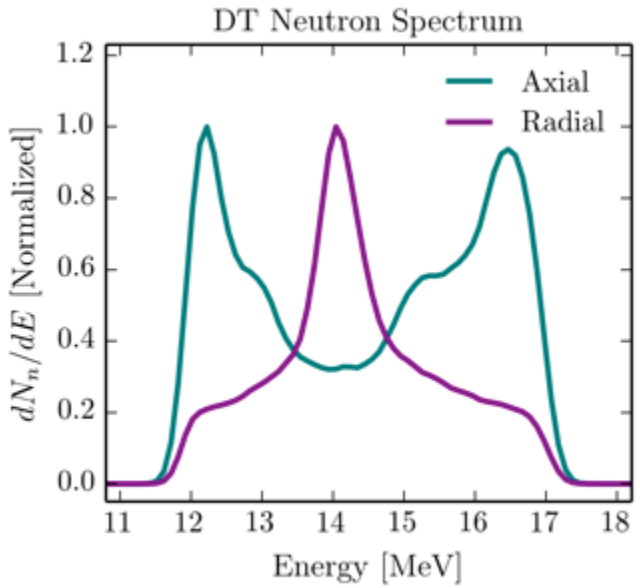

- Magnetization serves to:
  - Trap tritons
  - Direct them axially
  - Execute helical orbits
- Axial redirection forces tritons to see ρZ instead of ρR
  - $\rho Z = \mathrm{AR} * \rho R, \mathrm{AR} >> 1$
  - broadens the velocity distribution of tritons that have a significant probability of reaction

At large BR, helical orbits induce Doppler splitting in the radial view

Magnetizing the tritons modifies their trajectories, imprinting on DT spectrum

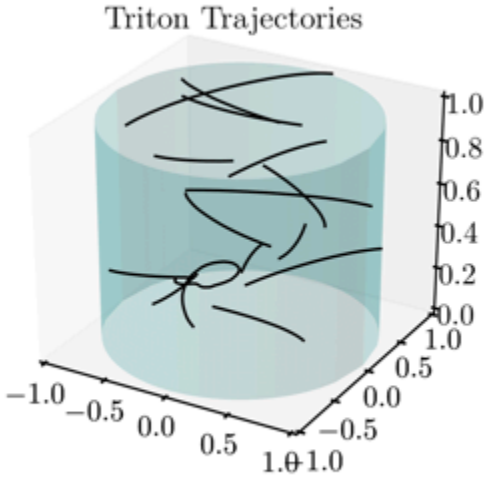

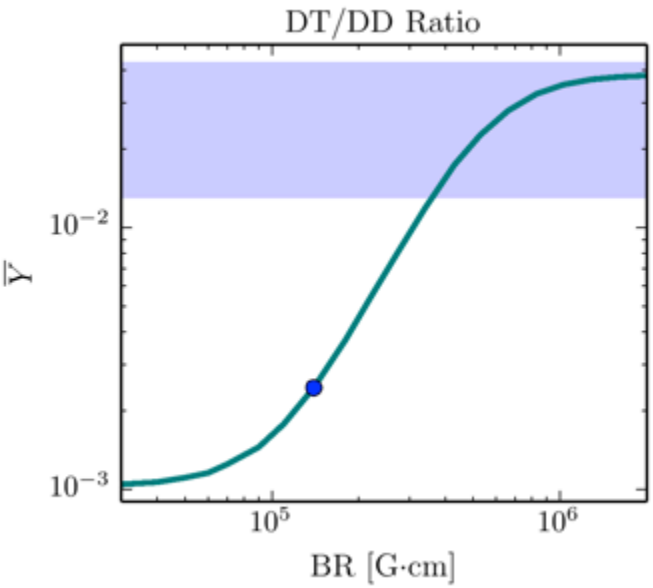

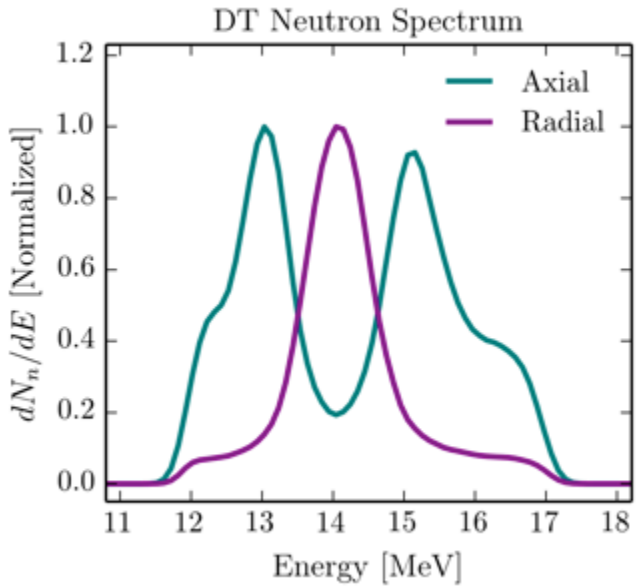

- Magnetization serves to:
  - Trap tritons
  - Direct them axially
  - Execute helical orbits
- Axial redirection forces tritons to see ρZ instead of ρR
  - $\rho Z = \mathrm{AR} * \rho R, \mathrm{AR} >> 1$
  - broadens the velocity distribution of tritons that have a significant probability of reaction

At large BR, helical orbits induce Doppler splitting in the radial view

Magnetizing the tritons modifies their trajectories, imprinting on DT spectrum

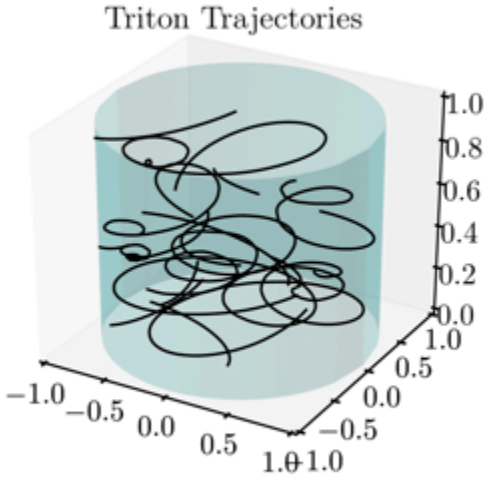

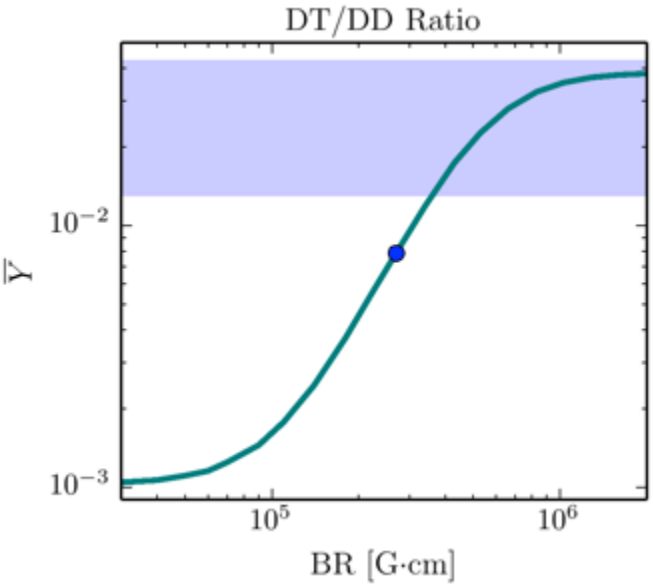

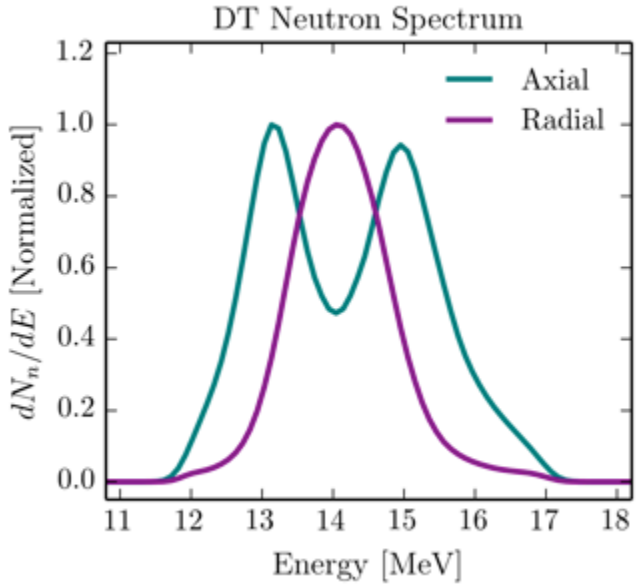

- Magnetization serves to:
  - Trap tritons
  - Direct them axially
  - Execute helical orbits
- Axial redirection forces tritons to see ρZ instead of ρR
  - $\rho Z = \mathrm{AR} * \rho R, \mathrm{AR} >> 1$
  - broadens the velocity distribution of tritons that have a significant probability of reaction

At large BR, helical orbits induce Doppler splitting in the radial view

Magnetizing the tritons modifies their trajectories, imprinting on DT spectrum

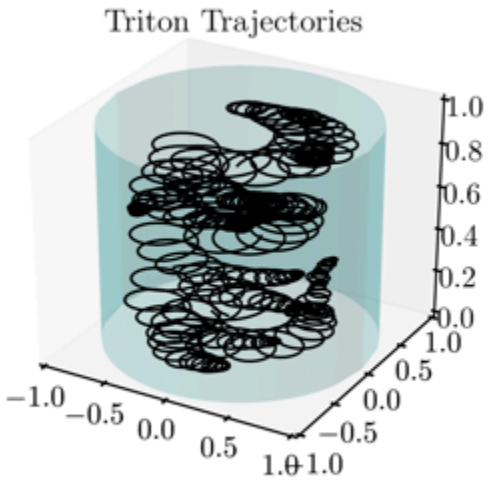

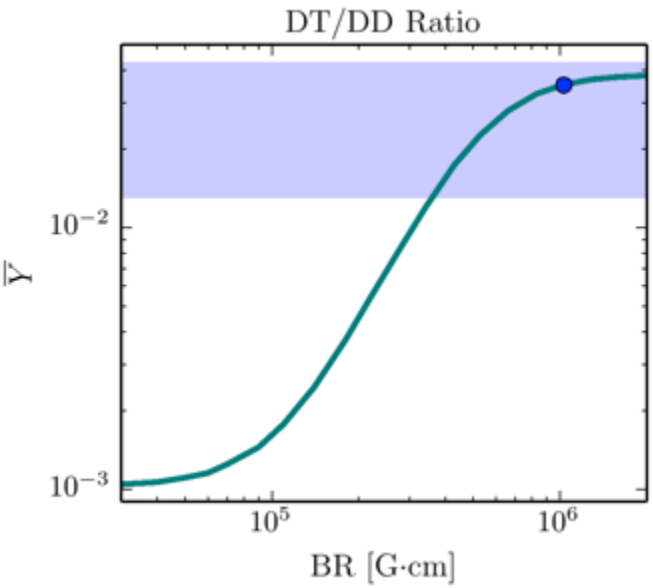

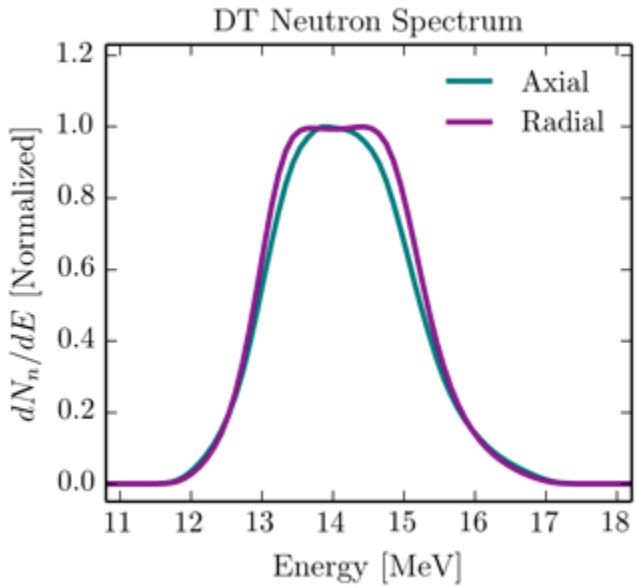

- Magnetization serves to:
  - Trap tritons
  - Direct them axially
  - Execute helical orbits
- Axial redirection forces tritons to see ρZ instead of ρR
  - $\rho Z = \mathrm{AR} * \rho R, \mathrm{AR} >> 1$
  - broadens the velocity distribution of tritons that have a significant probability of reaction

At large BR, helical orbits induce Doppler splitting in the radial view

DT Spectra are used in conjunction with measured DT/DD ratio to constrain the stagnation *BR*

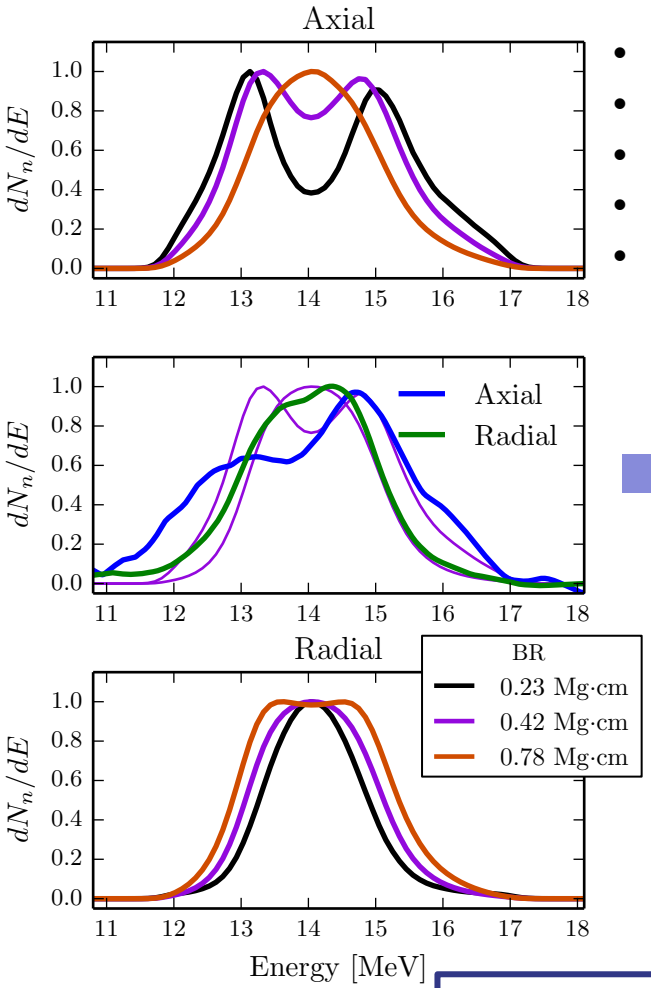

- $T_i \sim T_e$=3.1 keV
- ρ=0.5 g/cc
- R=50–100 μm
- ρR=2-5 mg/cm^2
- ρZ~0.3 g/cm^2

- Not a rigorous fit to the spectra
- Considering only the high energy half of the spectra (scattering)
- In reasonable agreement with integrated 2D simulations[*]

$$(B_z R)_{stag} = 5.3 \times 10^5 G \cdot \mathrm{cm}$$

$$F_t \approx 55\%$$

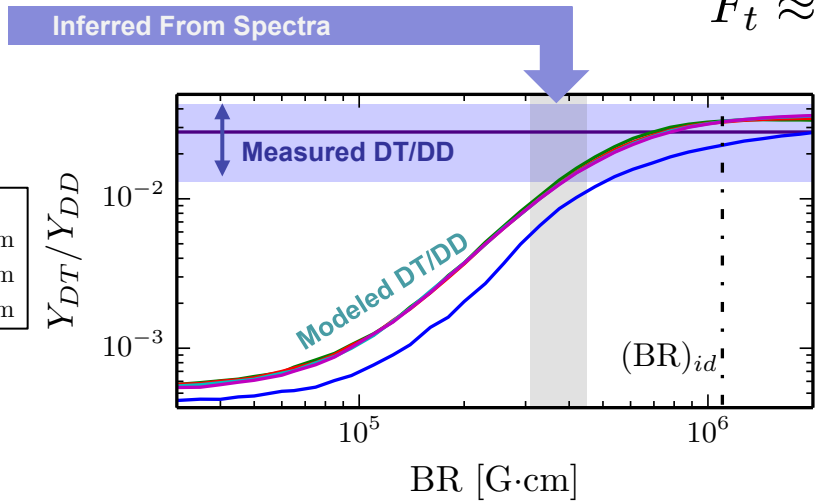

Axial nonuniformities and azimuthal field are the biggest missing features that can contribute to the modeled spectra

$$BR \approx 3.4(+1.4/-0.6) \times 10^5 \ \mathrm{G \cdot cm}, \sim 14 \times (BR)_o$$

[*] A.B. Sefkow, *et al.*, Phys. Plasmas, **21** 072711 (2014)

Experimentally inferred stagnation *BR* indicates we are trapping 1 MeV tritons and magnetizing electrons

- Modeling suggests we are depositing >35% of the triton energy
- Scales to >40% α deposition

$$BR \sim 4 \times 10^5 G \cdot \mathrm{cm} \rightarrow \frac{R}{r_\alpha} \sim 1.5 - 2$$

$$r_\alpha \approx 1.07 r_t$$

- Magnetizing fast tritons implies electrons are magnetized as well

$$\omega_{ct}\tau_{te} \approx \omega_{ce}\tau_{ee}$$

MagLIF works! We were able to compress flux, preheat the plasma and keep it hot, and magnetize the burn products!

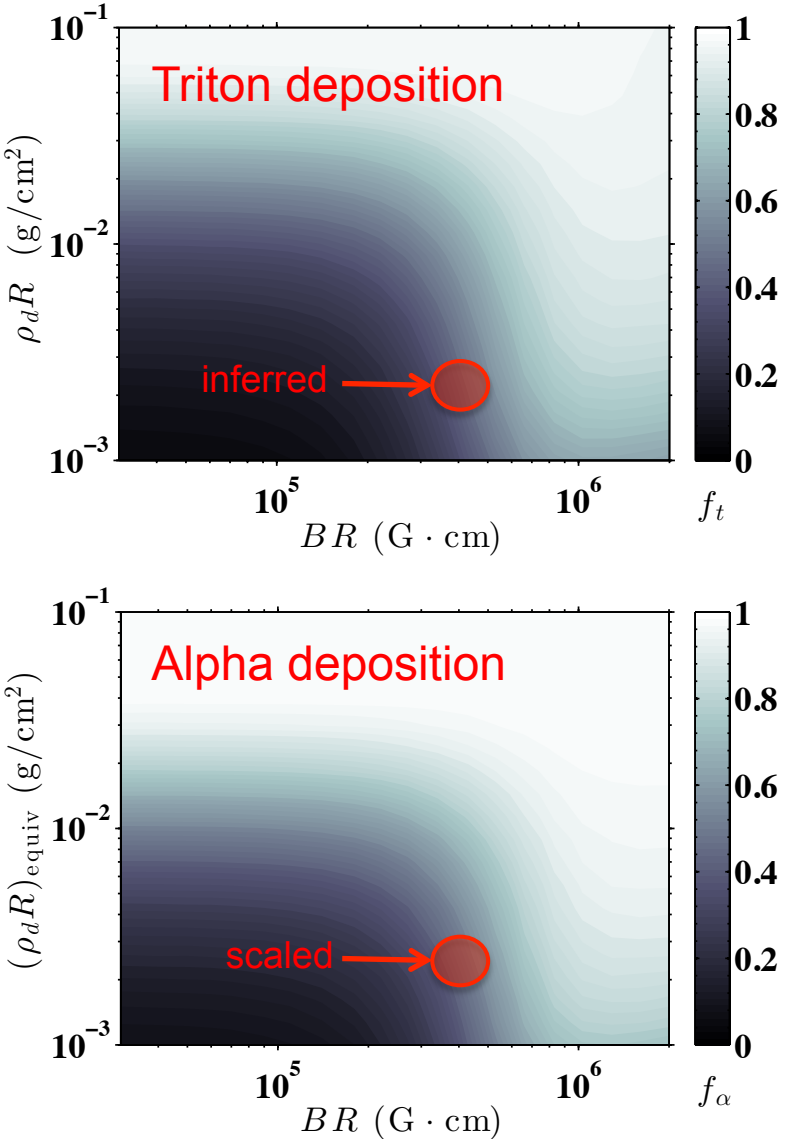

Currently using D2 fuel, DT would enable significant diagnostic advances

Sandia National Laboratories

- The Z facility and operations were not designed w/ tritium in mind
  - People enter chamber everyday
  - Entire center section is unloaded and manually refurbished
  - Facility has massive tanks of oil and water (~1000's of gallons)
- Routine use of tritium would enable or simplify
  - Magnetic Recoil Spectrometer
  - Burn history
  - Neutron imaging (primary and downscatter)
- Each of these would allow us to build on our understanding and better constrain our interpretations
- Would require us to rethink B-field measurement
  - May not be necessary if performance improves
  - May be able to use tertiary reactions to probe BR

We need the community's help to push our nuclear diagnostics further and learn more about stagnation in this interesting regime

- How can we field a burn history diagnostic on Z?
- How can we obtain better quality primary and secondary neutron spectra?
- How can we better understand the environmental influences on these measurements?
- Neutron Imaging

Stagnation is a fundamental concept that can be explored in a number of different ways

Sandia National Laboratories

- The key concepts that effect burn during stagnation are:
  - Stability and confinement
  - Conversion of kinetic to thermal energy
  - Mix

→ **All fundamentally 3D processes**

- These are all interrelated, but we can design experiments that minimize some aspects to look at others
  - **D_2 Gas puff**: Platform to look at energy conversion and non-thermal effects
    - High velocity (700-1000 km/s), low ρR (similar to exploding pusher)
    - No mix and no opacity
    - Ideal for studying residual kinetic energy, velocity distributions, thermalization processes, and non-thermal effects, electron-ion coupling
  - **Cold Compression**: Platform to Stability and confinement
    - Low velocity (25-50 km/s)
    - High pressure, high density allows long dwell time
    - Low atwood number limits decel-instability growth
    - Ideal for studying stagnation and confinement dynamics, symmetry effects

Deuterium gas puffs provide high velocity, high convergence implosions with no mix and no opacity

Sandia National Laboratories

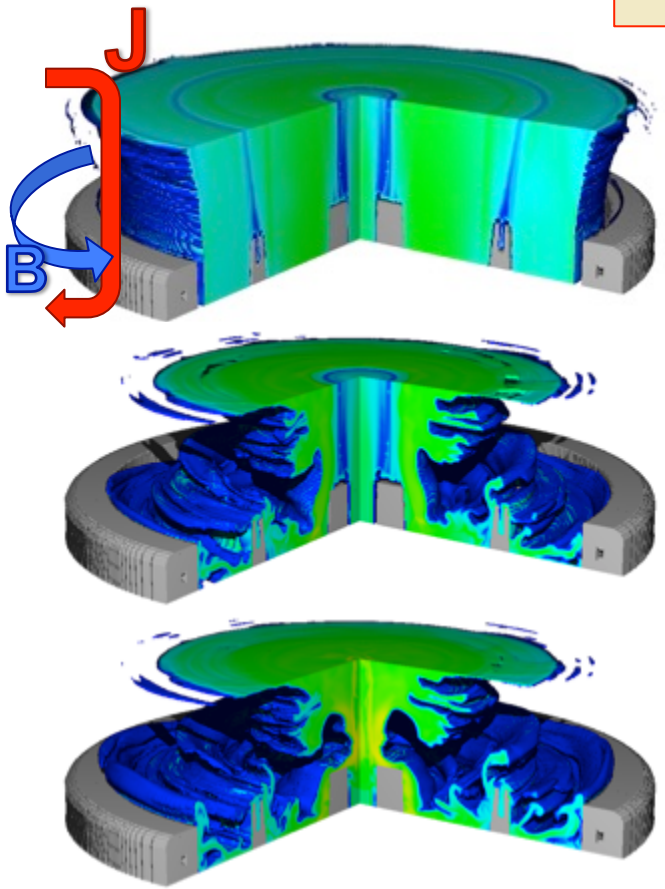

Produced 4x10^{13} DD neutrons

Doppler splitting: vel. = 500-700 km/s

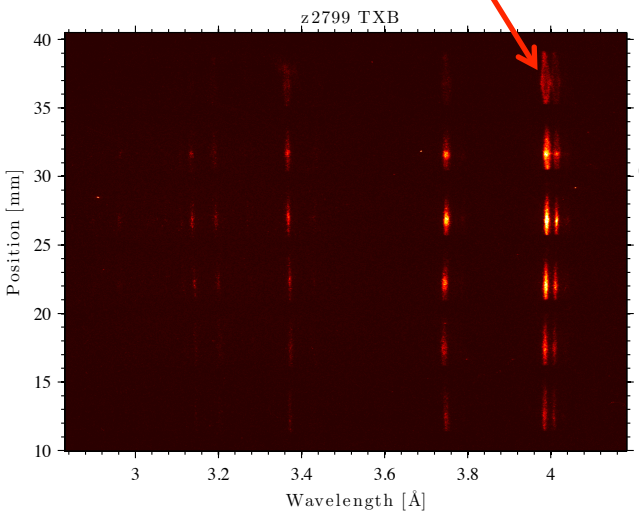

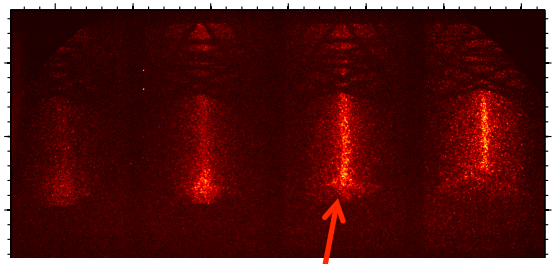

~1 mm radius pinch

- Ideal for studying the conversion of kinetic to thermal energy
- Study line broadening with neutrons and x-rays
- Also study non-thermal processes (e.g. "beam-target" neutrons)
- Working with Yitzhak Maron to analyze spectra

Neutron spectral analysis is complicated by the long source duration

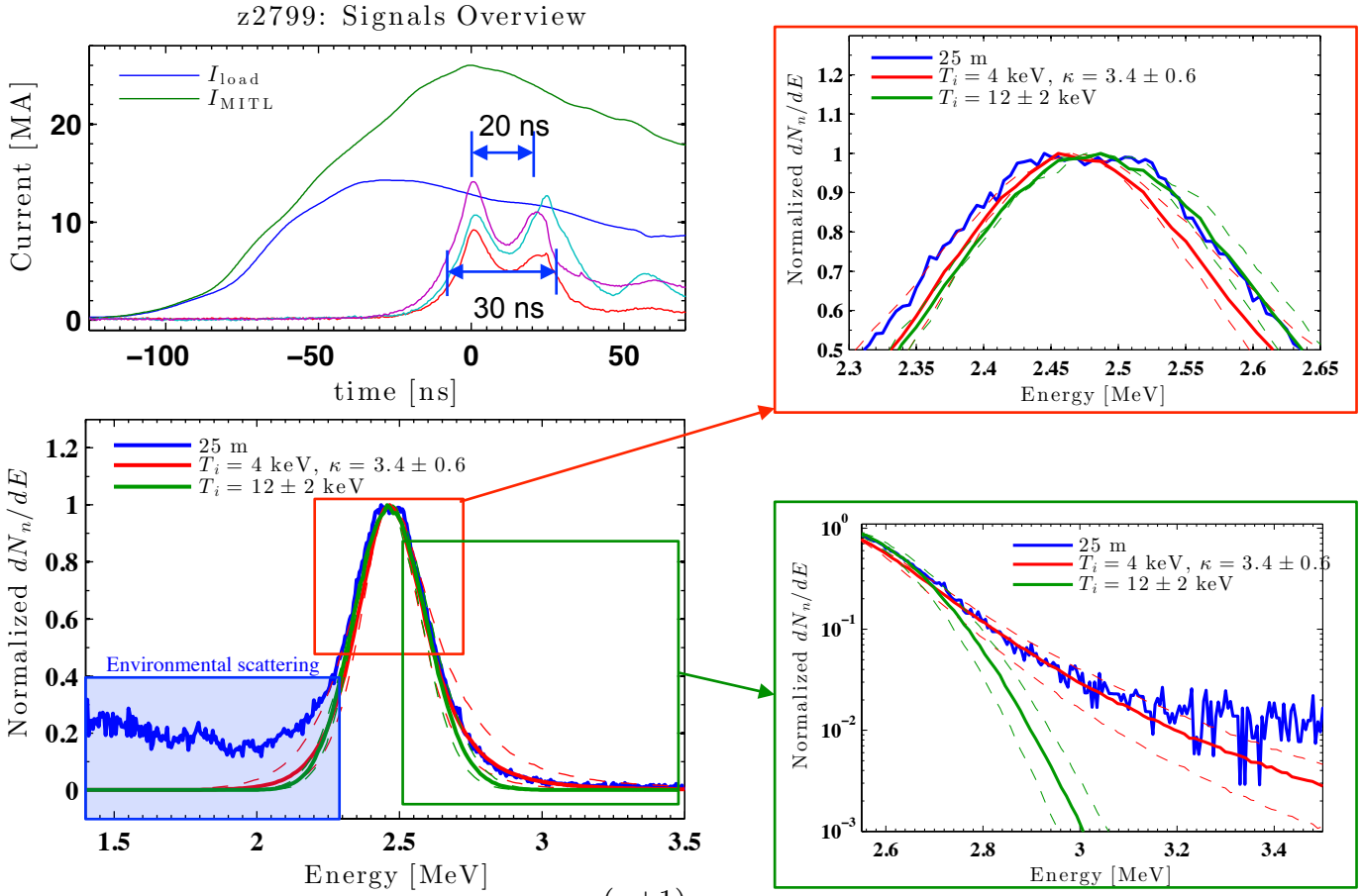

$$f_\kappa(v) = \frac{A_\kappa}{2\pi v_T^3}\left(1 + \frac{v^2}{(2\kappa - 3)v_T^2}\right)^{-(\kappa+1)}$$

$$A_\kappa = \frac{(2\kappa-3)^{-3/2}\Gamma(\kappa+1)}{\Gamma(\kappa-1/2)\Gamma(3/2)} \quad v_T = \sqrt{\frac{k_b T}{m}}$$

- Can fit spectrum well with different models
- Potentially sensitive to peak location, poorly known due to lack of absolute energy calibration
- Source duration effects can impact spectrum, even at 25 m
- High energy tail contains important information, but noisy
- Need a well-calibrated, well-shielded, time-integrated DDn spectrometer
- Need burn history to resolve some issues

We achieved a stable stagnation at ~100 Mbar and CR=7.6

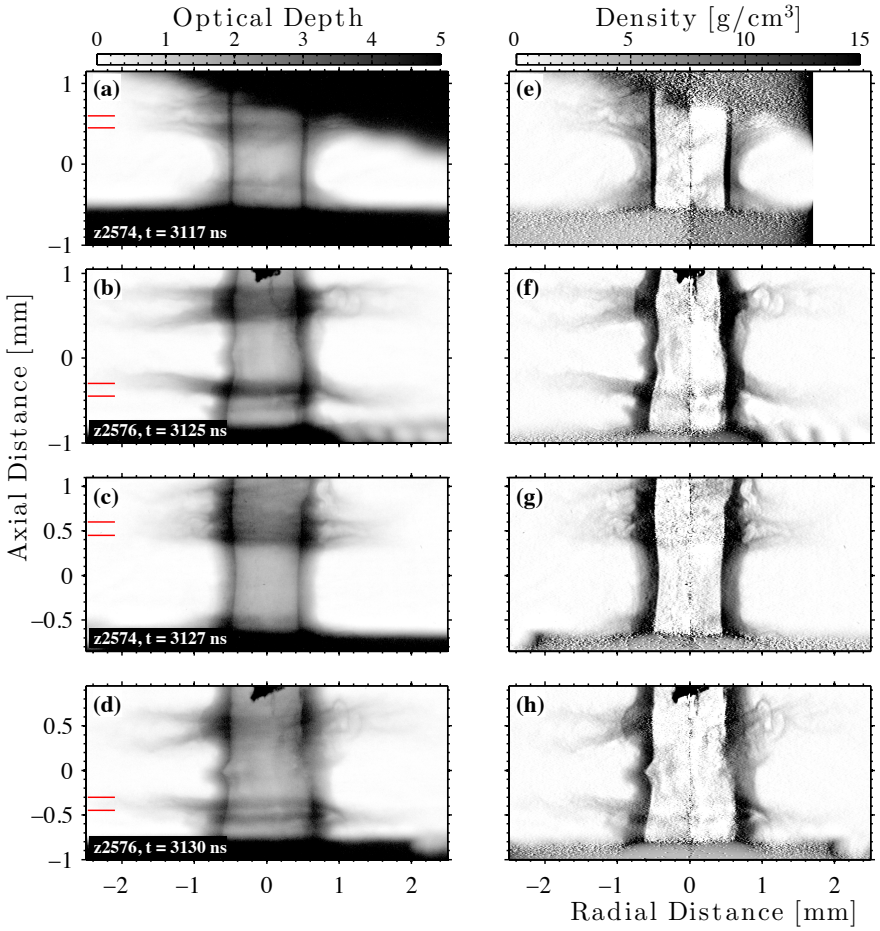

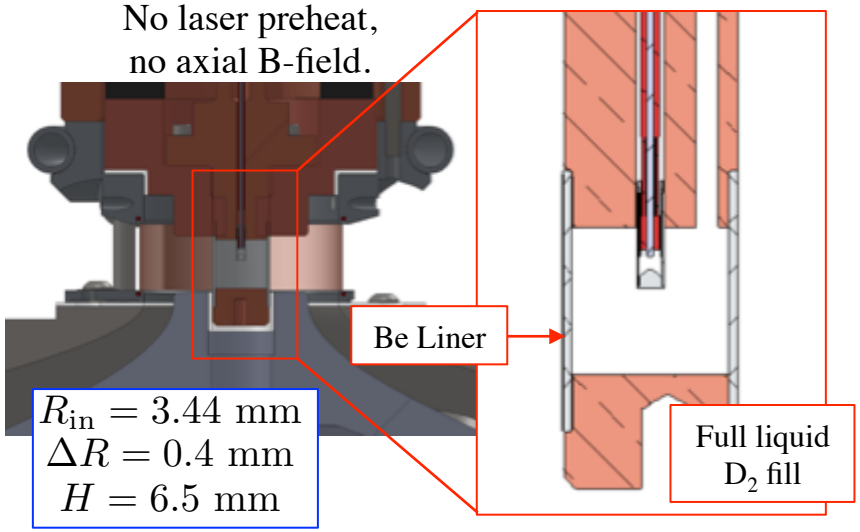

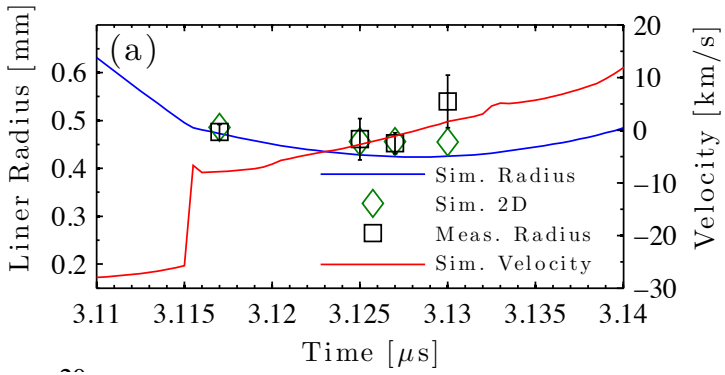

$$R_{\rm stag} = 450\ \mu{\rm m} \quad \Theta = k_B T/E_{\rm F} \approx 0.05$$
$$\rho_D = 10\ {\rm g/cm}^3 \quad \Gamma = ze^2/ak_B T \approx 6$$

- Excellent agreement with 1D simulations early in stagnation
- Deuterium is degenerate and strongly coupled at stagnation
- Disassembly is faster than 1D or 2D

Reflected shock dynamics reveal ~100 Mbar stagnation pressure

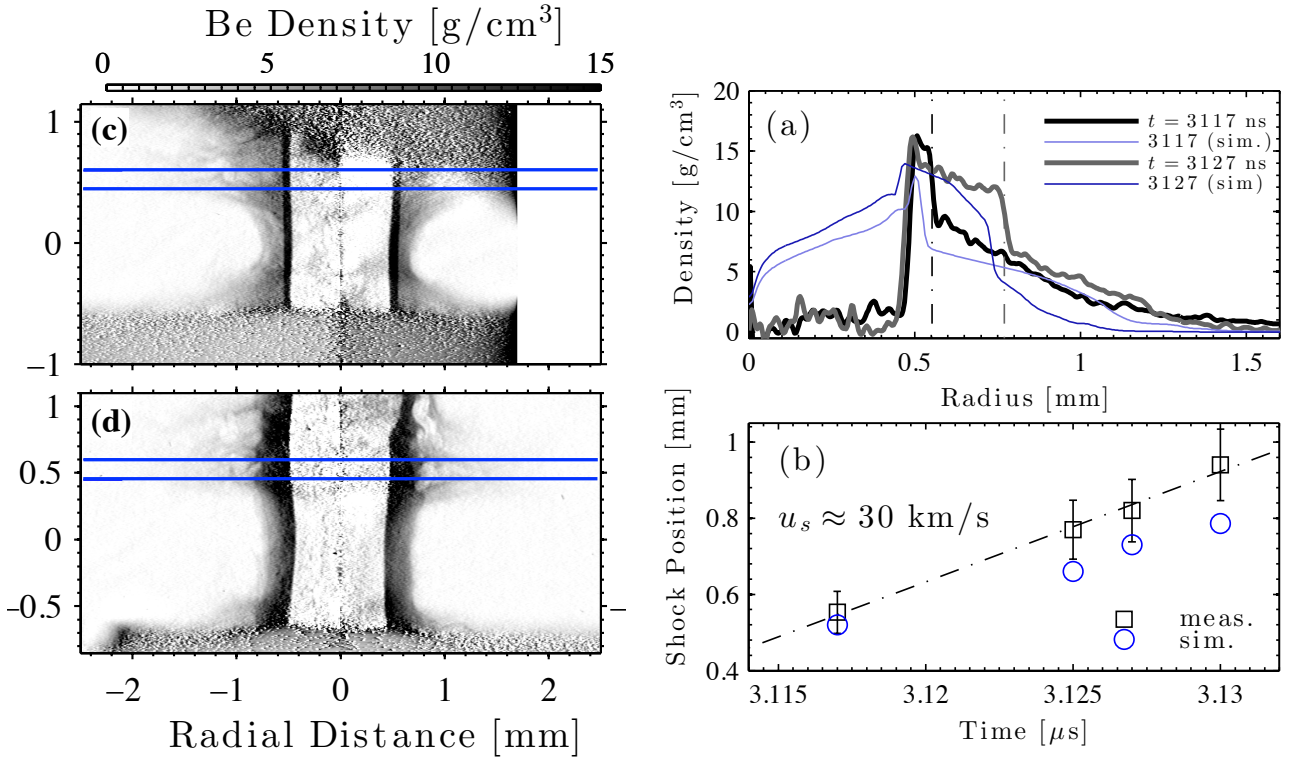

- Able to track the reflected shock in the liner in all four images (through the MRT spikes)
- Pre- and post-shock densities are known from radiograph
- Shock velocity inferred from all 4 images
- Unshocked fluid velocity from simulation

$$\Delta P = u_1^2 \rho_1 \left(1 - \frac{\rho_1}{\rho_2}\right) \approx 120 \text{ Mbar}$$

Using more drive current, we achieved a peak convergence of 19 at a pressure of 2.25 Gbar

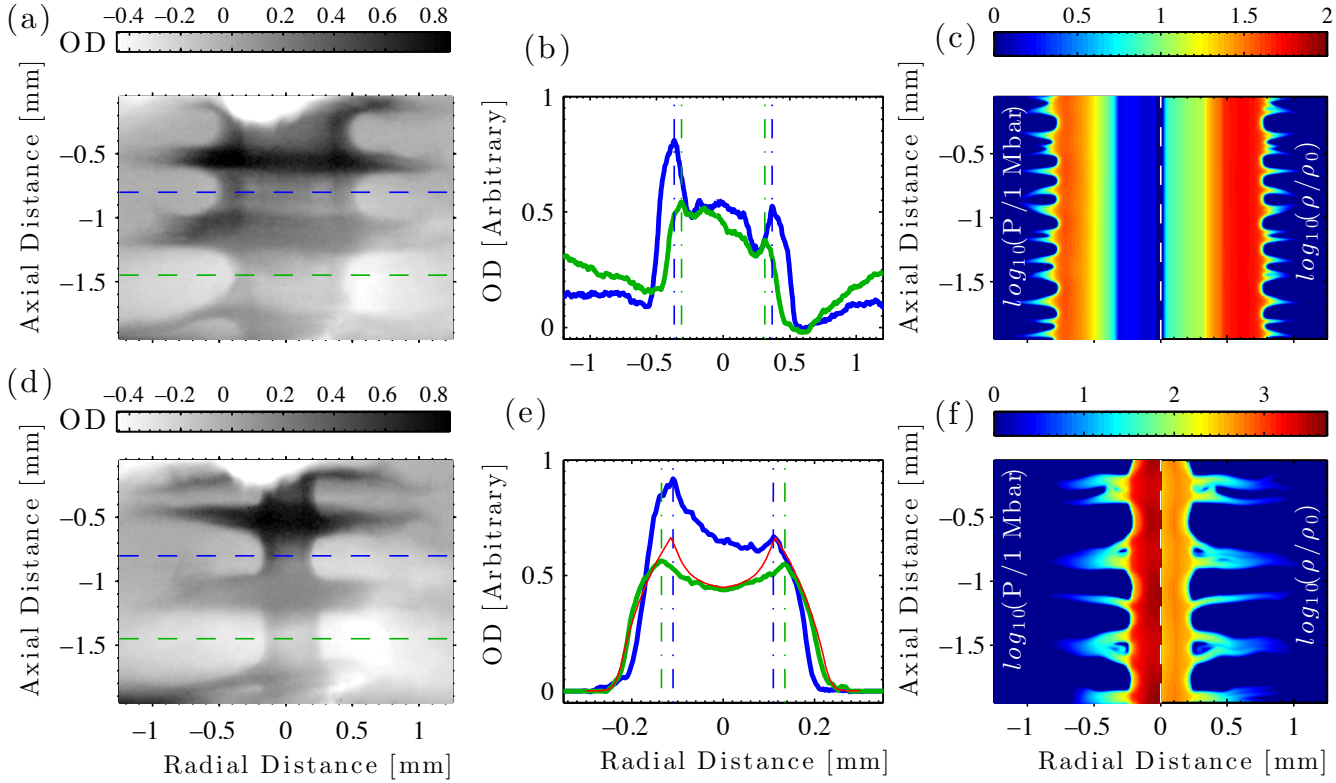

$$R_{\text{stag}} = 110\ \mu\text{m}$$
$$\rho_D = 58\ \text{g/cm}^3$$
$$\Theta \approx 0.07$$
$$\Gamma \approx 6$$

- Significant self-emission contaminated the images
- Good agreement (in some locations) with 1D simulations, but significant axial variations exist, similar to 2D
- MRT saturates and bubbles feed through earlier in experiment

In both experiments, liner areal density is more perturbed than predicted in 2D leading to degraded confinement

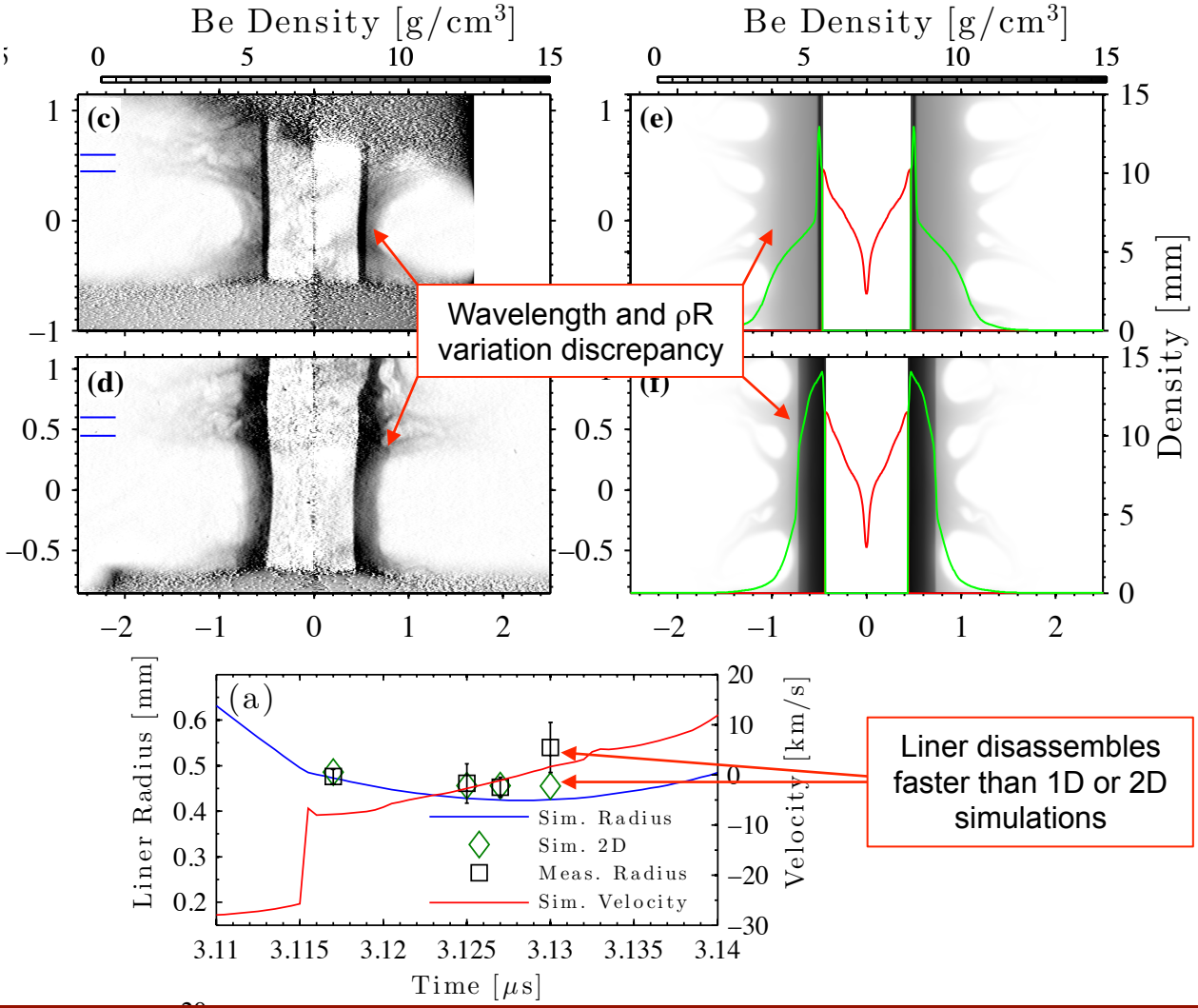

- This result is of general significance for any ICF system
- In-flight PDV measurements indicate excellent agreement during the implosion
- This platform is one of the most ideal one can envision for testing confinement (no preheat, no decel-RT growth, large spatial scales)

We are also using this platform to study deceleration phase instability growth at 100's of Mbar

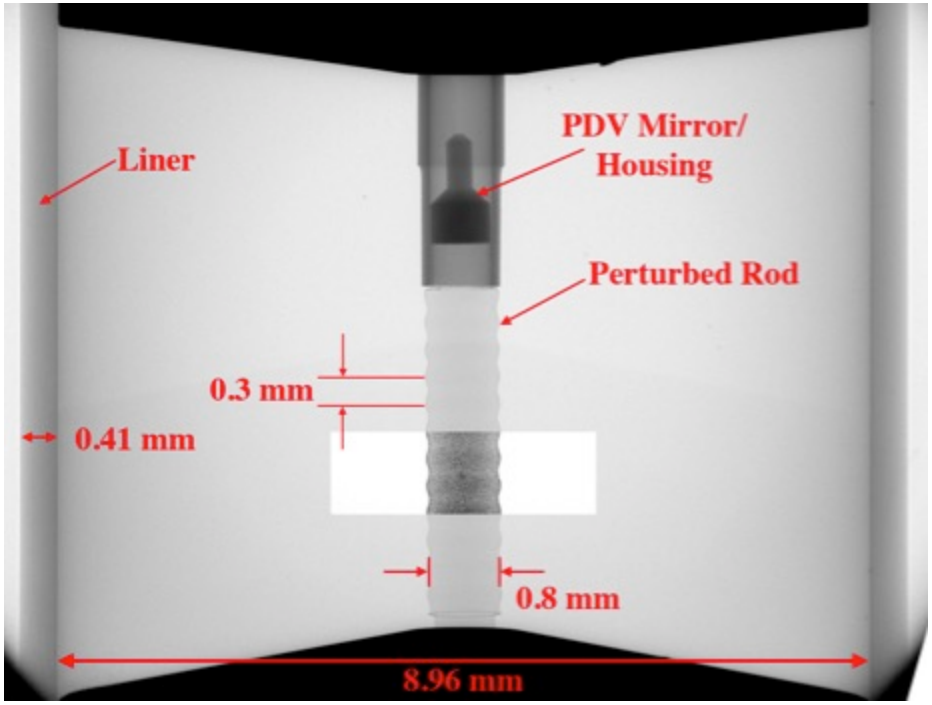

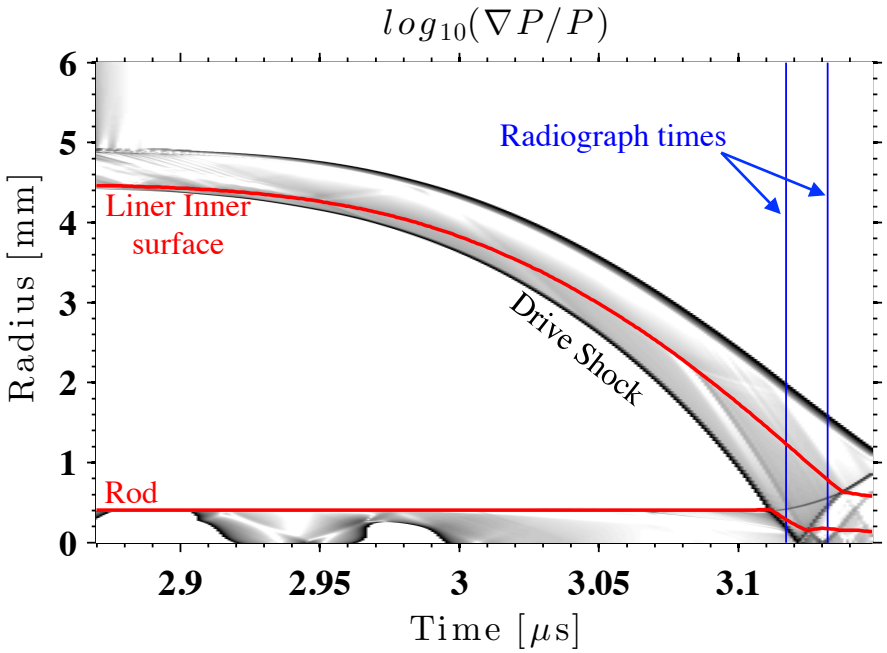

- A Be rod with a pre-imposed sinusoidal perturbation is placed on axis
- The target is filled with liquid D2
- The liner launches a shock in the D2 which grows and strikes the rod/fuel interface
- Interface is unstable to RM and RT
- After reflection, shock (now ~300 Mbar) crosses the interface again

Highly 3D structure is seen on the rod after second shock

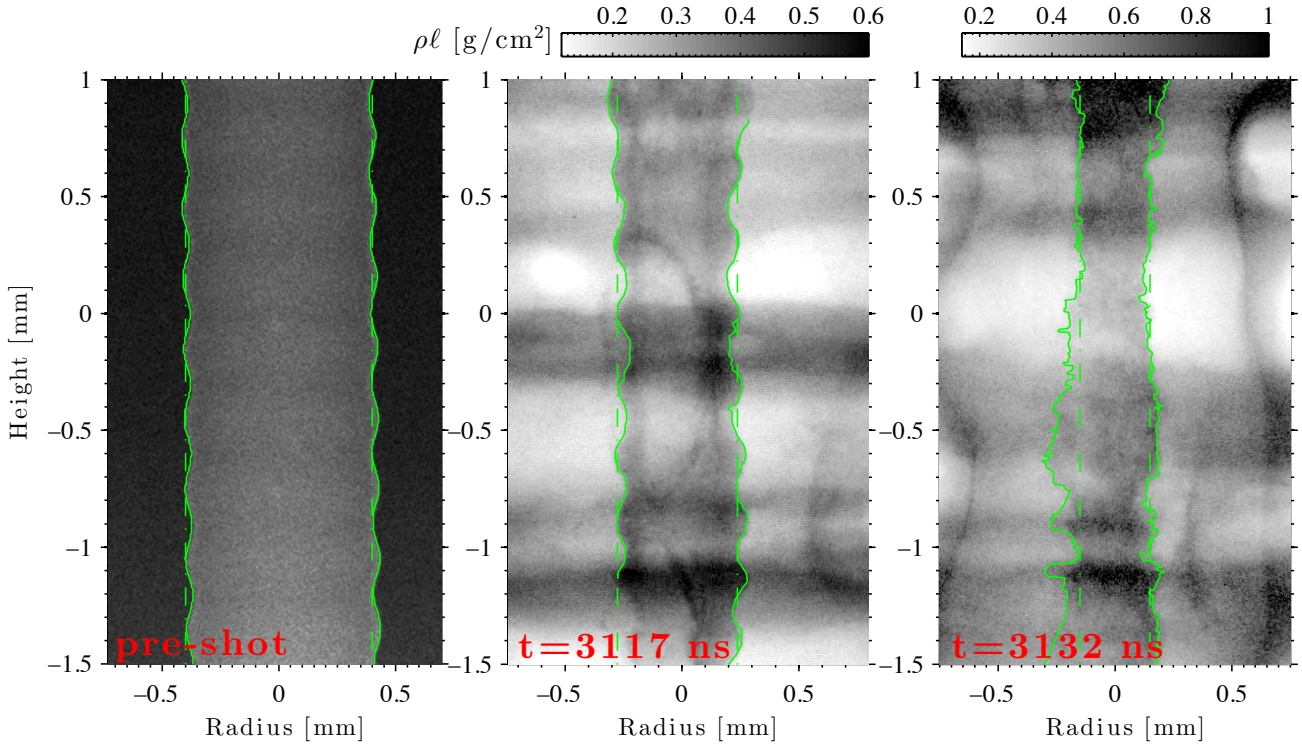

- Initial mode grows after 1st shock
- Unseeded, small scale perturbation appear
- After 2nd shock, initial mode is erased
- Small scale, highly 3D structures dominate

MagLIF Backups

Sandia National Laboratories